13th Acta Oncologica Symposium
BiGART2015

Biology-Guided Adaptive Radiotherapy

Aarhus
Denmark
June 10-12, 2015

Final programme and abstracts

Contents

Welcome!

It is our great pleasure to welcome you to Aarhus, Denmark for the 2015 Acta Oncologica symposium on Biology-Guided Adaptive Radiotherapy.

Key topics for the conference will include:

- **Biology of tumours and normal tissue** to guide patient selection, target volumes and dose prescription in radiotherapy and particle therapy
- **Functional imaging of tumours and normal tissues** with functional imaging techniques based on MRI and PET, and the use of such images for dose painting and normal tissue avoidance in radiotherapy and particle therapy
- **Treatment planning and delivery challenges** in adaptation of radiotherapy and particle therapy based on changes in tumour and normal tissue biology, anatomy and/or function
- **Clinical outcome** of adaptive radiotherapy and particle therapy

The meeting has attracted 180 physicians, physicists, radiobiologists and other scientists from Denmark and internationally. With a record-breaking 120 submitted abstracts, we look forward to an active audience in exciting scientific sessions with presentations from leading scientists from several continents.

All participants are invited to attend the social programme. Wednesday evening we have arranged a welcome reception and tour at the new Moesgaard Historic Museum in the forest south of Aarhus. Please remember to bring your entrance ticket, which will be given to you by check in or by contacting the registration desk. On Thursday evening you will have the chance to stroll through this year's version of the famous Sculpture by the Sea exhibition before enjoying the conference dinner at the Varna Mansion, a beautifully situated restaurant in the forest next to Hotel Marselis.

We hope you will enjoy the meeting and your time in Aarhus - the "city of smile"!

Ludvig Paul Muren Morten Høyer Jens Overgaard Cai Grau

Map

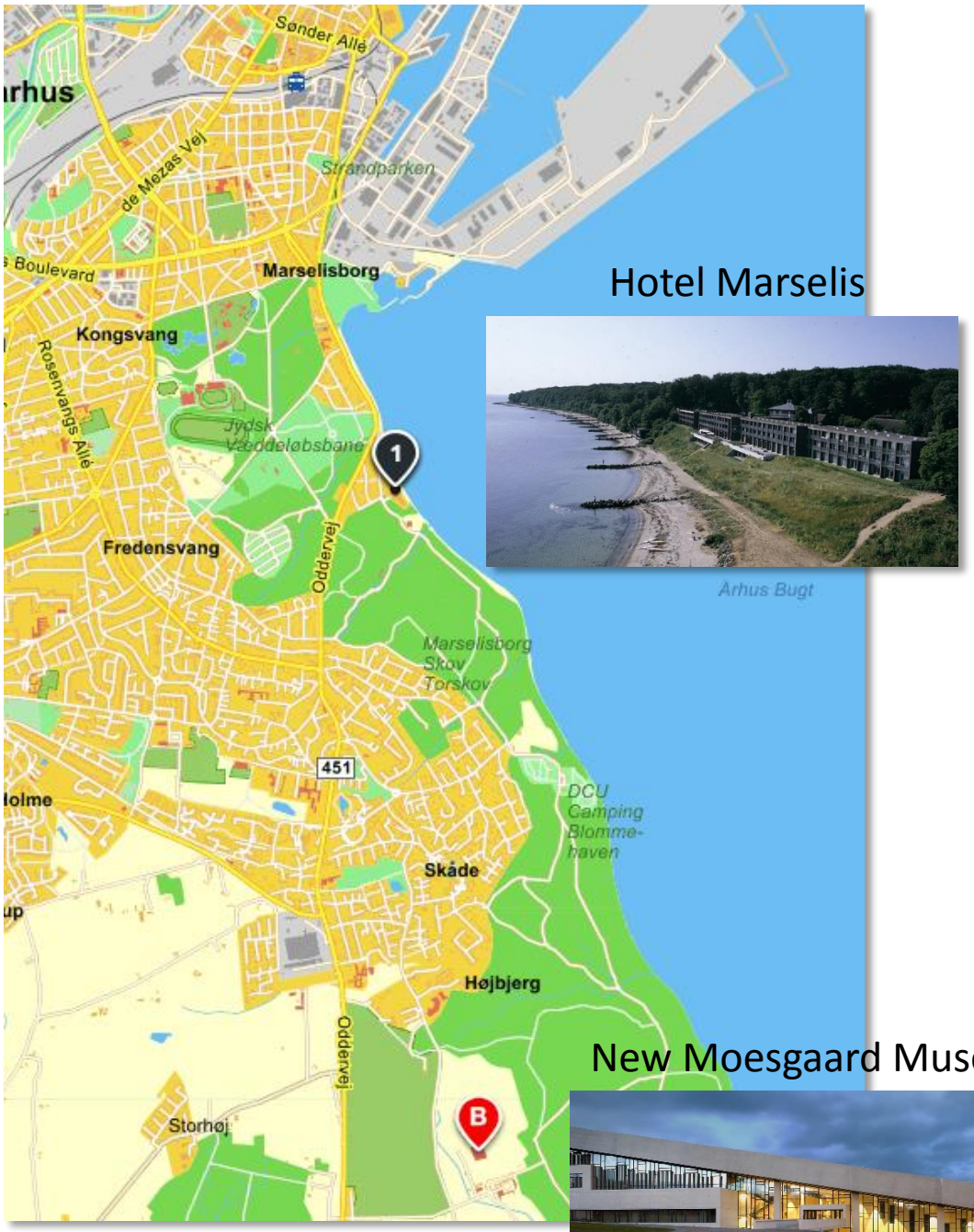

Hotel Marselis

New Moesgaard Museum

Faculty

Invited speakers
Beate Timmermann, Essen
Christoffer Johansen, Copenhagen
Daniel Zips, Tübingen
Ivan Vogelius, Copenhagen
Jan Bussink, Nijmegen
Jan Lagendijk, Utrecht
Jean-Philippe Pignol, Rotterdam
Joao Seco, Boston
Joe Deasy, New York
Josep M Borras, Barcelona
Karin Haustermans, Leuven
Klaus R. Trott, München
Marta Peroni, Villigen PSI
Michael Baumann, Dresden
Parag Parikh, St. Louis
Peter Hoskin, London
Philippe Lambin, Maastricht
Philippe Maingon, Lyon
Richard Hill, Toronto
Richard Pötter, Vienna
Thomas Björk-Eriksson, Skandion
Uulke vd Heide, Amsterdam
Vincenzo Valentini, Rome
Yolande Lievens, Ghent

Local faculty and organizers
Cai Grau
Jacob Lindegaard
Jan Alsner
Jens Overgaard
Kari Tanderup
Ludvig P. Muren
Markus Alber
Michael. R. Horsman
Morten Busk
Morten Høyer
Nicolaj Andreassen
Niels Bassler
Per R. Poulsen
Brita Singers Sørensen

Contact
Prof. Cai Grau
Department of Oncology,
Aarhus University Hospital,
Norrebrogade 44,
DK-8000 Aarhus C
Denmark
mail@bigart2015.dk

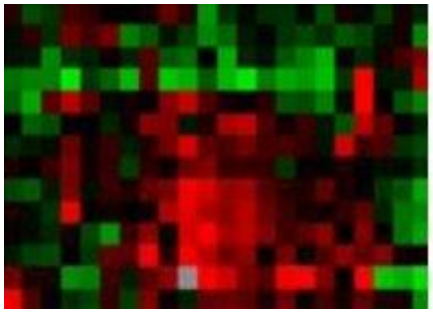
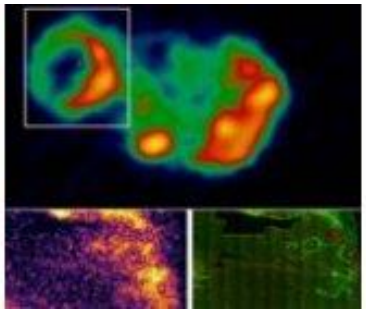


Scientific Programme

Wednesday June 10, 2015

13:00-13:10 **Opening session**
Cai Grau, Aarhus: Welcome to BiGART2015 and Aarhus. Practical information.

13:10-14:40 **Session 1: Radiobiology of human tumors: guidance for therapy**
Chairs: Michael Horsman and Marianne Nordsmark

Keynote lectures

13:10-13:30 **Richard Hill, Toronto**: Use of a small animal irradiator/imager for chemo-radiotherapy of orthotopic models of cervix cancer

13:30-13:50 **Jan Bussink, Nijmegen**: The tumor microenvironment in head and neck cancer: radiotherapy and EGFR

Proffered papers

13:50-14:00 **Christina Sæten Fjeldbo, Oslo:** Construction of a prognostic hypoxia gene classifier in cervical cancer that is reflected in dynamic contrast-enhanced (DCE) MR images

14:00-14:10 **Brita Singers Sørensen, Aarhus:** Relative biological effectiveness for tumor control and acute skin damage in a mouse model

14:10-14:20 **Ghazaleh Ghobadi, Amsterdam:** Histopathology-derived modeling of prostate cancer tumor control probability: implications for the dose to the tumor and the gland

14:20-14:30 **Thomas Wittenborn, Aarhus:** Targeting the microenvironment and vasculature of tumours to improve response to radiation administered using a dose and schedule equivalent to that for a stereotactic treatment: the effect of hypoxic modifiers

14:30-14:40 **Gregers Rasmussen, Copenhagen:** Association between immunohistochemical and imaging biomarkers in head and neck squamous cell carcinomas

14:40-15:10 **Coffee break and poster viewing**

15:10-17:00 **Session 2: Late normal tissue effects**
Chairs: Joe Deasy and Jan Alsner

Keynote lectures

15:10-15:30 **Klaus R. Trott, Münich:** Radiation-induced secondary cancers

15:30-15:40 **Nicolaj Andreassen, Aarhus:** Recent activities and future plans of the International Radiogenomics Consortium (RGC)

15:40-15:50 **Michael Baumann, Dresden:** European radiotherapy treatment plan databank

Proffered papers

15:50-16:00 **Azza Khalil, Aarhus:** New dose constraint reduces radiation-induced pneumonitis in locally advanced NSCLC treated with Intensity-Modulated Radiotherapy

16:00-16:10 **Marciana N. Duma, Münich:** Tangential field radiotherapy for breast cancer: the dose to the heart and heart subvolumes

16:10-16:20 **Laura Tuomikoski, Helsinki:** Post-RT saliva production can be predicted by measuring pre-RT salivary function and mean glandular doses

16:20-16:30 **Line Schack, Aarhus:** SNP analysis on late radiation induced toxicity analyzed by questionnaires and anal physiological methods in prostate cancer patients.

16:30-16:40 **Camilla Stokkevåg, Bergen:** Risk of radiation-induced secondary rectal and bladder cancer following radiotherapy of prostate cancer

16:40-16:50 **Laura Rechner, Copenhagen:** Risk-optimized proton therapy treatment planning to minimize second cancers after radiotherapy of the prostate

16:50-17:00 **Britta Weber, Aarhus:** Long-term outcomes and toxicity after proton beam radiotherapy of large non-peripapillary choroidal melanoma

17:15 **Bus departure for New Moesgaard Museum**

17:30 **Welcome reception – New Moesgaard Museum**

19:45 **Busses return to Hotel Marselis**

20:30 **Dinner at Hotel Marselis**

Thursday June 11, 2015

8:00-10:00	**Session 3: Recent developments in functional imaging** Chairs: Eirik Malinen and Stine Korreman
	Keynote lectures
8:00-8:20	**Uulke van der Heide, Amsterdam:** Recent developments in quantitative imaging for radiotherapy.
8:20-8:40	**Karin Haustermans, Leuven:** The role of functional imaging and molecular markers for organ-preserving strategies after chemo-radiotherapy for rectal cancer
	Proffered papers
8:40-8:50	**Niels Raaijmakers, Utrecht:** Validation is crucial in head and neck translational imaging research
8:50-9:00	**Haley Clark, Vancouver:** Preliminary findings using dynamic contrast-enhanced magnetic resonance imaging to identify functional aspects within the parotid
9:00-9:10	**Catharina Zegers, Maastricht:** Imaging of tumor hypoxia and metabolism in patients with head and neck squamous cell carcinoma
9:10-9:20	**Ane Iversen, Aarhus:** Metabolic imaging: the potential of [1-^{13}C]lactate/[1-^{13}C]pyruvate ratio to be a surrogate marker for hypoxia in hyperpolarized magnetic resonance spectroscopy
9:20-9:30	**Joachim Chan, Wirral:** Dose painting radiotherapy for high risk prostate cancer: delayed 18F-choline PET/CT imaging before neo-adjuvant hormone therapy improves detection rates
9:30-9:40	**Endre Grøvik, Oslo:** Feasibility of multi-echo dynamic MRI for simultaneous acquisition of T1-weighted and R2* contrast kinetics in rectal cancer
9:40-9:50	**Katherina Farr, Aarhus:** Perfusion SPECT imaging and radiation-induced injury in the lung after curative radiotherapy for NSCLC
9:50-10:00	**Søren Møller, Copenhagen:** Early changes in perfusion of glioblastoma during radio- and chemotherapy evaluated by T1*-dynamic contrast enhanced MRI
10:00-10:30	**Coffee break and poster viewing**
10:30-12:40	**Session 4: Clinical results – hypoxia, dose painting and adaptive radiotherapy** Chairs: Vincenzo Valentini and Jacob Lindegaard
	Keynote lectures
10:30-10:50	**Daniel Zips, Tübingen:** Hypoxia dose painting in head and neck cancer
10:50-11:10	**Peter Hoskin, London:** Hypoxia dose painting in prostate and cervix cancer
11:10-11:30	**Ivan Vogelius, Copenhagen:** FDG PET based dose painting in head and neck cancer

Proffered papers

11:30-11:40 **Marie Tvilum Petersen, Aarhus:** The clinical implication of introducing adaptive radiotherapy in the treatment of lung cancer patients

11:40-11:50 **Patrick Berkovic, Ghent:** Adaptive radiotherapy for locally-advanced non-small cell lung cancer, can we predict when and for whom?

11:50-12:00 **Anne Vestergaard, Aarhus:** Acute gastro-intestinal morbidity in a Phase II trial of online adaptive radiotherapy for urinary bladder cancer.

12:00-12:10 **Ralph Leijenaar, Maastricht:** Early prediction of pathological response in rectal cancer patients using "PET Radiomics" with independent validation

12:10-12:20 **Marianne Assenholt, Aarhus:** Application of coverage probability treatment planning for lymph node boosting in locally advanced cervical cancer

12:20-12:30 **Sara Thörnqvist, Bergen:** Adaptive radiotherapy strategies for pelvic tumours – a review of clinical implementations

12:30-12:40 **Hella Sand, Aalborg:** Correlation between pretreatment FDG-PET biological target volume and location of T-site failure after definitive radiation therapy for head and neck cancers

12:40-13:40 **Lunch break**

13:40-14:50 **Session 5: Novel concepts in design of clinical trials in radiotherapy**
Chairs: Philippe Maingon and Kari Tanderup

Keynote lectures

13:40-14:00 **Philippe Lambin, Maastricht:** Novel concepts of clinical research in radiation oncology: from clinical trials to rapid learning health care

14:00-14:20 **Joe Deasy, New York:** Data driven radiobiological modeling of tumor control probability

Proffered papers

14:20-14:30 **Armin Lühr, Dresden:** Individual benefit for advanced head and neck cancer patients in terms of NTCP differences from intensity-modulated proton therapy for complete or sequential boost treatment versus intensity-modulated photon therapy

14:30-14:40 **Morten Høyer, Aarhus:** Radiation dose to the gastro-intestinal tract and patient-reported symptom domains after prostate cancer radiotherapy

14:40-14:50 **Timo Deist, Maastricht:** Clinical routine data as a viable source for radiation-induced lung toxicity prediction models

14:50-15:20 **Coffee break and poster viewing**

15:20-16:30 **Session 6: How to establish clinical evidence in particle therapy?**
Chair: Phillipe Lambin and Morten Høyer

Keynote lecture
Michael Baumann, Dresden: Particle therapy, networks and infrastructure

Presentation by panelists (5 min each)

Philippe Maingon, Lyon
Richard Pötter, Vienna
Beate Timmermann, Essen
Thomas Björk-Eriksen, Uppsala
Jean-Philippe Pignol, Rotterdam
Cai Grau, Aarhus

Discussion

16:30-18:00 **Poster viewing, including poster discussion groups. Refreshments.**

18:00-19:30 **Sculpture by the Sea (on your own)**

19:30 **Conference dinner (Varna Mansion, next to Hotel Marselis)**

Friday June 12, 2015

8:00-10:00	**Session 7: Image-guidance for adaptive radiotherapy and proton therapy** Chairs: Jan-Jakob Sonke and Ludvig Muren
	Keynote lectures
8:00-8:20	**Jan Lagendijk, Utrecht:** The MR linac system and its impact on the radiotherapy process
8:20-8:40	**Parag Parikh, St. Louis:** Online adaptive radiation therapy in the abdomen: The challenge of bowel
8:40-9:00	**Joao Seco, Boston:** Image-guidance for adaptive proton therapy
9:00-9:20	**Marta Peroni, Villigen:** The adaptive challenge in proton therapy
	Proffered papers
9:20-9:30	**Christopher Kurz, Munich:** Comparing strategies for CBCT-based dose recalculation to foster adaptive IMRT and IMPT of head and neck cancer patients
9:30-9:40	**Lucas Persoon, Maastricht:** Is integrated transit planar EPID dosimetry able to detect geometric changes in lung cancer patients treated with volumetric modulated arc therapy (VMAT)
9:40-9:50	**Andreas Gravgaard Andersen, Aarhus:** A method to evaluate the robustness of single beam proton plans for pelvic lymph node irradiation with respect to interfractional motion
9:50-10:00	**Per Poulsen, Aarhus:** Calculation of interplay effects caused by liver tumor motion during scanning proton therapy in a commercial treatment planning system
10:00-10:20	**Coffee break** (please remember to take down your poster)
10:20-11:50	**Session 8: Radiotherapy in Europe 2020** Chairs: Michael Bauman and Jens Overgaard
10:20-10:30	**Jens Overgaard, Aarhus:** Introduction
	Keynote lectures
10:30-10:50	**Josep M Borras, Barcelona:** The need for radiotherapy in Europe 2020: Not only data but also a cancer plan
10:50-11:10	**Christoffer Johansen, Copenhagen:** Patient-reported outcome measures
11:10-11:30	**Vincenzo Valentini, Rome:** Can automation reduce costs?
11:30-11:50	**Yolande Lievens, Ghent:** Cost calculation: a necessary step on the winding road towards widespread adoption of advanced radiotherapy technology
	Discussion
11:50-12:00	**Ludvig Muren, Aarhus:** Closing of the meeting

Posters

All posters are on display throughout the entire meeting

Poster discussion group 1: Functional imaging in RT: PET

1. Kathinka Elinor Pitman, Oslo: Variability of dynamic 18F-FDG-PET data in breast cancer xenografts
2. Linda Wack, Tübingen: Comparison of [18F]-FMISO, [18F]-FAZA and [18F]-HX4 for hypoxia PET imaging – a simulation study
3. Daniel Warren, Oxford: A predictive model of three-dimensional hypoxia distributions in tumour
4. Azadeh Abravan, Oslo: Correlation between normal tissue dose and 18F-FDG-PET uptake for non-small cell lung cancer patients receiving thoracic radiotherapy and erlotinib
5. Marta Lazzeroni, Stockholm: Evaluation of early response in H&N cancer patients based on effective radiosensitivity derived from repeated FDG-PET scans
6. Espen Rusten, Oslo: Early radiotherapy response monitoring of anal carcinoma with 18F-FDG-PET
7. Mikkel Vendelbo, Aarhus: PET-based assessment of tumor IGF1- and insulin receptor expression and its linkage to anti-receptor treatment response
8. Morten Busk, Aarhus: Pre-clinical assessment of the robustness and reliability of PET-based identification and quantification of tumor hypoxia

Poster discussion group 2: Functional imaging in RT: MRI

9. Anna Li, Oslo: Hypoxia imaging with dynamic contrast enhanced MRI and focal brachytherapy of cervical cancers
10. Catarina Dinis Fernandes, Amsterdam: Characterising irradiated prostate tissue in radio-recurrent PCa patients using mp-MRI and histopathology
11. Kathrine Røe Redalen, Lørenskog: Quantitative diffusion-weighted MRI of rectal cancer is strongly influenced by the choice of b-values
12. Oscar Casares-Magaz, Aarhus: biomechanical image-based rectal properties following radiotherapy of prostate cancer

Poster discussion group 3: In - room imaging

13. Jenny Bertholet, Aarhus: Targeting accuracy in image-guided stereotactic liver radiation therapy with and without time resolved rotation corrections
14. Lone Hoffmann, Aarhus: Positional stability of fiducial markers in oesophageal cancer patients during radiotherapy treatment
15. Mariwan Baker, Herlev: Using Real-time Four-dimensional Ultrasound Imaging to Determine Prostate Displacement during Trasabdominal Ultrasound Image-guided Radiotherapy
16. Mai Lykkegaard Schmidt, Aarhus C: Time-resolved differential motion of tumor and lymph nodes during conebeam computed tomography (CBCT) of lung cancer patients

17. Esben Worm, Aarhus: Is a delay between marker insertion and planning CT needed in fiducial marker guided liver SBRT?
18. Maria Najim, Sydney: Retrospective review to assess volumetric and dosimetric change in organs at risk (OAR) during IMRT/VMAT treatment for HN cancer
19. Ulrik Vindelev Elstrøm, Aarhus: Cone-beam CT-based Dose Calculation in Radiotherapy of Head and Neck Cancer
20. Lotte Lutkenhaus, Amsterdam: A comparison of two adaptive strategies for radiotherapy of urinary bladder cancer using biological models

Poster discussion group 4: Image analysis

21. Søren Haack, Aarhus: Diffusion Weighted MRI during Radiotherapy of Locally Advanced Cervical Cancer – Treatment response assessment using different segmentation methods
22. Martin Nielsen, Aalborg: A new method to validate CT-CT deformable image registration using an auto-segmented bronchial branch point grid
23. Turid Torheim, Ås: Cluster analysis of DCE-MRI pharmacokinetic parameter maps is related to locoregional and metastatic relapse for cervical cancer patients
24. Sara Carvalho, Maastricht: The impact of region of interest definition on PET textural features of involved lymph nodes in NSCLC – a separate region per node or a combined one?
25. Ruta Zukauskaite, Odense: Comparison of local rigid and deformable image registration in head and neck cancer
26. Jonathan Sykes, Sydney: Performance evaluation of head and neck contour adaptation with cone beam CT using commercial software systems
27. Giske Fiskarbekk Opheim, Herlev: How different delineation strategies affect parameter estimation in diffusion MRI study of treatment response in brain metastases
28. William (Bill) Nailon, Edinburgh: Identifying Focal Prostate Cancer by Image Analysis

Poster discussion group 5: Outcome and modelling

29. Anne Winther Larsen, Aarhus: Influence of PET-staging on outcome in limited disease small-cell lung cancer treated with definitive chemoradiotherapy
30. Christina Maria Lutz, Aarhus: The reliability of dose-response model selection
31. Anne Ramlov, Aarhus: Impact of lymph node dose on nodal control in patients with locally advanced cervical cancer
32. Christina Daugaard Lyngholm, Aarhus: Recurrence pattern and survival in DBCG-1989-TM patients, with a special focus on the significance of age
33. Ferenc Lakosi, Liège: Clinical efficacy and toxicity of radio-chemotherapy and MRI-guided brachytherapy for locally advanced cervical cancer patients: a mono-institutional experience
34. Emely Lindblom, Stockholm: Radiobiological modelling of tumour response based on the 5 Rs of radiobiology in search for optimal radiotherapy treatment parameters for non-small-cell lung cancer
35. Yasmin Lassen, Aarhus: Pseudoprogression after proton radiotherapy for pediatric low grade glioma

36. Jørgen Johansen, Odense: Validation of a normal tissue complication probability (NTCP) model for radiation-induced hypothyroidism in two independent cohorts

Poster discussion group 6: Planning challenges: Photons

37. Ditte Sloth Møller, Aarhus: Adaptive radiotherapy for advanced lung cancer ensures target coverage and decreases lung dose
38. Susanne Rylander, Aarhus C: A comparison study for US- and MR based dose planning in high-dose-rate interstitial prostate brachytherapy
39. Marius Røthe Arnesen, Oslo: Dose painting by numbers in a standard treatment planning system using inverted dose prescription maps
40. Bernt Louni Rekstad, Oslo: Anal carcinoma - a candidate for FDG-PET guided high-dose simultaneously integrated boost
41. Gitte Persson, Copenhagen: Deep Inspiration Breath-Hold Radiotherapy for Lung Cancer - Can Dose to Heart and Mediastinal Structures be Decreased?
42. Stine Korreman, Roskilde: Loss of TCP by geometrical uncertainties in dose painting strategies
43. Anders Traberg Hansen, Aarhus: Exploring the optimal dose-prescription strategy for liver SBRT including the effects of target motion
44. Patrik Sibolt, Roskilde: Adaptation requirements due to anatomical changes in free-breathing and deep-inspiration-breath-hold for standard and dose escalated radiotherapy of lung cancer patients

Poster discussion group 7: Particle therapy challenges

45. Eirik Malinen, Oslo: Dose or 'LET' painting – what is optimal for hypoxic tumors?
46. David Hansen, Aarhus: A simulation study comparing proton CT and dual energy CT for stopping power estimation
47. Maria Fuglsang Jensen, Aarhus: Flexible spot scanning patterns improve dose quality and -robustness in intensity-modulated proton therapy (IMPT) treatment planning
48. Ellen Marie Høye, Aarhus: Improving the stability of a radiochromic deformable 3D dosimeter
49. Vicki Trier Taasti, Aarhus C: A new approach for stopping power ratio calibration in proton beam therapy using spectral CT
50. Anne Ivalu Sander Holm, Aarhus: Dose escalation IMRT and IMPT study using FET-PET in high-grade gliomas – initial experiences
51. Ida Mølholm, Lyngby: The dosimetric impact of an MRI contrast agent in photon and proton radiotherapy
52. Shirin Rahmanian, Heidelberg: Toward a New Microscopic Dosimetry of Ion therapy

Poster discussion group 8: Delivery solutions

53. Sidsel Damkjær, Næstved: Improved dose coverage of internal mammary nodes using deep inspiration breath hold for right-sided breast cancer radiotherapy
54. Tine Bisballe Nyeng, Aarhus: Dosimetric evaluation of interfractional shifts in oesophageal cancer patients
55. Rune Hansen, Aarhus: Calypso-guided MLC tracking on a TrueBeam accelerator
56. Annette Boejen, Aarhus: A learning program qualifying radiation therapists to manage daily online adaptive radiation treatment
57. Jakob Toftegaard, Aarhus: Design improvement for TrueBeam MLC tracking investigated with an MLC tracking simulator
58. Toke Ringbæk, Marburg: Planning evaluations of new 2D ripple filters in carbon ion treatment plans using TRiP98 and Monte Carlo code SHIELD-HIT12A
59. Alina Santiago, Marburg: Interfractional local changes in the radiological depth correlate with dosimetric deterioration in particle beam therapy for stage I NSCLC patients under jet ventilation
60. Caroline Grønborg, Aarhus C: Population-based vs patient-specific margins for intra-fractional motion in adaptive bladder radiotherapy

General poster display

61. Ahmad Ali, Cairo: MIM: A New Auto-Contouring and Deformable Registration Software for Adaptive Lung Radiation Therapy
62. Mette Winther, Aarhus: Evaluation of miR-21 and miR-375 as prognostic biomarkers in esophageal cancer
63. Alexandr Kristian, Oslo: Dynamic 18F-FDG PET of breast cancer xenografts and correlation with treatment outcome
64. Anne Winther Larsen, Aarhus: Loco-regional failures in limited disease small-cell lung cancer patients treated with definitive chemoradiotherapy
65. Kirsten Legaard Jakobsen, Herlev: Soft tissue vs. bony anatomy registration in an adaptive plan selection protocol for bladder cancer
66. Mirjana Josipovic, København: Image quality and registration uncertainty in image guided deep inspiration breath hold radiotherapy of lung cancer
67. Noha Jastaniyah, Riyadh: A volumetric analysis of GTVD and CTVHR as defined by the GEC ESTRO recommendations in FIGO stage IIB and IIIB cervical cancer patients treated with IGABT in a prospective multicentric trial (EMBRACE)
68. Taran Paulsen Hellebust, Oslo: Influence of rectum and bladder filling and position on the motion of the central clinical target volume for cervical cancer patients
69. Jacob Lilja-Fischer, Aarhus: Response evaluation of the neck in oropharyngeal cancer: value of MRI and influence of p16 in selecting patients for post-radiotherapy neck dissection
70. Jasmin Mahdavi, Lyngby: Dosimetric effect of unwanted air gaps under bolus in volumetric modulated arc therapy (VMAT)
71. Steffen Nielsen, Aarhus: Hypoxia-regulated Gene Expression as an Endogenous Marker in Prostate Adenocarcinoma

72. Maria Sjölin, Herlev: The effect of different dosimetric leaf gap on patient specific quality assurance
73. Oscar Casares-Magaz, Aarhus: Towards spatial dose-response relationships for the rectum in prostate radiotherapy
74. Britta Weber, Aarhus: VMAT makes it possible to treat more advanced stages of NSCLC compared to 3D-CRT
75. Nina Boje Kibsgaard Jensen, Aarhus: Application of library plan selection and margin reduction in locally advanced cervical cancer
76. Ziad Saleh, West Harrison: Multiple-image based approach to evaluate the performance of deformable image registration and identify scan outliers in a longitudinal data set
77. Steffen Hokland, Aarhus: Evaluation of external beam radiotherapy CT-based dose plans recalculated on MRI-generated density maps
78. Aniek Even, Maastricht: Dual-energy CT for the combined assessment of changes in lung perfusion and morphology after radiotherapy in non-small cell lung cancer patients
79. Angela Botticella, Leuven: Optimization of gross tumour volume definition in lung-sparing volumetric modulated arc therapy for pleural mesothelioma: Implications for radiotherapy planning
80. Ester Thøgersen, Aarhus: Quantification of interfractional movement of the oesophagus and the influence on the dose to the oesophagus
81. Bregtje Hermans, Maastricht: Weekly cone beam computed tomography for detection of discrepancies between planned and delivered dose in head and neck cancer patients treated with radical (chemo)radiotherapy
82. Jacob Rasmussen, Copenhagen: Spatio-temporal stability of pre-treatment 18F-Fludeoxyglucose uptake in head and neck squamous cell carcinomas sufficient for dose painting
83. Jens Edmund, Herlev: CBCT guided treatment delivery and planning verification for MRI-only radiotherapy of the brain
84. Grete May Engeseth, Bergen: Effect of range uncertainty and setup errors in cranio-spinal treatment plans
85. Maria Luisa Belli, Milano: PET positive lymph nodes variations during treatment as predictors of treatment outcome
86. Roshan Karunamuni, La Jolla, California: Adaptive replanning for brain IMRT treatment to achieve sparing of eloquent cortex in glioblastoma
87. David Hansen, Aarhus: A Gadgetron based hyperpolarised 13C analysis module for multi-vendor clinical translation
88. Finn von Eyben, Odense: Management of prostate cancer with dominant intraprostatic lesion: a systematic revoew and meta-analysis

SPONSOR

ACTA ONCOLOGICA

Abstracts

Wednesday June 10, 2015

Session 1: Radiobiology of human tumors: guidance for therapy

13:10-13:30: Richard Hill, Toronto, Canada

Use of a small animal irradiator/imager for chemo-radiotherapy of orthotopic models of cervix cancer

R.P. Hill, N. Chaudary, D.W. Hedley, S, Jelveh, P. Lindsay, H. Mackay, M. Milosevic. Ontario Cancer Institute and Princess Margaret Cancer Centre, Toronto, Canada

Objective: The recent availability of small animal irradiators and suitable immune-deprived mouse models has allowed preclinical studies using xenograft models with radiochemotherapy that more closely mimic clinical studies. We have generated a series of early-passage xenografts from cervix cancer patients that were initiated and passaged orthotopically in the cervix of mice and have used an XRad225Cx small animal irradiator/imager to deliver fractionated dose treatment and chemotherapy (CRTx) to these xenograft models. The CRTx was combined with (1) AMD3100, a drug that blocks the interaction of the CXCR4 chemokine receptor with its ligand CXCL12 or (2) inhibitors of the Hedgehog pathway since our recent studies have shown this pathway is significantly upregulated in many cervix cancers. Methods: Irradiation treatment was delivered to tumours of ~5 mm diameter growing in the cervix of mice using an 8-beam protocol with imaging of the target immediately prior to each fraction. The radiation treatment (15 x 2Gy fractions delivered 5 days/wk) was combined with weekly cisplatin (4 mg/kg/wk) to match current external beam treatment procedures for cervix cancers. Tumour growth delay analysis was performed using the imaging features of the irradiator to assess tumour size as a function of time during and after the treatment. Metastases were assessed in the para-aortic lymph nodes. Results: There was limited response of the primary tumour to treatment with cisplatin alone but significant response to fractionated radiation treatment, which was enhanced when combined with cisplatin. Combining CRTx with either AMD3100 or Hedgehog (Hh) pathway inhibitors further enhanced the treatment response of the primary tumours and growth of lymph node metastases in the aortic chain was also significantly suppressed. Analysis of the response of small intestinal stem cells as assessed using a GI-tract clonal assay indicated that cisplatin enhances radiation effects but that there is no further enhancement of early gut toxicity by AMD3100 or Hh pathway inhibitors. Studies on late G-I toxicity are underway. Conclusions: The combination of CRTx with AMD3100 or a Hedgehog pathway inhibitor has potential for clinical application in the treatment of patients with cervical cancer.

Wednesday June 10, 2015

13:30-13:50: Jan Bussink, Nijmegen, The Netherlands

The tumor microenvironment in head and neck cancer: radiotherapy and EGFR

Jan Bussink. Department of Radiation Oncology, Radboud University Medical Center, Nijmegen, The Netherlands

The potential of personalized treatment has been widely recognized. Based on preclinical studies in murine tumor models and human xenografts several improvements have been implemented in clinical practice over the last decennia. These include the introduction of hypoxia modification and targeting the epithelial growth factor receptor (EGFR) in combination with radiotherapy. By adaptations based on the characteristics of the tumor of the patient, it is expected that treatment outcome can be improved and that the overall treatment-related side effects can be reduced. The heterogeneity of the patient population drives the search for tumor specific biomarkers and has established the value of non-invasive molecular imaging techniques. This heterogeneity, as well as the observation that specific characteristics of the microenvironment are maintained when human tumors are transplanted in immune compromised mice, makes these relevant models for testing new therapies. In this presentation recent developments of the application of radiolabeled EGFR antibodies for quantifying EGFR expression in human head and neck cancer xenografts will be presented.

Wednesday June 10, 2015

13:50-14:00: Christina Sæten Fjeldbo, Oslo, Norway

Construction of a prognostic hypoxia gene classifier in cervical cancer that is reflected in dynamic contrast-enhanced (DCE) MR images

Fjeldbo C S1, Julin C H1, Lando M1, Forsberg M F1, Alsner J2, Kristensen G B3, Malinen E4, Lyng H1. Departments of 1Radiation Biology, 3Gynaecologic Oncology, 4Medical Physics, The Norwegian Radium Hospital, Oslo University Hospital, Oslo, Norway. 2Department of Experimental Clinical Oncology, Aarhus University Hospital, Aarhus, Denmark.

Introduction: Combining functional imaging with global gene expression provides a better biological understanding of the images that may be used for treatment planning. We have previously identified a prognostic 31-gene hypoxia signature in locally advanced cervical cancer that was associated with the DCE-MR image parameter ABrix. To bring the signature closer to clinical use, the present work aimed to construct a hypoxia classifier based on the 31 genes that retained an association to ABrix and separated the patients into groups with different outcome. Materials and methods: A training cohort of 42 patients and two validation cohorts of 108 and 131 patients were included. Gene expression was assessed by two different Illumina versions (WG6, HT12), for which the latter required transformation before classification. DCE-MR images were available for 64 patients. The amplitude ABrix in the 'Brix' pharmacokinetic model was extracted from each image. Progression-free survival was used as endpoint. Results: Different classifiers were constructed by separating patients in the training cohort into a more and less hypoxic group based on ABrix and including genes ranked by their difference in expression between the groups. By evaluating the ability of the classifiers to separate the patients correctly according to ABrix, a 6-gene classifier with a strong correlation to ABrix (ρ=0.66;P<0.001) was chosen. In validation cohort 1, the prognostic value of the classifier was validated, classifying the patients into two groups with 5-years survival probabilities of 85% and 60% (P=0.004). In validation cohort 2, its ABrix-association (ρ=0.47;P=0.027;n=22) and prognostic value (P=0.01) were validated. Conclusion: A robust, prognostic hypoxia classifier has been constructed. The classifier might be used alone or in combination with DCE-MR imaging to achieve an early indication of a patient's risk of failure and allocate high risk patients to adjuvant hypoxia-targeted therapy.

Wednesday June 10, 2015

14:00-14:10: Brita Singers Sørensen, Aarhus, Danmark

Relative Biological Effectiveness for Tumor Control and Acute Skin Damage in a Mouse Model

Sørensen BS, Horsman MR, Alsner J, Overgaard J, Durante M, Scholz M, Friedrich T, Bassler N. Department of Experimental Clinical Oncology, Aarhus University Hospital, Aarhus, Denmark. GSI Helmholtzzentrum für Schwerionenforschung (GSI), Department of Biophysics, Darmstadt, Germany. Department of Physics, Aarhus University, Aarhus, Denmark

Particle therapy provide a more favorable dose distribution compared to x-rays, but limited focus has been on the actual biological responses. Effects of carbon ion radiation in experimental tumor models has been investigated in a limited number of studies, the majority of these with tumor growth delay as biological endpoint. To elucidate the biological variation in radiation response in particle therapy, more in vivo studies are needed. The aim of the present study was to compare the biological effectiveness of carbon ions relative to x-rays between the clinical relevant endpoint tumor control and acute skin reaction of CDF1 mice. CDF1 mice with C3H mouse mammary carcinoma placed subcutaneously on the foot of the right hind limb were irradiated with single fractions of either photons or 12C ions, using a 30-mm spread-out Bragg peak. Endpoint of the study was local control (no tumor recurrence within 90 days). For the acute skin reaction, non-tumor bearing CDF1 mice were irradiated with a comparable radiation scheme, and monitored for acute skin damage. The TCD50 (dose producing tumor control in 50% of mice) values with 95% confidence interval were 29.7 (25.37- 34.78) Gy for C ions and 43.94 (39.24- 49.2) Gy for photons. The corresponding RBE values were 1.48 (1.28-1.72). For acute skin damage the MDD50 (dose to produce moist desquamation in 50% of mice) values with 95% confidence interval were 26.34 (22.99-30.19) Gy for C ions and 35.84 (32.94-38.98) Gy for photons, resulting in a RBE of 1.36 (1.20-1.45). We have established TCD50 and MDD50 values for local tumor control and acute skin damage and the corresponding RBE values for carbon ions in a mouse model. The RBE was larger for a tumor than skin when irradiated with large doses of high-LET (linear energy transfer) carbon ions. This study add information to the variation in biological effectiveness in different tumor and normal tissue models, which could reflect the variation found in patient cohorts.

Wednesday June 10, 2015

14:10-14:20: Ghazaleh Ghobadi, Amsterdam, The Netherlands

Histopathology-derived modeling of prostate cancer tumor control probability: implications for the dose to the tumor and the gland

Ghobadi G.1, de Jong J.2, Hollmann B.G.1, van Triest B.1, van der Poel H.G.3, Vens C. 1,4, van der Heide U.A.1. 1 Department of Radiation Oncology; 2 Department of Pathology; 3 Department of Urology; 4 Division of Biological Stress Response, The Netherlands Cancer Institute, Amsterdam, The Netherlands.

Objective: We aim to evaluate the impact of dose differentiation on the tumor control probability (TCP) in prostate radiotherapy (RT) using histopathological data of prostatectomy specimens. To compare different dosing regimens to the gross target volume (GTV) or the clinical target volume (CTV) we estimated the patients' TCP considering the cell numbers (N0) and Gleason Scores (GS) of the identified tumors within those regions. Material and methods: N0 and GS of each separate tumor were derived from histopathology of 25 specimens of intermediate-risk prostate cancer patients. Index lesions and tumors ≥0.5cm3 were considered GTV. The whole gland excluding the GTV was set as CTV. N0 of each tumor was incorporated into the linear quadratic model to estimate patient's response to simulated RT while assuming either a constant α and β for all tumor foci or values that depend on the GS. α and β were calibrated to clinical response data reaching 80% TCP after a conventional dose of 78Gy/2Gy and α/β=1.93Gy, consistent with clinical data. Results: We found that 19/25 patients showed multi-focal disease. CTV often included tumors (by definition <0.5cm^3) and in 11 cases of these multifocal cancers it contained GS 4+3 or 4+4 lesions. Compared to the GTV, however, the pathology of CTV was on average more favorable. For 78Gy, we found an α of 0.14Gy^{-1} for a TCP of 80%. With this α, a GTV dose of 79Gy combined with a CTV dose of 72Gy did not affect the TCP in the population. By varying α between 0.16 and 0.118Gy^{-1}, depending on GS of the individual tumor, a GTV dose of 80Gy combined with a 70Gy dose to the CTV also gave an 80% TCP. Conclusions: Based on tumor cell density data, we suggest that a dose differentiation of 7Gy between GTV and CTV would not compromise TCP of the patient population. When associating the GS with radiosensitivity, a further GTV-CTV dose differentiation of 10Gy might be feasible.

Wednesday June 10, 2015

14:20-14:30: Thomas Wittenborn, Aarhus, Denmark

Targeting the microenvironment and vasculature of tumours to improve response to radiation administered using a dose and schedule equivalent to that for a stereotactic treatment: the effect of hypoxic modifiers

Wittenborn T.R. and Horsman M.R.. Department of Experimental Clinical Oncology, Aarhus University Hospital, Aarhus, Denmark

Introduction: Hypoxia is a characteristic feature of tumours that reduces the efficacy of radiation therapy. Such hypoxia may play a more significant role with high radiation doses per fraction as used in stereotactic radiation schedules. This was investigated using various agents known to enhance tumour radiation response and that do so by primarily targeting hypoxia. Materials and methods: Restrained, non-anaesthetised CDF1 mice with a 200mm3 C3H mammary carcinoma growing in the right rear foot, had their tumour locally irradiated with 3x15 Gy during a 1-week period, followed 3-days later by a clamped top-up dose to produce a dose-response curve; the endpoint was tumour control 90 days after treatment. The hypoxic modifiers were nimorazole (200 mg/kg injected i.p. 30 minutes before radiation); nicotinamide (120 mg/kg injected 20 minutes before radiation) and carbogen (95% O2 + 5% CO2) breathing (started 5 minutes before and continued during irradiation); OXi4503 (10 mg/kg injected i.p. 1 hour after irradiation); and hyperthermia (41.5OC for 1-hour starting 4 hours after irradiation). Results: The radiation dose controlling 50% of clamped tumours (TCD50) following 3x15 Gy was 30 Gy. Giving nimorazole or nicotinamide+carbogen prior to the final 15 Gy irradiation non-significantly ($\chi 2$; $p<0.5$) reduced this TCD50 to 20-23 Gy; when administered with all three 15 Gy irradiations these values were significantly reduced to <2.5 Gy. Injecting OXi4503 or heating after irradiating significantly reduced the TCD50 to 9-12 Gy regardless of whether administered with one or all three 15 Gy treatments. Combining OXi4503 and heat with the final 15 Gy had a significantly larger effect (TCD50 = 2 Gy). Conclusions: All hypoxic modifiers enhanced radiation response, but the effects were different depending on the agent or how often it was administered. These differences may be related to different effects on hypoxia and this is currently under investigation.

Wednesday June 10, 2015

14:30-14:40: Gregers Rasmussen, Copenhagen, Denmark

Association between immunohistochemical and imaging biomarkers in head and neck squamous cell carcinomas

Rasmussen GBD (1), Vogelius IR (1), Rasmussen JH (1), Fischer M (2), Therkildsen MH (3), Cullen KJ (4), Ioffe OB (4), Specht L (1), Bentzen SM (1,4). Departments of (1) Oncology, (2) Clinical Physiology, and (3) Pathology, Rigshospitalet, Copenhagen, Denmark and (4) University of Maryland Greenebaum Cancer Center, Baltimore, USA

Introduction: There is an exciting complementarity between the spatial resolution provided by molecular imaging of a single, often unspecific, biomarker on one hand and the more detailed biological profile achievable from a diagnostic biopsy using a panel of immunohistochemical (IHC) markers on the other. A number of previous studies have shown a relationship between glucose transport protein expression and FDG PET uptake. Here, we study 18F-Fludeoxyglucose (18F-FDG)-uptake on PET versus IHC cancer biomarker expression in head and neck squamous cell carcinomas (HNSCC). Materials & Methods: IHC staining for Bcl-2, beta-tubulin-I and II, p53, glutathione-transferase-pi and p16 was performed on formalin fixed paraffin embedded diagnostic biopsies from 102 HNSCC cases treated at Rigshospitalet 2005-2009. The proportion of positive cells was used for analyses (p16 scored according to EORTC guidelines). In all cases, FDG Standardized uptake value (SUV) metrics were extracted for the primary tumor, TSUVmax. Univariate linear regression and multiple linear regression analyses were performed. Results: In univariate analyses, TSUVmax showed negative associations with Bcl-2 (p=0.002) and p16 (p=0.005) indices and positive association with beta-tubulin-I index (p=0.003). On multivariate analysis, TSUVmax remained associated with both beta-tubulin-I and Bcl-2 (p=0.03) with p16 being borderline significant (p=0.05). All correlations had R^2<0.2, Conclusion: Statistically significant correlations were observed between the expression of immunohistochemical biomarkers, that have previously shown to be of prognostic importance for HNSCC, and FDG PET TSUVmax that has also been shown to be prognostic. The results suggest that IHC and imaging biomarkers may capture partially associated tumor biological features. Improved understanding of HNSCC biology as well as more accurate prognostic and predictive models may arise from multiplexed modeling of data from multiple types of assays.

Session 2: Late normal tissue effect

Wednesday June 10, 2015

15:10-15:30: Klaus R. Trott, Münich, Germany

Radiotherapy-induced Second Cancers

Department of Radiation Oncology, Technische Universität München, Klinikum rechts der Isar, Germany

Second cancers may occur in patients who have been cured by radiotherapy. In some cases they can be ascribed to the radiation treatment which cured the patient. This would, undoubtedly, be considered the most serious normal tissue complication imaginable. Results of numerous studies have been published recently which estimated the absolute risk of developing a second cancer caused by modern radiotherapy to be in the same order of magnitude as that of severe (grade 3+) non-malignant complications. The risk of radiotherapy-induced second cancers varies dramatically between individual patients. The main factors which determine the risk are the anatomical dose distribution outside the treated volume, the organs at risk, the age of the patient, the sex of the patient. The mathematical models used to calculate the risk of radiation-induced cancer in radiation protection should never be used for risk estimation in individual patients treated with radiotherapy. Only results of dedicated studies in cancer patients treated with radiotherapy provide reliable risk estimates, moreover, some may even provide evidence on which treatment plan optimisation can be based.Radiation-induced cancer can occur close to the PTV in the high-dose volume but also at very much lower doses in the <1% isodose. There is no evidence that the dose dependence of second cancer risk differs from the linear no-threshold equation up to the prescribed tumour dose range. The most critical organ in radiotherapy of cancer patients in the typical cancer age of >50 years with regard to radiation-induced second cancers is the lung. A significantly increased risk has been found for organ doses of < 1Gy as well as for local lung doses >40 Gy. The most critical organ in radiotherapy of cancer patients in young adults, adolescents and children is the female breast. Recent results of the follow-up of female patients after paediatric radiotherapy suggest that, in some clinical situations, the risk of radiation-induced breast cancer may be comparable to the risk of patients carrying a BRACA1 mutation so that systematic early detection procedures have to be recommended. The radiobiological mechanisms involved in the induction of second cancers which may determine the risk are very complex and vary between organs, dose levels and dose distributions, sex and age. Some mathematical models to estimate risk have been published but they are not compatible with the evidence arising from the results of recent clinical studies.

Wednesday June 10, 2015

15:30-15:40: Nicolaj Andreassen, Aarhus, Denmark

Recent activities and future plans of the International Radiogenomics Consortium (RGC)

Dept. of Oncology, Aarhus University Hospital, Aarhus, Denmark

The RGC was established in 2009 in order to foster collaborative research initiatives addressing possible associations between genetic variation and normal tissue toxicity. It currently has approximately 180 members from more than 100 institutions in 21 countries. The RGC has conducted two large individual patient data meta-analyses . The RGC TGFB1 meta-analysis included 2,782 breast cancer patients. Though the study was powered to detect a very small difference in normal tissue complication risk, no association was identified. The RGC ATM meta-analysis, by far the largest of its kind, included more than 30,000 toxicity assessments from 2,759 prostate cancer patients and 2,697 breast cancer patients. It demonstrated an impact of the ATM rs1801516 SNP that corresponds to an odds ratio of around 1.2 for late toxicity and 1.4 for acute toxicity. Six genome wide association studies (GWASs) have been carried out within the framework of or by members of the RGC. The largest of these studies included more than 3,500 patents. These studies have provided evidence that numerous SNPs affect risk of different types of normal tissue toxicity. Putative associations have been shown for SNPs in genes involved in steroid hormone metabolism, muscle regeneration, smooth muscle contraction, inflammation and body weight regulation. Thus, the studies may expand our understanding of the pathophysiology underlying normal tissue toxicity. The RGC recently obtained 6 million Euros of funding from the European Commission for the REQUITE project that will prospectively collect clinical data and biological specimens from 5,300 patients with prostate, breast or lung cancer in order to establish and validate predictive models. As part of a collaboration with the 'GameOn OncoArray project', the RGC has access to genome wide SNP genotyping at a very affordable cost (less than 50 £ per patient). The RGC is currently planning collaborative radiogenomics studies addressing head & neck cancer.

Wednesday June 10, 2015

15:40-15:50 Michael Baumann, Dresden, Germany

European Treatment Plan Data Bank – towards a leading research infrastructure for radiation oncology

Mechthild Krause 1,2,3,3, Thomas Skripcak 1,3, Monique Simon 1,3, Armin Lühr 1,3, Daniel Büttner 1,3, Steffen Löck 2,3,4, Michael Baumann 1,2,3,4

1 German Cancer Consortium (DKTK) Partner Site Dresden and German Cancer Research Center (DKFZ), Heidelberg, Germany; 2 Department of Radiation Oncology Medical Faculty and University Hospital Carl Gustav Carus, Technische Universität Dresden, Germany; 3 OncoRay – National Center for Radiation Research in Oncology Dresden, Germany, 4 Helmholtz-Zentrum Dresden-Rossendorf, Institute of Radiooncology, Dresden, Germany

It is long recognized that effects of radiotherapy on normal tissues and tumors depend on biological effective dose, irradiated volume and dose-distribution, as well as on dose-modifying internal and external factors. The effect of biological effective dose and dose distribution is of such overwhelming importance that it has been accepted as a surrogate marker in radiation oncology for decades. This surrogate marker is routinely applied in treatment planning and selection of the optimal treatment plan for individual patients as well as for design of treatment strategies for patient populations. Therefore treatment plan data bases, connected to basic clinical parameters and outcome parameters, may constitute a powerful resource for research in radiation oncology, similarly important as tissue banks or liquid biopsy repositories in other branches of oncology.

Several points need to be taken into consideration for European initiatives on state-of-the-art treatment plan data bases (TPDB). The most important include:

- TPDB need to be big, integrative, data-protected, ownership/reciprocity-based, and build on existing expertise and infrastructures. Treatment plans in individual patients are variable within and between centers. In addition overall oncology treatment strategies and patient populations may be extremely variable. In a time of personalized medicine this calls for stratification of patients based on clinical, biological and radiobiological/physical parameters for meaningful results. Therefore, to be powerful TPDB need to include very large data sets coming from many centers. As these centers will use different infrastructures for treament plan generation and application, as well as for storage, a European Research Infractructures needs to have the necessary interfaces to recruit and analyse such data of different sources. Beside a dynamic technical basis, ontology and harmonization processes by the medical community are mandatory. Patients, their advocates and national as well as European law mandate elaborated safety rules for data protection, and a transnational initiative is even more complex than national registers. Ownership and reciprocity are important considerations, as all academic institutions and research networks contributing to a large scale infrastructure wish to keep their rights for research and publication. Last not least some well functioning regional or national data bases are already established and it would be extremely counterproductive to re-invent the wheel.
- TPDB must be user friendly, without (or better with little) additional efforts e.g. duplication of entry functions, and idealy must provide added value for everybody involved in this task.
- TPDB must be able to communicate with other TPDBs (national, international, registers of prospective trials, etc)

- TPDB must include latest search and cross-link technologies (e.g. data warehouse functions)
- TPDB must be able to access latest analysis tools and to submit the results of such analysis back tot he individual institutions which provided the base-data
- TPDB must be low cost, web-based and open access. A community of developers should be established around this infrastructure
- To fully integrate TPDBs in an information science environment for „Systems Radiation Oncology Research“, TPDB need highly developed links to outcome data, to spatially resoluted outcome data (imaging), and to biological data-bases including high-throughput technologies.

The talk will review the aim of TBDBs, some of these requirements and the current state of development of such initiatives within Europe.

Wednesday June 10, 2015

15:50-16:00: Azza Khalil, Aarhus, Denmark

New dose constraint reduce radiation-induced pneumonitis in locally advanced NSCLC treated with Intensity-Modulated Radiotherapy

Azza A. Khalil1, Lone Hoffmann2, Ditte S. Møller2, Katherina P. Farr1, Marianne M. Knap1. 1 Department of Oncology and 2 Department of Medical Physics, Aarhus University Hospital

Introduction: Intensity Modulated Radiotherapy (IMRT) in locally advanced NSCLC allows treatment of patients (pts) with large tumour volumes but normal tissue damage particularly radiation pneumonitis (RP) remains a limiting factor. The incidence of sever RP using 3D conformal radiotherapy (CRT) in our department was 16.4%, 2% of which was lethal. The aim of this study was to prospectively monitor the normal tissue complications following the introduction of IMRT in our clinic. Material and Methods: IMRT technique was introduced in 2011 and monitored in three phases. In phase I, 12 pts were treated using only one dose contraint (V20) in which the total lung volume receiving 20 Gy was limited to 40%. In phase II, 25 pt were treated with an additional dose constraint of Mean Lung Dose (MLD) ≤19 Gy. In phase III, 50 pt were treated with an additional dose constraint (V5) in which the total lung volume receiving a dose of 5 Gy should not exceed 60%. Patients were continuously monitored and the incidence of RP documented. The results of pts in phase I &II (IMRT-1) were compared to pts in phase III (IMRT-2) as well as with a matching group of pts treated with CRT in 2007-2010. Results: The median follow up time was 17 months. IMRT was delivered using 4 to 8 beam arrangements. Introducing IMRT led to an increase in the incidence of RP to 30%, 16% of which were lethal (IMRT-1). Introducing the dose constraint V5, generally lead to a significant reduction in the dose delivered to the lungs and heart. The lung volume receiving low doses <20 Gy significantly decreased from 51±2% to 41±1% ($p<0.0001$). Introducing V5 constrain in IMRT-2 did not significantly decrease the incidence of severe (grade≥3) RP but significantly decreased the lethal pneumonitis to <5% ($p=0.029$). Conclusion: Prospectively monitoring patients and introduction of new constraint as regards the volume of lung receiving low doses can help reduce the incidence of severe lethal radiation pneumonitis.

Wednesday June 10, 2015

16:00-16:10: Marciana Nona Duma, Münich, Germany

Tangential field radiotherapy for breast cancer: the dose to the heart and heart subvolumes

Marciana Nona Duma, M.D.1, Anne-Claire Herr, 1,2, Markus Oechsner, PhD 1, Stephanie Elisabeth Combs, M.D. 1, Klaus Rüdiger Trott, 1,3, Michael Molls, M.D. 1

1: Department of Radiation Oncology, Technische Universität München, Klinikum rechts der Isar, Germany
2: Medical School, Technische Universität München, Germany
3: Cancer Institute, University College of London, London

Purpose/Objectives: The aim of the present study was to analyze the heart doses in patients treated with 3D-conformal radiotherapy (3D-CRT) by tangential fields in half beam technique. The aim is to relate dose distribution within the different heart structures with late radiation induced heart injury assessed by non invasive functional imaging.. Material/Methods: From March 2009 to November 2010 201 patients were treated with conventional 3D-CRT for left sided breast cancer. All planning CTs were reviewed and patients were visually divided into two groups. Patients with a large dose to the heart (87 patients) and patients with a low dose to the heart (114 patients). Out of these two groups we chose a representative sample of 46 patients, 22 with a high dose (HiD) an 24 with a low dose(LoD) to the heart. The heart, the left ventricle, the left anterior descending artery (LAD), the right coronary artery (RCA) and the ramus circumflexus (RCX) were contoured. A helper structure (HS) in the LAD region was generated. We analyzed the mean dose (Dmean), the maximum dose (Dmax) and the V10, V20, V30, V40, the length of the LAD that received 20Gy and 40Gy. Average±standard deviations and Pearson correlations are presented. Results: The two groups had a significant different Dmean of the heart ($p<0.001$). The average Dmean to the whole heart was 4.0±1.3Gy (HiD) and 2.3±0.8Gy (LoD), respectively. The average Dmean to the LAD/HS was 26.2±7.4Gy / 23.3±6.9Gy (HiD) and 13.0±7.5Gy / 13.0±7.2Gy (LoD). The length of the LAD that received 20Gy / 40Gy was 4.5±1.8cm / 2.9±2.3cm (HiD) and 1.9±1.7cm / 0.7±1.1cm (LoD). Conclusion: Even a rough contouring of the LAD region (i.e helper structure) provides clinically valuable information on the LAD dose. The Dmean heart is not always a good surrogate parameter for the dose to the LAD. It might underestimate clinically significant doses in 1/3 of the patients in LoD group.

Wednesday June 10, 2015

16:10-16:20: Laura Tuomikoski, Helsinki, Finland

Post-RT saliva production can be predicted by measuring pre-RT salivary function and mean glandular doses

Tuomikoski L, Kapanen M, Collan J, Keyriläinen J, Loimu V, Seppälä T, Saarilahti K, Tenhunen M. HUCH Cancer Center, Department of Radiation Oncology, Helsinki University Central Hospital, Helsinki, Finland

Introduction: A predictive model to evaluate stimulated post-RT salivary function was validated for 70 patients undergoing IMRT for cancer of the head-and-neck region. Materials and Methods: Tc-99m-pertechnetate scintigraphy of salivary gland ejection fraction (sEF) and direct measurement of total stimulated saliva output F_{stim} were performed for 70 patients before RT and both 6 (70 patients) and 12 months (50 patients) after RT. The input parameters for the predictive model were 1) the total stimulated saliva output F_{stim} before RT, 2) the mean dose D_{mean} for the major salivary glands and 3) the proportion of single gland saliva output of the total saliva production m_i defined by scintigraphy. Thus, the salivary flow 6 months after RT was modelled by equation

$$F_{stim}(t) = F_{stim}(0) \cdot \sum_i m_i \cdot rEF(D_{mean,i}) ,$$

where $rEF(D_{mean,i})$ is the population-based sigmoidal dose-response function. The values of salivary flow predicted by the model were compared to measured values of saliva secretion 6 months after RT. In addition, the measured relative ejection fraction (rEF_{meas}=sEF(post-RT)/sEF(pre-RT)) values were evaluated among the patients to detect variations possibly related to the individual radiosensitivity. For this purpose the distances $d_i=rEF_{meas,i}$-rEF(Dmean,i) of glandular rEF_{meas} values from mean dose-response curve were recorded. Results: A significant correlation ($r=0.83$, $p<0.001$) was found between the modelled and the measured values of stimulated salivary flow 6 months after RT. Some patients showed systematically large $|d|$ values for both left and right parotid glands. For most of these patients scintigraphy was repeated 12 months after RT, where it was seen that the large deviations from the mean dose-response curve remained. Conclusions: The predictive model can be used for the evaluation of post-RT salivary flow. The detected systematic deviations from mean dose-response curve may reflect individual differences in radiosensitivity.

Wednesday June 10, 2015

16:20-16:30: Line Schack, Aarhus, Denmark

SNP analysis on late radiation induced toxicity analyzed by questionnaires and anal physiological methods in prostate cancer patients.

Schack LH (1), Petersen SE (2), Lundby L (3), Høyer M (2), Bentzen L (2), Overgaard J (1), Andreassen CN (2), Alsner J (1). 1) Department of Experimental Clinical Oncology, Aarhus University Hospital, Denmark. 2) Department of Oncology, Aarhus University Hospital, Denmark. 3) Department of Surgery P, Aarhus University Hospital, Denmark.

Introduction: From a previous study we have access to a cohort of 42 prostate cancer patients with clinical data for radiation induced toxicity measured by anal physiological methods and validated questionnaires. Eleven single nucleotide polymorphisms (SNPs) have previously been suggested to be predictive of different late radiation induced toxicity endpoints by GWAS studies or candidate gene studies. This study aimed to test each of the eleven SNPs against the particular physiological data and questionnaire data corresponding to the endpoints previously reported to be associated with each SNP. Materials and methods: Patients received EBRT 70-78 Gy for prostate cancer. Functional toxicity endpoints include Vienna Rectoscopy Score (VRS) (teleangiectasia, congested mucosa and ulceration) and maximum resting pressure (MRP) of anal sphincters. An RT-AnoRectal Dysfunction score (RT-ARD) was obtained from questionnaires. For each SNP, the reported risk allele was identified and the number of risk alleles was correlated to physiological data and questionnaire data corresponding to the endpoints published. Results: For two SNPs, all patients were homozygous and could not be tested against morbidity endpoints. Significant Spearman's rank correlations were found between rs1801516 (ATM) and RT-ARD score ($\rho = 0.31$, $p = 0.049$), MRP ($\rho=-0.31$, $p = 0.045$), and the questionnaire endpoint "incontinence for loose stools" ($\rho = 0.42$, $p = 0.005$). rs1800469 (TGFB1) was significantly associated with congested mucosa ($\rho = 0.38$, $p = 0.019$) but not the questionnaire endpoint "mucus in stool" ($\rho = 0.12$, $p = 0.43$). The seven other SNPs were not statistically correlated to the endpoints hypothesized. Conclusion: Weak correlations were found between SNP rs1801516 (ATM) and RT-ARD, MRP and "incontinence for loose stools" as well as between SNPs rs1800469 (TGFB1) and congested mucosa and "mucus in stool". We could not reproduce correlations between the remaining SNPs and endpoints tested.

Wednesday June 10, 2015

16:30-16:40: Camilla Stokkevåg, Bergen, Norway

Risk of radiation-induced secondary rectal and bladder cancer following radiotherapy of prostate cancer

Stokkevåg CH (1,2), Engeseth GM (1), Hysing LB (1), Ytre-Hauge KS (2), Ekanger C (1), Muren LP (3). 1 Department of Oncology and Medical Physics, Haukeland University Hospital, Bergen, Norway. 2 Department of Physics and Technology, University of Bergen, Bergen, Norway. 3 Department of Medical Physics, Aarhus University Hospital, Aarhus, Denmark.

Introduction: An elevated risk of radiation-induced secondary cancer (SC), particularly in directly irradiated tissues such as the bladder and rectum, has been observed in prostate cancer patients after radiotherapy (RT), rising to as high as 1 in 70 with more than ten years follow-up. In this study we have estimated SC risks following RT with both previous and contemporary techniques, including proton therapy, using risk models based on different dose-response relationships. Materials and methods: RT plans treating the prostate and seminal vesicles with either conformal RT (CRT), volumetric modulated arc therapy (VMAT) or intensity-modulated proton therapy (IMPT) were created for ten patients. The risks of radiation-induced cancer were estimated for the bladder and rectum using dose-response models reflecting varying degrees of cell sterilisation: a linear model, a linear-plateau model and a bell-shaped model also accounting for fractionated RT. Results: The choice of risk models was found to rank the plans quite differently, with the CRT plans having the lowest SC risk using the bell-shaped model, while resulting in the highest risk applying the LNT model. Considering all dose-response scenarios, VMAT resulted in up to twice as high risk compared to IMPT. Risks of radiation-induced bladder cancer were five times higher if exposed at 50 relative to 80 years. Conclusions: The SC risk estimations for the bladder and rectum revealed no clear relative relationship between the contemporary techniques and CRT, with divergent results depending on choice of model. However, the SC risks for these organs when using IMPT were lower or comparable to VMAT. SC risks should be assessed when considering referral of prostate cancer patients to proton therapy, taking also general patient characteristics such as age into account.

Wednesday June 10, 2015

16:40-16:50: Laura Rechner, Copenhagen, Denmark

Risk-optimized proton therapy treatment planning to minimize second cancers after radiotherapy of the prostate

Laura A. Rechner1,2, John G. Eley1, Rebecca M. Howell1, Rui Zhang1,3, Dragan Mirkovic1, and Wayne D. Newhauser1,3,4. 1 Dept of Radiation Physics, The University of TX MD Anderson Cancer Center, 2 Dept of Oncology, Section Radiotherapy, Rigshospitalet, 3 Dept of Physics and Astronomy, Louisiana State University, 4Dept of Medical Physics, Mary Bird Perkins Cancer Center

Introduction Proton therapy reduces the predicted risk of second cancer compared with photon therapy. However, no previous studies have directly optimized beam angle or fluence for proton therapy to further minimize those risks. The objectives of this study were to demonstrate the feasibility of risk-optimized proton therapy (ROPT) and to find the plan with the minimum risk of second cancer in the bladder and rectum for a prostate cancer patient with and without consideration of normal tissue (NT) constraints for acute toxicity. Methods We used 6 risk models to predict the excess relative risk (ERR) of second cancer in the bladder and rectum. One risk model incorporated the effects of fractionation, initiation, inactivation, repopulation, and promotion (iirp model) (Shuryak et al Rad. Env. Bio. 2009 I & II, 2011), and the other risk models spanned a range of simplified relationships ranging from linear-exponential to linear-non-threshold (NRC 2006, Rechner et al PMB 2012). Initial plans were created using a commercial treatment planning system to produce the input data for the in-house risk-optimizer. Results The iirp model selected anterior and lateral beams, resulting in an ERR of 0.73 in the bladder and 0.14 in the rectum, which was a reduction of 21% for the bladder and 30% for the rectum compared to the lateral-opposed beam arrangement. When the linear-exponential model with a maximum risk at 10 Sv was used, the same ROPT plan was selected as for the iirp model. When all other models were used, the ROPT plan was a lateral-opposed pair. When NT constraints were ignored, different ROPT plans were selected that did not meet the constraints. Conclusions We conclude that ROPT planning is feasible and that, for the iirp model, the ROPT plan for a prostate cancer patient reduced the predicted risk of second cancer. We also conclude that applying NT constraints is required during ROPT planning. Future research is needed to validate the risk models.

Wednesday June 10, 2015

16:50-17:00: Britta Weber, Aarhus, Denmark

Long-term outcomes and toxicity after proton beam radiotherapy of large non-peripapillary choroidal melanoma

Weber B, Paton K, Ma R, Pickles T. Department of Oncology, Aarhus University Hospital, Aarhus Denmark, Department of Ophthalmology and Visual Sciences, Vancouver Hospital Eye Care Center, Vancouver, British Columbia, Canada, Radiation Oncology, BCCA, Vancouver, Canada

Background: To report on outcomes and toxicity after proton beam radiotherapy for large non-peripapillary choroidal melanoma considered unsuitable for other eye-sparing therapies in Canada. Materials and Methods: We included patients with non-peripapillary tumors (>2mm from the optic disc) treated with proton therapy at TRIUMF, the only ocular proton therapy facility in Canada, from 1995-2013. An existing database including patient, tumor, and treatment characteristics was updated with ocular complications and follow up status from chart reviews. Results: In total, 77 patients were included in the analysis. The median age was 60 years and the median observation time 47 months (0-221 months). More than half of the patients (53%) had a tumor located anterior to the equator and 35% had involvement of the ciliary body. The median tumor diameter was 13.6 mm and the median thickness was 7.1 mm. The 5 -(10) year actuarial rate was 85 (85)% for ocular tumor control, 72 (57)% for metastasis-free survival, 77 (63)% for overall survival, 22 (22)% for enucleation and 38 (38)% for complete blindness. 80% of patients with blindness had developed neovascular glaucoma. For patients with good vision (≥20/50) at baseline, the 5-(10) year actuarial rate was 40 (40)% for conservation of vision of 20/50 or better, 44 (44)% for conservation of vision of 20/200 or better and 67 (67)% for conservation of vision of counting fingers or better. On univariate analysis, patients with ciliary body involvement had significant worse metastasis-free survival and overall survival rates compared to patients without ciliary body involvement ($p<0.001$). Conclusions: Proton therapy resulted in acceptable local control and survival rates in patients with large anteriorly located tumors. The risk of complete blindness and severe toxicity requiring enucleation was low and a substantial proportion maintained a useful vision.

Session 3: Recent developments in functional imaging

Thursday June 11, 2015

8:00-8:20: Uulke van der Heide, Amsterdam, The Netherlands

Recent developments in quantitative imaging for radiotherapy.

Uulke van der Heide. The Netherlands Cancer Institute, Department of Radiation Oncology, Amsterdam, The Netherlands.

MRI is increasingly used in radiotherapy for its superior soft-tissue contrast. In particular T2-weighted MRI scans are now used widely to facilitate tumor delineation for radiotherapy treatment planning. Increasingly, also functional techniques such as diffusion-weighted MRI (DWI) and dynamic contrast-enhanced (DCE-) MRI are added to an MRI exam. A key advantage of these techniques is that they provide quantitative data. DWI produces an ADC map, and DCE-MRI results in parameter maps reflecting tracer kinetics. T1 and T2-weighted MRI can also be replaced by T1 and T2 mapping, quantifying the relaxation times. This facilitates comparison of imaging results between institutes and scanner types. Within a multicenter project using quantitative MRI for imaging cancer in the prostate, we tested the consistency of sequences that were optimized for each scanner. Consistent quantification with a bias of a few percent between different scanners and institutes was feasible for T2 mapping, as well as for diffusion-weighted MRI. With newer scanners and sequences, typically more precise results were obtained. For radiotherapy this is particularly interesting. A key property of RT that sets it apart from other treatment modalities of cancer, is the capacity to spatially modulate the level of radiation dose within a treatment depending on the presence of macroscopic tumor (GTV) or microscopic disease (CTV). We can expand this concept by modulating the dose based on the probability of tumor presence. For prostate cancer, we used data from multiple quantitative MRI techniques to create a map reflecting the tumor probability. With radiobiological modeling this can be converted directly into a dose prescription, where the dose in modulated based on the likelyhood of tumor presence. Validation of this approach is in progress.

Thursday June 11, 2015

8:20-8:40: Karin Haustermanns, Leuven, Belgium

The role of functional imaging and molecular markers for organ-preserving strategies after chemo-radiation for rectal cancer

Joye I, Debucquoy A, Haustermans K. KU Leuven - University of Leuven, Department of Oncology, Leuven, Belgium

Nowadays chemoradiation followed by surgery is the standard treatment for locally advanced rectal cancer. The response to this preoperative treatment is highly heterogeneous: while 15-27% of the patients achieve a pathological complete response (pCR), a partial response is seen in 54-75% and the remaining tumors show no response at all. The advent of highly-conformal RT techniques such as Volumetric Modulated Arc Therapy (VMAT) allows clinicians to precisely irradiate the target volume while minimizing the dose to the organs at risk. In rectal cancer radiotherapy, VMAT is well-known for its superiority over 3D-conformal radiotherapy regarding sparing of the bowel structures. The better sparing of the bowel structures facilitates dose escalation, which can in turn contribute to a better tumoral response. Patients who achieve a pCR have a favorable long-term outcome with excellent local control and disease-free survival, regardless of their initial T- and N-stage. This observation raises the question as to whether invasive surgery could be avoided in a selected cohort of patients who obtain a good clinical response to preoperative RCT. In this respect, there has been growing interest in functional imaging techniques as diffusion-weighted MRI (DW-MRI) and 18F-FDG PET/CT. Up to now, DW-MRI and 18F-FDG PET/CT as sole modalities are not accurate enough to safely select patients for organ-sparing strategies. Combination of different imaging modalities at various time points and the integration of multimodal imaging with clinical data and molecular biomarkers might contribute to safely select candidates for organ-preserving strategies.

Thursday June 11, 2015

8:40-8:50: Niels Raaijmakers, Utrecht

Validation is crucial in head and neck translational imaging research

Terhaard C.H.J.(1), Philippens M.E.P. (1), Jager E.A.(1), Schakel T.(1), Caldas-Magalhaes J. (1), Ligtenberg H. (1), Kasperts NKA (1), Pameijer F.A. (2), Willems S.M. (3), Raaijmakers C.P.J (1). University Medical Center Utrecht, the Netherlands, Department of Radiotherapy (1), Department of Radiology (2), Department of Pathology (3).

Introduction: Delineation of the tumor, based on imaging, is the weakest link in radiotherapy. The value of new and existing imaging techniques should be demonstrated by comparison with the ground truth: histopathology. Total laryngectomy specimens (TLE) are an appropriate model, since the resected tissue remains cohesive. Materials & Methods: For 30 patients who received TLE because of cancer, before surgery PET, CT and MRI images were made in a radiation mask. After surgery, a CT scan was made of the fixated specimen. The specimen was sliced and digitally reconstructed in 3D and registered to the CT, MRI and FDG-PET scan. DW MRI scans were performed in some but not all patients. CT and MR were delineated by three observers, for the PET scan manual delineation was compared with automatic delineation. Results: Comparative examination between 3 pathologists revealed a slight variation with respect to tumor delineation. Variation between the three observers for the CT and MRI delineations was much larger. The average volume on CT as well as on MRI was twice as large as the gold standard. Automatic delineations using FDG-PET, had the least tumor overestimation, but also some underestimation. To reduce tumor volume overestimation in MRI, guidelines were drawn up for tumor definition based on the guidelines of Becker for cartilage invasion. The histological background of DWI, was determined by correlating ADC with histological variables. ADC values appeared significantly correlated with cellularity, stromal component, and nuclear-cytoplasmic ratio. EPI based DWI was not feasible for tumor delineations due to geometrical distortions.
Conclusion: The current practice of tumor delineation using CT, PET and MRI results in significant tumor volume overestimation. The GTV-CTV and, thereby, the chance of complications could be significantly reduced by improving tumor definition Image validation studies are a recommended tool to develop evidence based delineation guidelines.

Thursday June 11, 2015

8:50-9:00: Haley Clark, Vancouver, Canada

Preliminary findings using dynamic contrast-enhanced magnetic resonance imaging to identify functional aspects within the parotid

Clark H D, Moiseenko V, Rackley T, Thomas S, Wu J, Reinsberg S. Department of Physics and Astronomy, University of British Columbia, Vancouver, Canada. Department of Medical Physics, British Columbia Cancer Agency, Vancouver, Canada.

Introduction: Radiotherapy-induced salivary function loss impacts strongly on quality of life. Presently used consensus guidelines for parotid gland sparing assume it is a parallel organ and that mean dose is the strongest predictor of functional loss. In recent years evidence has mounted to suggest heterogeneity of functional burden distribution among tissues within the parotid. Conclusive proof and underlying mechanisms are yet to be established. Preliminary findings of a novel approach for identifying functionally dominant tissues using dynamic contrast-enhanced magnetic resonance imaging are described. Methods: Dynamic contrast-enhanced magnetic resonance images (3D, T1-weighted, gradient echo, 600s duration, 3.8s resolution) were collected on a 3T scanner with an intravenously administered gadolinium agent. Salivation was induced 120s after contrast injection using a citric acid solution. Contrast agent time courses C(t) were constructed by averaging neighbouring voxels. Both intra- and inter-tissue variations were inspected. Results: The average normalized running variance of C(t) over the full 600s scan demonstrates clear distinction in tissue contrast dynamics and apparent stimulatory response. Parotid was significantly distinct from masseter and pharynx tissues (Wilcoxon sign-rank test $p < 0.0001$); masseter and pharynx were not ($p = 0.07$; two-tailed t-test $p = 0.72$). Anterior and posterior aspects of right parotid were distinct (Wilcoxon $p < 0.001$). Large variations were observed during initial contrast uptake and following 10-30s after stimulation. Nearby tissue stimulatory response occurs later and with reduced amplitude. Conclusions: Salivary action appears to be detectable. Probing by inducing salivary secretion during imaging is a novel technique that has potential to non-invasively identify functionally dominant regions suitable for radiotherapy sparing techniques. The efficacy of normal tissue avoidance could be boosted using this information.

Thursday June 11, 2015

9:00-9:10: Catharina Zegers, Maastricht, The Netherlands

Imaging of tumor hypoxia and metabolism in patients with head and neck squamous cell carcinoma

Catharina M.L. Zegers1, Frank Hoebers1, Wouter van Elmpt1, Michel C. Öllers1, Felix M. Mottaghy2, Philippe Lambin1. 1 Dept. of Radiation Oncology (MAASTRO) and 2 Dept. of Nuclear Medicine, MUMC, Maastricht, The Netherlands

Introduction: Tumor hypoxia and a high tumor metabolism increase radioresistance in patients with head and neck cancer. The aim of this study was to evaluate the correlation between hypoxia [18F]HX4 and metabolic [18F]FDG PET uptake. Materials and methods: HX4 and FDG PET/CT images of 20 HNSCC patients were acquired prior to radiotherapy, in an immobilization mask, with a median time interval of 7d (NCT01347281). Gross tumour volumes of the primary lesions (GTVprim) and pathological lymph nodes (GTVln) were included in the analysis. The standardized uptake values (SUVmax, SUVmean) within the GTVs were determined. The hypoxic fraction (HF) defined as the fraction of the GTV with a tumor-to-muscle ratio TMR>1.4 was calculated. Additionally, FDG PET/CT images were rigidly registered to the HX4 PET/CT images to compare the spatial uptake pattern. Pearson's correlation coefficients were calculated. Results: PET/CT scans including 20 GTVprim and 12 GTVln were analyzed. There was a significant correlation between the tumor volume and the HX4 parameters SUVmax ($R=0.39$, $P=0.03$), TMR ($R=0.62$, $P<0.001$), HF ($R=0.52$, $P<0.01$) and FDG parameters SUVmean ($R=0.39$, $P=0.03$) and SUVmax ($R=0.50$, $P<0.01$). There was also a significant correlation between all FDG and HX4 parameters, with the most pronounced correlation between FDG SUVmean and HX4 TMR ($R=0.61$, $P<0.001$). Voxel wise comparison of the HX4 and FDG uptake within the GTVs showed a large diversity for the primary lesion ($R=0.47\pm0.31$, range -0.04 to 0.85), whereas a good correlation was observed for the lymph nodes (0.73 ± 0.12 range: 0.59 to 0.91). Conclusions: There is a correlation between HX4 and FDG uptake parameters on a global tumor level. On a voxel level there is a good spatial correlation between HX4 and FDG uptake for the lymph nodes, but this is less pronounced for primary lesions. These complementary imaging data allow the characterization of radioresistant tumor volumes that can be used for radiotherapy dose-painting.

Thursday June 11, 2015

9:10-9:20: Ane Iversen, Aarhus, Denmark

Metabolic imaging: the potential of [1-^{13}C]lactate/[1-^{13}C]pyruvate ratio to be a surrogate marker for hypoxia in hyperpolarized magnetic resonance spectroscopy

Ane B Iversen1, Steffen Ringgaard2, Christoffer Laustsen2, Hans Stødkilde-Jørgensen2, Morten Busk1 and Michael R. Horsman1. 1) Department of Experimental Clinical Oncology, Aarhus University Hospital, Noerrebrogade 44, Blgd. 5, 8000 Aarhus C, Denmark 2) Institute for Clinical Medicine - The MR Research Centre, Palle Juul-Jensens Boulevard 99, 8200 Aarhus N, Denmark

Introduction: Hypoxic tumor cells are treatment resistant; therefore, identification of hypoxia is crucial. Hyperpolarized magnetic resonance spectroscopy (HPMRS) is a new technique that allows measurement of biochemical reactions in vivo and it has been suggested that the conversion of pyruvate to lactate, may allow non-invasive identification of hypoxia. The aim of the study was to investigate this potential. Materials and methods: C3H mammary carcinomas grown to a volume of 200 mm3 in the right foot of a female CDF1 mouse were used. Non-anaesthetized mice were gassed (air, 10% or 100% oxygen) prior to and during all measurements. Oxygen partial pressure (pO2) was measured using an Eppendorf oxygen electrode. The probe was inserted in the tumor with an average of 5 repeated parallel insertions giving a mean number of 63 pO2 values. The endpoint was the percent of pO2 values ≤5 mmHg. Additional mice were transferred to a 9.4 T MRI and through an intravenous line hyperpolarized [1-^{13}C]pyruvate, prepared in a Spinlab, was injected and HPMRS performed. The ratio of [1-^{13}C]lactate/[1-^{13}C]pyruvate was calculated using iNMR. Statistical comparisons were done using a Student's t-test ($p < 0.05$). Results: The Eppendorf measurements resulted in a mean (with 1 S.E.) of 36 % (30-43) values ≤ 5 mmHg in air-breathing mice. This was significant reduced to 9% (3-14) with 100% oxygen breathing and increased to 72% (62-81) under 10% oxygen. The mean (with 1 S.E.) HPMRS lactate/pyruvate ratio was 35 (32-38) in air-breathing mice and non-significantly changed to 40 (36-44) under 100% oxygen. Conclusions: The Eppendorf measurements clearly showed that breathing 100% oxygen increased oxygenation status, while it decreased with 10% oxygen. However, no change was observed during 100% O2 breathing using HPMRS; this may be due to the excessive production of lactic acid even in well-oxygenated tumor cells (Warburg effect), which may limit the influence of oxygen pressure on glycolytic flux.

Thursday June 11, 2015

9:20-9:30: Joachim Chan, Wirral, United Kingdom

Dose painting radiotherapy for high risk prostate cancer: delayed 18F-choline PET/CT imaging before neo-adjuvant hormone therapy improves detection rates

Chan J. (1)(2), Mahmood S. (1), Brunt J.N.H. (1), Vinjamuri S. (3), Syndikus I. (1). (1) Clatterbridge Cancer Centre NHS Foundation Trust, Wirral, UK; (2) Institute of Translational Medicine, University of Liverpool, UK; (3) Royal Liverpool and Broadgreen University Hospitals NHS Trust, Liverpool, UK.

Introduction: We have compared the size of dominant intraprostatic lesions (DILs) identified on 18F-choline PET/CT before and during hormone treatment in high-risk prostate cancer patients. Materials and Methods: As part of the BIOPROP trial (NCT02125175), delayed 18F-choline PET imaging (60 and 90 min uptake time) has been performed on 28 patients prior to and 12 patients during hormone treatment. Functional MRI was used as the reference standard. DILs were outlined on both scans. Volumes were compared by paired 2-tail T-test. Results: For all 40 patients, mean age was 66 (49-77), mean PSA was 15.3 (3.6-59.1), median Gleason was 7 (6-9), staging T2 in 14 patients and T3 in 26 patients. PET imaging prior to treatment identified a DIL in all 28 patients, but 1 had no DIL on MRI (PET DIL volume was 4.20 ml). Of 27 patients in whom DIL could be identified on both PET and MRI, mean PET DIL and MRI DIL volumes were 2.97 ml (SD 2.05) and 2.66 ml (SD 1.64) respectively ($p = 0.44$). Of note, 5 patients had unexpected PET uptake in pelvic lymph nodes. For 12 patients, PET imaging was performed after starting hormone therapy, with mean time to PET scan of 93 days (42-193). A DIL could not be identified by PET in 4 patients (mean MRI DIL volume was 2.33 ml, SD 1.79). Of the other 8 patients, mean PET DIL and MRI DIL volumes were 1.85 ml (SD 2.01) and 4.79 ml (SD 5.46) respectively ($p=0.06$). Conclusions: Compared to functional MRI, intra-prostatic tumour lesions are similar in size on 18F-choline PET/CT with delayed imaging time if performed before hormonal therapy. The sensitivity and detection rate is reduced if patients have already commenced hormone therapy. Therefore PET imaging for dose-painting radiotherapy planning in high-risk prostate cancer patients should be performed before anti-androgen treatment.

Thursday June 11, 2015

9:30-9:40: Endre Grøvik, Oslo, Norway

Feasibility of multi-echo dynamic MRI for simultaneous acquisition of T1-weighted and R2* contrast kinetics in rectal cancer

Grøvik E., Redalen KR., Melles WA., Gjesdal KI.. The Intervention Centre, Oslo University Hospital, Oslo, Norway. Department of Oncology, Akershus University Hospital, Lørenskog, Norway. Department of Radiology, Akershus University Hospital, Lørenskog, Norway. Sunnmøre MR-klinikk, Ålesund, Norway

Introduction: In rectal cancer, the use of conventional MRI is established. However, integration of functional MRI, enabling quantitative assessment of intratumoural biological and -physiological characteristics, may provide a more comprehensive depiction of tumour aggressiveness and may be valuable for further developments of individualised, multimodal treatment. We have evaluated the feasibility of a novel split dynamic MRI technique acquiring both high spatial and multi-echo high temporal resolution data during a single bolus injection, enabling assessment of T1-weighted and R2* contrast kinetics. Materials and methods: Simulations were performed to evaluate the accuracy of the split dynamic technique and to identify temporal sampling requirements for accurate estimation (relative error ± standard deviation less than 10%) of quantitative kinetic parameters. Subsequently, the technique was implemented and optimised on a 1.5T Philips Achieva MR scanner and evaluated in rectal cancer patients enrolled in the prospective study OxyTarget (NCT01816607). Results: Simulations revealed a required temporal resolution of 13, 16 and 4 seconds for accurate estimation of Ktrans, ve and vp, respectively. For accurate measurement of peak change in R2*, simulations suggested a sampling interval between 2 and 6 seconds. Optimisation of sequence parameters minimized susceptibility and saturation effects and provided high image quality. Intriguingly, we identified the peak change in R2* as a particularly interesting parameter, being high in malignant lesions and low or absent in benign lesions. Conclusions: A single bolus multi-echo split dynamic MRI technique has, for the first time in rectal cancer, been optimised for use in staging and evaluation of response to neoadjuvant chemoradiotherapy. This technique enables detailed assessment of dynamic T1-weighted and R2* contrast kinetics, yielding comprehensive additional information on pathophysiological processes in rectal cancer.

Thursday June 11, 2015

9:40-9:50: Katherina Farr, Aarhus, Denmark

Perfusion SPECT imaging and radiation-induced injury in the lung after curative radiotherapy for NSCLC

Farr KP, Khalil AA, Møller DS, Bluhme H, Kramer S, Morsing A, Grau C. Department of Oncology, Department of Medical Physics and Department of Nuclear Medicine and PET Centre Aarhus University Hospital, Aarhus Denmark

Introduction: Curative radiotherapy (RT) for non-small-cell lung cancer (NSCLC) gives a large dose to the surrounding normal lung tissue, resulting in regional lung damage and leading to clinically significant complications. The purpose of the study was to assess dose and time dependence of RT-induced changes in regional lung function measured with single photon emission computed tomography (SPECT) of the lung. Materials and Methods: NSCLC patients scheduled to receive RT of minimum 60 Gy were included prospectively in the study. Lung perfusion SPECT/CT was performed before and 1, 3, 6 and 12 months after RT. Reconstructed SPECT/CT data were fused to the RT planning CT using MIM Software. RT dose to the whole lung was segmented into regions corresponding to 0-5, 5-20, 20-40, 40-60 and over 60 Gy. Fractional lung function in these regions was calculated from SPECT before and serially after RT. Changes (%) in regional lung perfusion were correlated with regional dose. Results: A total of 71 patients were included. Fifty three had 1 and 3 months follow-up (FU) scans, 44 had 6 months FU scan, and 29 had 12 months FU scans. Preliminary analysis of 20 patients showed a statistically significant dose-dependent reduction in regional perfusion at 3 months FU. Largest relative decrease in lung perfusion was at dose region receiving 40-60 Gy (46 %). Dose regions of 20-40 Gy and >60 Gy had perfusion reduction of 22 and 35 % respectively. Lung regions receiving low dose of 0-5 Gy and 5-20 Gy had corresponding increase in relative lung perfusion (3.3 and 1.3 % respectively). Analysis of the whole patient cohort at different time points after RT is underway. Conclusion: Our analysis suggests that following RT perfusion lung function changes in a dose-dependent manner. Lung regions receiving high dose demonstrate a decrease in relative function with a corresponding though much smaller increase in regions receiving low dose, possibly due to function being shunted to these areas.

Thursday June 11, 2015

9:50-10:00: Søren Møller, Copenhagen, Denmark

Early changes in perfusion of Glioblastoma during radio- and chemotherapy evaluated by T1*-dynamic contrast enhanced MRI

Møller S (1), Lundemann M (1), Law I (2), Poulsen HS (1,3), Larsson HBW (1,4), Engelholm SA (1). (1) Dept. of Oncology, Rigshospitalet, Copenhagen. (2) Department of Clinical Physiology, Nuclear Medicine & PET, Rigshospitalet, Copenhagen. (3) Dept. of Radiation Biology, Rigshospitalet, Copenhagen. (4) Functional Imaging Unit, Glostrup Hospital

Introduction: The survival times of patients with glioblastoma differ widely and biomarkers that would enable individualized treatment are needed. The objective of this study was to measure tumor perfusion using T1*-dynamic contrast enhanced MRI (DCE-MRI) in patients with glioblastoma during early stages of radio- and chemotherapy (Tx) and identify possible biomarkers of treatment outcomes. Materials and methods: An exploratory prospective study was planned. Patients underwent DCE-MRI at baseline, after approximately 1- and 6 weeks of Tx and 3- and 6 months post Tx. DCE-MRI at 3 Tesla generated maps of cerebral blood flow (CBF) cerebral blood volume (CBV), permeability (CBKi) and volume of distribution (CBVd) using a combination of model-free deconvolution and Patlak plots. Regions of interest in contrast enhancing tumor, and normal appearing white matter were contoured. Progression-free survival (PFS) was the primary clinical outcome. Patients with PFS>6 months were compared with those with PFS<6 months. Parameters of perfusion and changes in these during Tx were compared for these two groups at all time points using non-parametric statistics. Results: Eleven eligible patients were included and 46 DCE-MRI examinations were carried out. Regional CBF (rCBF) in tumor increased for all patients early during Tx (p=0.005) and then fell to a level below baseline at post-Tx examinations (p=0.016). A similar but non-significant trend was seen for rCBV. There was no detectable difference between patients with PFS>6 months vs PFS< 6 months with regards to baseline values or changes during- and after Tx. Conclusions: Regional cerebral blood flow (CBF) in tumor was increased significantly after only one week of radio-chemotherapy and was decreased three months post-treatment. Although no correlations to outcomes could be found, the results of this exploratory study may be hypothesis generating and will be examined in a larger patient group.

Session 4: Clinical results – hypoxia, dose painting and adaptive radiotherapy

Thursday June 11, 2015

10:50-11:10: Peter Hoskin, Northwood, UK

Hypoxia dose painting in prostate and cervix cancer

Peter J Hoskin. Mount Vernon Cancer Centre, Northwood, UK

Prostate and cervix cancer are both tumours which exhibit hypoxia and where there is clinical data to show that hypoxic tumours have a worse outcome. Hypoxia can be measured in these sites using non-invasive functional imaging data from which can be imported into radiotherapy planning systems. In this way biological subvolumes representing more hypoxic regions of the tumour can be defined. Delivery of differential dose distributions with higher doses to the hypoxic subvolumes is best achieved with high dose rate brachytherapy which enables rapid delivery of high dose per fraction radiation overcoming organ motion in the pelvis.

Thursday June 11, 2015

11:10-11:30 Ivan Vogelius, Copenhagen, Denmark

FDG PET based dose painting in head and neck cancer

Ivan Vogelius, Department of Oncology, Rigshospitalet, Copenhagen, Denmark

Introduction:

A data driven dose painting strategy with the aim of increasing radiation dose to regions with high risk of relapse is presented. The dose prescription strategy is developed based on the spatial distribution of recurrence risk observed in a retrospective cohort. A prospective phase I protocol increasing the dose to regions with high risk of recurrence, predominantly the FDG positive regions, will be discussed along with the results from the first 15 patients treated in the protocol (accrued Dec 2013 - August 2014). In addition, a description of the risk of competing events in the retrospective series will be presented with the aim of discussing patient selection for dose painting.

Methods and materials:

The presented data is based on a large retrospective cohort of 287 patients treated with radical (chemo)radiotherapy for squamous cell cancer of the head and neck from 2005-2009. In addition, 15 patients enrolled in the prospective phase I trial will be discussed. Patients in the phase I protocol are selected to be HPV negative or heavy smokers. The phase I protocol delivers five different dose levels (dose painting by regions) of up to 79.7 Gy in 34 fractions to the FDG PET positive region.

Results:

A substantial benefit is expected from modeling work. The 15 patients cleared the protocol-defined criterion for toxicity, but some concerning late toxicity will be discussed. Different approaches to patient selection and a description of the risk of failing at competing events will be discussed in more detail from the original 287 patient cohort. To date, we have seen only 1 treatment failure in the 15 patients of the phase I trial - a simultaneous lower neck, mediastinal and lung failure,

Thursday June 11, 2015

11:30-11:40: Marie Tvilum Petersen, Aarhus, Denmark

The Clinical Implication of Introducing Adaptive Radiotherapy in the Treatment of Lung Cancer Patients

Petersen M.T. (1), Khalil A.A. (1), Hoffmann L. (2), Møller D.S. (2), Knap M.M. (1). (1) Department of Oncology, Aarhus University Hospital, Aarhus, Denmark and (2) Department of Medical Physics, Aarhus University Hospital, Aarhus, Denmark

Introduction In April 2013 an adaptive strategy with daily online tumour match was introduced when treating locally advanced lung cancer patients (pts) with curative intended radiotherapy (RT). This study aims to evaluate the impact of introducing adaptive strategy on toxicity of the treatment as well as localization of intra-thoracic failure. Patients and methods Fifty one consecutive lung cancer pts receiving RT with an adaptive strategy and small PTV margins were analysed. A control group of 51 consecutive pts treated prior to April 2013 with bone match, no adaptive strategy and larger margins was included. All pts were toxicity-scored using CTCAE 4.03 grading scale. Pts were followed with CT-scans every third month. CT-images showing intra-thoracic recurrences were identified. The recurrence gross tumour volume was delineated and registered with the original radiation treatment plan to identify the site of failure. Data were analyzed using the Kaplan-Meier-analysis. Results The median follow-up time was 16.2 months (2.8-34.9). Within a year, 40% of the pts in the adaptive group (ART) and 61% in the control group (CRT) experienced thoracic failure, showing improved intra-thoracic control in the ART group (p=0.03). Median progression free survival time for the ART-group was 10.2 months (95%-CI: 8.3-12.2), and 7.6 months (95%-CI: 6.4-8.7) for the CRT group. Severe pneumonitis (grade 3-5) decreased from 21.6% in the CRT group to 17.6% in the ART group (non-significant, p=0.6). No significant difference in severe dysphagia was found between the two groups. Sixty-one patients showed thoracic failure. Of the first 13 patients, 7 had failure in the treatment field, 5 had out-of-field failure and 1 had marginal failure. Analysis is in progress. Conclusion Implementation of an adaptive strategy and tumour match for locally advanced lung cancer patients increases the intra-thoracic control rate without increasing toxicity of the treatment.

Thursday June 11, 2015

11:40-11:50: Patrick Berkovic, Ghent, Belgium

Adaptive radiotherapy for locally-advanced non-small cell lung cancer, can we predict when and for whom?

*Berkovic P, *Paelinck L, *Lievens Y, *Goddeeris B, *Derie C, **Gulyban A, *Surmont V, *De Neve W, *Vandecasteele K. *Department of Radiation Oncology, Ghent University Hospital, Ghent, Belgium **Department of Radiation Oncology, Liège University Hospital, Liège, Belgium

Introduction To analyze volume reduction and dosimetric consequences for stage III NSCLC tumors treated with concurrent or sequential chemoradiotherapy (cCRT or sCRT). To create a predictive tool to identify who may benefit from adaptive radiotherapy (ART), and if so, when. Material and Methods Forty-one patients were treated with cCRT (n=21) or sCRT to a median dose of 70Gy, 2 Gy/F. At every fraction a cone beam CT (CBCT) was performed. The gross tumor volume (GTV-T) was adapted (exclusion of lymph nodes) to create the GTV-T-F1. Every fifth fraction (F5 to F30), the GTV-T-F1 was adapted on the CBCT to create a GTV-T-Fx. Dose volumes histograms were recalculated for every GTV-T-Fx, enabling to create look-up tables to predict the theoretical dosimetric advantage on common lung dose constraints. Results The average GTV reduction was 42.1% (range: 4.0-69.3%); 50.1% and 33.7% for the cCRT and sCRT patients respectively. A linear relationship between GTV-T-F1 volume and absolute volume decrease was found for both groups. The mean V5, V20, V30 and mean lung dose increased by 0.77, 3.1, 5.2 and 3.42% respectively. A larger increase ($p < 0.05$) was observed for peripheral tumors and cCRT. Look-up tables were generated. The dosimetric impact of ART is higher in case of large initial GTV-T, performed around the 15th and 20th fraction for cCRT and sCRT respectively. Conclusions ART offer the most beneficial effects when performed around fraction 15, especially for patients with a large initial GTV-T.

Thursday June 11, 2015

11:50-12:00: Anne Vestergaard, Aarhus, Denmark

Acute gastro-intestinal morbidity in a Phase II trial of online adaptive radiotherapy for urinary bladder cancer.

Vestergaard A, Als AB, Muren LP, Lindberg H, Jakobsen KL, Dysager L, Jensen HR, Petersen JB, Elstrøm UV and Høyer M. Department of Medical Physics & Department of Oncology, Aarhus University Hospital, Department of Oncology, Copenhagen University Hospital, Herlev, Department of Oncology & Laboratory of Radiation Physics, Odense University Hospital, Odense, Denmark

Introduction: Adaptive radiotherapy (ART) using plan selection is being introduced in the treatment of urinary bladder cancer to account for the inter-fractional motion while sparing normal tissues. This study reports final outcome from a multicenter Phase II trial of ART for bladder cancer, with reduction of peak grade 2 or higher diarrhea as primary endpoint. Materials and methods: Sixty five patients were included in the trial, however five patients did not meet the inclusion criteria and six patients did not complete ART. The remaining 54 patients were treated with plan selection from an individual predefined library of three treatment plans corresponding to small, medium and large size bladder, created from the first four CBCTs of each patient. All patients received 60 Gy in 30 fractions to the bladder while 40 patients also received 48 Gy to the pelvic lymph nodes as a simultaneous integrated boost treatment. Patients were set-up by use of cone-beam CT (CBCT) and treatment was delivered by volumetric modulated arc therapy (VMAT). The first five fractions were delivered using large non-adaptive margins. A Fishers exact test was used to compare the frequency of peak grade 2 or higher diarrhea to a previously treated cohort (Søndergaard Acta Oncol 2014). Results: The median frequency of which plans were selected was 48%, 25% and 27% for small, medium and large size plan, respectively. The median course-averaged PTV for the adaptive treatment was 441 cm3 compared to 642 cm3 if treated with non-adaptive radiotherapy. Twelve patients (22%) had grade 2 or higher diarrhea, including only two cases with grade 3 diarrhea. This was compared to 30% in the previously treated cohort and was not statistical significant (p=0.2). Conclusion: Adaptive plan selection in radiotherapy of bladder cancer leads to a considerable normal tissue sparing and this might reduce the frequency of grade 2 or higher acute gastrointestinal morbidity.

Thursday June 11, 2015

12:00-12:10: Ralph Leijenaar, Maastricht, The Netherlands

Early prediction of pathological response in rectal cancer patients using "PET Radiomics" with independent validation

Leijenaar RTH *, Carvalho S *, Buijsen J *, van Stiphout RG **, Valentini V ***, Dekker A *, Lambin P *. * Department of Radiation Oncology (MAASTRO), Maastricht, the Netherlands; ** Department of Oncology, University of Oxford, Oxford, United Kingdom; *** Department of Radiation Oncology, Gemelli-ART, Università Cattolica S. Cuore, Rome, Italy

Purpose: Early prediction of response to chemo-radiotherapy (CRT) in locally advanced rectal cancer (LARC) is essential to tailor treatment. We investigated and independently validated the value of pre-treatment PET Radiomics in predicting pathological tumor stage (ypTN). Methods: We included 324 patients accrued at our institute (training cohort) and 57 patients accrued at an external institute (validation cohort). Patients received CRT, followed by total mesorectal excision and underwent baseline 18F-FDG PET imaging. Tumor volumes were delineated with a signal to background based SUV threshold. In total, 166 radiomic features were extracted, comprising: a) first-order statistics, b) intensity volume histogram, c) shape, and d) texture. The feature space was reduced based on reliability (determined in other cohorts) and hierarchical cluster analysis. A logit model to predict responders according to pathology (ypT012N0), was built using a cross-validated forward feature selection scheme. Model performance was defined as the area under the receiver operating characteristic curve (AUC). Out-of-sample performance in the training cohort was determined using 100 rounds of 10-fold stratified cross-validation, followed by independent external validation. Results: We identified 145 (45%) and 28 (49%) responders in the training and validation cohort, respectively. Feature reduction resulted in 34 highly robust and non-redundant features. Model development lead to an 8-feature model with an out-of-sample AUC of 0.63±0.09. Independent validation resulted in an AUC of 0.77 (95% CI: 0.64-0.90). Conclusion: A multivariable Radiomic model predicted pathological response in LARC patients and independently validated in an external cohort. Radiomics may facilitate early and accurate prediction of tumor response to treatment and identify patients eligible for a wait and see or organ preserving approach, or patients who may benefit from treatment intensification.

Thursday June 11, 2015

12:10-12:20: Marianne Assenholt, Aarhus, Denmark

Application of coverage probability treatment planning for lymph node boosting in locally advanced cervical cancer

Assenholt MS(1), Ramlov A(1), Jensen MF(1), Nout RA(2), Fokdal L(1), Tanderup K(1,) Alber M(1) Lindegaard JC(1). 1) Department of Clinical Oncology, Aarhus University Hospital, Aarhus, Denmark 2) Department of Radiotherapy, Leiden University Medical Center, Leiden, The Netherlands.

Introduction: Traditional nodal boosting by external beam radiotherapy (EBRT) in locally advanced cervical cancer (LACC) invariably cause collateral high dose (>50 Gy) delivery to surrounding normal tissues including pelvic bones. Coverage probability treatment planning (CoP) of a simultaneous integrated boost (SIB) may reduce this problem. CoP is based on statistical modelling of the geometric uncertainties and the voxel-by-voxel probability of target occupation. With CoP a steep inhomogeneous dose distribution placed in the centre of the pathological node is generated. Materials and methods: Seven patients with LACC and a total of 19 pathological nodes were treated with EBRT using IMRT. Nodal gross tumour volume (GTV-N) was first delineated on a planning MRI. Internal target volume (ITV-N) was then defined as GTV-N + any additional nodal extension on a fused planning PET-CT. A 5 mm isotropic margin was added for PTV-N. Bone match on daily cone-beam CT (CBCT) were performed prior to each EBRT fraction. Sixteen of 19 nodes were visible on CBCT and were delineated on 9-10 CBCTs. Two dose plans were generated for each patient; a standard ICRU and a CoP. Constraints for CoP were developed in Hyperion and transferred to Eclipse: ITV-N D98>100%, PTV-N D98>90% and ITV-N D50>103%. The constraint for the ICRU plan was: PTV-N 95-107%. Both plans were based on 45 Gy/25 fx whole pelvic IMRT with a SIB of 55-60 Gy. Results: CoP reduced the volume of body and bony structures receiving over 50 Gy by 27.2 cm3 [range 15.1; 42.7] and 7.8 cm3 [range 1.8; 16.4], respectively. Nodal dose coverage (ICRU vs. CoP) was: D98%: 100.2 % (std. 0.7) vs. 99.6 % (std.0.9), D50%: 101.3 % (std.0.4) vs. 102.0 % (std.1.0), Dmin: 99.6 % (std.1.2) vs. 98.3 % (std.1.5), Dmax: 102.1 % (std.0.7) vs. 103.9 % (std.1.7). Conclusion: Collateral dose to normal tissue can substantially be reduced by use of CoP without compromising dose to boosted nodes. CoP is now routinely used for SIB planning in LACC.

Thursday June 11, 2015

12:20-12:30: Sara Thörnqvist, Bergen, Norway

Adaptive radiotherapy strategies for pelvic tumours – a review of clinical implementations

Hysing L.B.1, Tuomikoski L., Vestergaard A., Tanderup K., Muren L.P., Heijmen B.J.M.. 1. Dept. Medical Physics,Haukeland UH,Bergen, NO 2. Dept. Oncology, Helsinki University Central Hospital,Helsinki,FI 3. Dept. Medical Physics, Aarhus UH,Aarhus,DK 4. Dept. Radiation Oncology, Erasmus MC Cancer Institute, Rotterdam, NL

Introduction Variation in shape, size and relative position of the tumor and organs at risk (OAR) is one of the major challenges for dose delivery in radiotherapy (RT). Adaptive RT (ART) was proposed to customise the treatment to the motion/response pattern of the individual patient. The ART concept with motion monitoring, evaluation and adaptation of treatments results in additional workload, thus complicating clinical implementation. This study is a systematic review investigating the workflows that have been clinically implemented for prostate, bladder, gynaecological (gynae) and rectal cancers. Method Identification of papers was based on searches in PubMed. Subsequently, studies describing an ART workflow including treatment monitoring and evaluation, decision and execution of adaptions were included in the review. For each site, the search and paper selection were performed independently by two researchers. The studies referred to by the selected papers were also screened with the same inclusion criteria to avoid exclusion of any relevant studies. Results In total 36 studies with treatment of more than 3100 patiens (pts) satisfied the inclusion criteria. For prostate, 1219 pts were re-planned, mainly to adapt to the prostate motion in relation to bony anatomy. For gynae and rectal cancer, 1208 and 25 pts were re-planned to account for tumour regression observed by MRI/CT. For bladder and cervix, 163 and 64 pts were treated with plan selection to account for target shape changes. In 26% of the studies, dosimetric comparison with conventional RT showed either a reduction of the PTV, improved CTV coverage or OAR sparing with ART. Convincing outcome data with ART for gynea and prostate cancers has been published. Conclusion ART has been clinically implemented for pelvic tumors from year 1989 mainly with offline re-plan strategies. Sofar, clinical implementation have been slow, considering the vast amount of literature on technical aspects and simulation studies.

Thursday June 11, 2015

12:30-12:40: Hella Sand, Aalborg, Denmark

Correlation between pretreatment FDG-PET biological target volume and location of T-site failure after definitive radiation therapy for head and neck cancers

a) Sand H, b) Brunø AH, b) Andersen LJ, a) Carl J. a) Department of medical physics, Oncology, Aalborg Universityhospital, Aalborg, DK; b)Department of Oncology, Aalborg Universityhospital, Aalborg, DK.

Introduction: A number of studies suggest that 18F-fluorodeoxyglucose (FDG) might be a useful tracer for detecting intratumor regions of increased radiation resistance in head and neck cancer (HNC). We hypothesize that failures of HNC arise from the positron emission tomography (PET)-active volume with the strongest FDG-signal. Materials and Methods: Seventeen patients with loco-regional T-site failure of squamous cell HNC after definitive radiotherapy were included in the study. All patients had a pretreatment FDG-PET/computed tomography (CT) scan and a subsequent FDG-PET/CT scan visualizing the loco-regional recurrence. On the pretreatment FDG-PET/CT images manual delineation of the Gross Tumor Volume (GTV) was originally performed by an experienced radiation oncologist and a nuclear medicine physician in cooperation. All N-sites included in the original GTV were subsequently erased. This corrected GTV was called GTVmanPre. Furthermore, we delineated the primary tumor on the pretreatment PET and the T-site failure on the recurrence PET by means of a 41% fixed threshold of the maximum signal intensity value corrected for the background activity and called these autosegmented volumes GTV41Pre and GTV41Fail. Any evident physiological FDG-uptake and possible metastatic lymph nodes in the autosegmented volume were manually erased. Finally the overlap of the pretreatment volumes and the failure volume were delineated by means of Boolean operators and called ‘GTVmanPre ∩ GTV41Fail’ and ‘GTV41Pre ∩ GTV41Fail’. Results: The median GTVmanPre was 9,72 cm3 [0,47-98,03 cm3], while the median GTV41Pre was 4,42 cm3 [1,01-36,34 cm3]. On average GTV41Pre makes up 25% of GTVmanPre. ‘GTVmanPre ∩ GTV41Fail’ vs GTVmanPre was 18% and ‘GTV41Pre ∩ GTV41Fail’ vs GTV41Pre was 20%. Conclusions: Our results indicate that it is most possible that a T-site failure arise from within the PET-active volume with the strongest FDG-signal. Therefore a dose-escalation in this area could be considered.

Session 5: Novel concepts in design of clinical trials in radiotherapy

Thursday June 11, 2015

13:40-14:00: Philippe Lambin, Maastricht, The Netherlands

Modern Clinical Research: How Rapid learning health care and cohort multiple randomised clinical trials complement traditional evidence based medicine.

Philippe Lambin. Radiation Oncology, Maastro Clinic, Maastricht, The Netherlands

Background: Trials are vital in informing routine clinical care; however current designs have major deficiencies. An overview of the various challenges that face modern clinical research and the methods that can be exploited to solve these challenges, in the context of personalised cancer treatment in the 21st century is provided. Aim: The purpose of this manuscript is to present and discuss two important and complementary alternatives to traditional evidence based medicine, specifically rapid learning health care and cohort multiple randomised controlled trial design. Rapid learning health care is an approach that proposes to extract and apply knowledge from routine clinical care data rather than exclusively depending on clinical trial evidence. The cohort multiple randomised controlled trial design is a pragmatic method which has been proposed to help overcome the weaknesses of conventional randomised trials, taking advantage of the standardized follow-up approaches more and more used in routine patient care. This approach is particularly useful when the new intervention is a priori attractive for the patient (such as proton therapy, patient decision aids or expensive medications), when the outcomes are easily collected, and when there is no need of a placebo arm. Discussion: Truly personalised cancer treatment is the goal in modern radiotherapy. However, personalised cancer treatment is also an immense challenge. The vast variety of both cancer patients and treatment options makes it extremely difficult to determine which decisions are optimal for the individual patient. Nevertheless, rapid learning health care and cohort multiple randomised controlled trial design can help meet this challenge.

Thursday June 11, 2015

14:20-14:30: Armin Lühr, Dresden, Germany

Individual benefit for advanced head and neck cancer patients in terms of NTCP differences from intensity-modulated proton therapy for complete or sequential boost treatment versus intensity-modulated photon therapy

Jakobi A1, Bandurska-Luque A1, Stützer K1, Haase R1, Löck S1, Wack LJ2, Mönnich D2,3, Thorwarth D2, Kovacevic M1, Perez D1,3, Lühr A1,3, Zips D2, Krause M1,3, Baumann M1,3, Perrin R1, Richter C1,3. 1: OncoRay – National Center for Radiation Research in Oncology, Faculty of Medicine and University Hospital C. G. Carus, TU Dresden, HZDR, Dresden, Germany 2: University Hospital for Radiation Oncology, Tübingen, Germany 3 DKTK & DKFZ, Germany

Introduction: A treatment planning study was conducted for head and neck cancer (HNC) patients to evaluate the benefit of intensity-modulated proton therapy (IMPT) used for complete treatment or for sequential boost treatment compared to photon therapy (IMRT). Materials&Methods: For 45 HNC patients IMRT and IMPT treatment plans were created including a dose escalation via simultaneous integrated boost with a one-step adaptation strategy after 25 fractions for sequential boost treatment. Dose accumulation was performed for pure IMRT treatment (pIMRT), pure IMPT treatment (pIMPT) and for an IMRT treatment for the elective target followed by a sequential boost with IMPT (Mix). Treatment plan evaluation was based on normal tissue complication probabilities (NTCP). Individual NTCP differences between pIMRT and pIMPT (ΔNTCP) as well as between pIMRT and Mix (ΔNTCPMix) were calculated. Results: Target coverage was similar in all three cases. NTCP values could be reduced in all patients using IMPT treatment. However, ΔNTCPMix values were between 10 and 50% of the ΔNTCP values. Using a benefit of 10% NTCP reduction as threshold for patient assignment to IMPT, the majority of the patients would not benefit from a proton boost, but about 50% would benefit from the pure IMPT treatment considering xerostomia and dysphagia risk as main factors. ΔNTCP>10% for other toxicity risks like mucositis or trismus occurred only in 6 and 4 of 45 patients, respectively. Conclusions: The use of IMPT generally reduces the expected toxicity risk while maintaining good tumor coverage in the examined HNC patients. A mixed modality treatment using IMPT solely for boosting offers only a small benefit for the majority of patients. Pure IMPT treatment may be beneficial in terms of expected toxicity risk reduction for the main toxicities xerostomia and dysphagia for about half of the examined patient cohort. Using IMPT for those patients, special attention to adaptation needs is required.

Thursday June 11, 2015

14:30-14:40: Morten Høyer, Aarhus, Denmark

Radiation dose to the gastro-intestinal (GI) tract and patient-reported symptom domains after prostate cancer radiotherapy

Thor M1, Olsson CE2, Oh JH, Petersen SE1, Alsadius D2, Muren LP3, Pettersson N2, Bentzen L3, Høyer M3, Steineck G2, Deasy JO1. 1 Dept of Medical Physics, Memorial Sloan Kettering Cancer Center, NYC, US; 2 Dept of Oncology, Institute of Clinical Sciences at University of Gothenburg, Gothenburg, SE. 3 Depts of Medical Physics/Oncology, Aarhus University Hospital, Aarhus, DK

Introduction: The aim of this study was to investigate the wider range of GI morbidity than typically addressed in common scoring systems and to explore the interplay between patient-reported GI symptoms after primary radiotherapy (RT) for localized prostate cancer, and to what extent these are explained by dose to the GI tract. Materials and methods: The subjects investigated were taken from two Scandinavian prostate cancer cohorts (N=490) treated with primary external-beam RT to 70-78Gy@2Gy/fraction. The anal sphincter (AS) included the anal canal, inner and outer sphincters, and the rectum (R) was defined from AS up to the recto-sigmoid flexure. Symptom domains were obtained by applying a novel factor analysis-method to two PRO-based GI symptom profiles (43 symptoms in total; median time to follow-up: 3.2-6.4 years). Dose-response outcome variables were defined from the identified symptom domains (Boolean 'or condition' used when combining symptoms). Maximum and mean dose (Dmax and Dmean) to AS or R were tested as predictors for each outcome variable using logistic regression and Area Under the Receiver Operating Characteristic Curve (Az). Results: The symptom domains (number of symptoms) Leakage (4-6), Pain (3-6), and Urgency (2-3) were identified in both cohorts and Mucous (4) in one cohort. AS-Dmean significantly predicted all domains (p=0.001-0.05; Az=0.58-0.69), AS-Dmax predicted Leakage and Pain (p=0.001-0.05; Az=0.58-0.69), R-Dmean predicted Urgency and Leakage (p=0.03-0.05; Az=0.58-0.59) and R-Dmax predicted Leakage only (p=0.002-0.04, Az=0.58-0.67). Conclusions: We have demonstrated that grouping interacting GI symptoms is feasible and that GI morbidity post-RT include the symptom domains Leakage, Pain, Urgency, and Mucous. Models including the anal sphincter typically yielded stronger relationships with all domains. Further attention to the anal sphincter region has the potential to increase understanding of GI tract dose-response relationships.

Thursday June 11, 2015

14:40-14:50: Timo Deist, Maastricht, The Netherlands

Clinical routine data as a viable source for radiation-induced lung toxicity prediction models

Deist, T. M.; Jochems, A.;Oberije, C.; Vandecasteele, K.; Lievens, Y.; Dekker, A.; Lambin, P. Department of Radiation Oncology (Maastro Clinic), GROW – School for Oncology and Developmental Biology, Maastricht University Medical Centre; Department of Radiation Oncology, Ghent University Hospital;

Introduction Personalized medicine may guide the way to a new era of healthcare. Predicting patient-specific treatment outcomes and adjusting treatments accordingly requires reliable prediction models and abundant patient data. With the increasing number of treatment options, it is not feasible to timely conduct clinical trials for every scenario due to budget limitations and organizational lead times. Further, selection criteria bias the patient sample. One alternative is clinical routine data which are widely available but are prone to suffer from incompleteness and errors. Appropriate statistical models do however mitigate these limitations. We show the value of this data by building a prediction model for radiation-induced lung toxicity. Materials/Methods Clinical routine data of 719 lung cancer patients were collected (2008-2015) at MAASTRO Clinic, the Netherlands, including gender, smoking status, histology, n-staging, WHO performance status, tumor dose, chemotherapy types, cardiac comorbidity, and dyspnea (CTCv.3 or v.4) before radiotherapy (RT) and the maximal value up to 6 months after RT. An external data set of 109 patients was provided by Ghent University Hospital, Belgium. To predict post-RT increases in dyspnea scores, a Bayesian network was learned on the combined data set. Model performance is expressed by the 10-fold cross-validation AUC. Results The Bayesian network with all the above variables exhibits an AUC of 0.79. On a validation set of 90 patients, excluded before the model learning, the model achieves an AUC of 0.83. Conclusions The results show the clinical routine data's potential to generate predictions of patient-specific treatment outcomes. Not only are they readily available in clinics at no extra cost, they are continuously growing and perfectly represent the real patient population. Personalized healthcare will stand or fall with uncovering an abundant source of patient data, clinical routine data might just be the one.

Session 6: How to establish clinical evidence in particle therapy?

Thursday June 11, 2015

Michael Baumann, Dresden, Germany

Particle therapy, networks and infrastructure

Michael Baumann 1,2,3,4 , Mechthild Krause 1,2,3,4 , Esther Troost 1,2,3,4 , Christian Richter 1,2,3,4 , Wolfgang Enghardt 1,2,3,4

1 German Cancer Consortium (DKTK) Partner Site Dresden and German Cancer Research Center (DKFZ), Heidelberg, Germany; 2 Department of Radiation Oncology Medical Faculty and University Hospital Carl Gustav Carus, Technische Universität Dresden, Germany; 3 OncoRay – National Center for Radiation Research in Oncology Dresden, Germany, 4 Helmholtz-Zentrum Dresden-Rossendorf, Institute of Radiooncology, Dresden, Germany

Radiotherapy with particles, i.e. with protons or heavier ions, is one of the most exciting areas of research in radiation oncology today. The main advantage of proton therapy compared with state-of-the-art photon therapy is a decrease of the volume of normal tissues irradiated to intermediate and low doses, while irradiation of normal tissues to high doses or the conformality of the dose to the tumor are usually similar for protons and photons. Exceptions include situations where critical normal tissues can be excluded by proton therapy from the irradiated volume completely or to a large extent. Therefore, the most important clinical research question is to evaluate whether sparing of normal tissue by proton therapy leads to clinical relevant benefits which balance the higher costs of this treatment. After relevant sparing of normal tissues has been demonstrated, studies utilizing dose intensification strategies may become another important research avenue in those tumors where local or locoregional tumor control today are unsatisfactory. An important consideration in clinical research using protons is that only few centers (often with different technologies and patient populations) are currently active. This necessitates fresh thinking on study design in radiation oncology, as large scale randomized trials will not be feasible in many situtations. Model-based approaches are an important component of the trial methodology arsenal, however, alternatives (including multicenter stepwise randomized trials, pseudoransomized trials and prospective matched pair trials) may be superior in different clinical situations. All of these approaches need complex high-level network formation and dedicated clinical research infrastructures to reach the necessary power for meaningful clinical trials. This is even more important in the context of biologically stratified radiotherapy, which is anticipated to become a clinical reality in the coming decade for several tumor entities. Although proton (or other particle) therapy holds particular promise to further advance Personalized Radiation Oncology, problems in trial design, data sampling and integration, or analysis may dilute the effects to such an extent that it may not be possible to demonstrate it according to generally accepeted scientific standards. This would be a major hurdle for further implementation and reimbursement of this promising technology, as well as for sound medical stratification of access of of patients in need for this therapy.
The lecture will discuss some most important opportunities and problems of proton therapy in the context of biologically stratified, personalized radiation oncology, thereby also touching trial design, network formation and technology development.

Thursday June 11, 2015

Thomas Björk-Eriksson, Uppsala, Sweden

Skandion Clinic – A proton pencil beam scanning only facility based on distributed competence and shared governance.

Thomas Björk-Eriksson. Skandion Clinic, Uppsala, Sweden

Advanced and expensive radiation therapy facilities like proton therapy clinics must be organised to serve a large population. This has traditionally been obtained by setting up facilities in large population centres and frequently also in private care. However, for more sparsely populated regions and in public health care other solutions must be developed. Based on modern cutting edge information and communication technology a model for distributed expert support for a proton facility located close to a in a communication hub in the central part of Sweden, Uppsala, has been designed. In this model all tumour diagnostics and treatment planning will be performed locally in the collaborating seven University Hospitals and mutually discussed in video conferences where all data will be available and simultaneously demonstrated. The approved treatment plan will then be downloaded in a common database and used in the treatment of patients at the Skandion Clinic.This model for distributed expert collaboration and shared governance will secure clinical competence for all inhabitants served by the collaborating regional centres. This closely integrated referral network for proton radiotherapy will further be an efficient base for clinical research and education. The Skandion Clinic is run by the seven regions of Sweden with University hospitals through the Joint Authority of County Councils (Kommunalförbundet avancerad strålbehandling, KAS). Skandion Clinic will start with patient treatments in the beginning of June 2015.

Session 7: Image-guidance for adaptive radiotherapy and proton therapy

Friday June 12, 2015

8:20-8:40: Parag J. Parikh, St Louis, MO, USA.

Online adaptive radiation therapy in the abdomen: The challenge of bowel

Parag J. Parikh. Department of Radiation Oncology, Washington University School of Medicine, St Louis, USA

Online adaptive radiation therapy has become a clinical reality using an MRI guided radiation therapy system since September 2014 in St. Louis. There have been many challenges in the implementation of this, from patient selection, training and culture shifts. One of the most intriguing structures to adapt on is the small bowel. This talk will review some key points of the MR guided online adaptive radiation therapy system, and then challenges and opportunities with regards to the small bowel.

Friday June 12, 2015

9:00-9:20: Marta Peroni, Villigen, Switzerland

The adaptive challenge in proton therapy

Peroni M. Paul Scherrer Institut, Villigen, Switzerland

Since its early stages, external beam therapy has been heavily relying on image guidance, with the goal of conforming dose distribution to the target, whilst at the same time sparing the surroundings organ at risks. The favourable inverted dose profile of protons can be shaped and placed at any depth in the patient, though it is not always easy to define where. The management of uncertainties, including setup errors, heterogeneities, stability of Hounsfield units, physiological motion and anatomo-pathological changes, plays therefore a key role in the clinical routine. In this context, proper imaging of uncertainties and motion as well as innovative monitoring of the patient positioning at different time scales (intra- and inter-fraction) is the necessary step for safely adapt the delivery and to extend treatment indications. While in conventional therapy the adaptive paradigm and motion compensated deliveries are becoming consolidated realities, proton therapy inherently higher sensitivity makes the online changes of the Bragg peaks even more challenging. In this talk, we will review some approaches to address the challenge of adapting proton plan to compensate for the daily or continuous modifications in the context of a spot scanning delivery system.

Friday June 12, 2015

9:20-9:30: Christopher Kurz, Munich, Germany

Comparing strategies for CBCT-based dose recalculation to foster adaptive IMRT and IMPT of head and neck cancer patients

Kurz, C., Dedes, G., Resch, A., Reiner, M., Janssens, G., Orban de Xivry, J., Kamp, F., Wilkens, J. J., Thieke, C., Nijhuis, R., Ganswindt, U., Belka, C., Parodi, K. and Landry, G. Department of Radiotherapy and Department of Medical Physics, Ludwig-Maximilians-University, Munich, Germany

Introduction: In IMRT and IMPT of H&N cancer, inter-fractional changes can compromise treatment quality and demand for a plan adaptation. To this aim, a 3D dose calculation based on the actual patient anatomy is required. This contribution investigates two different approaches for dose recalculation on the basis of cone-beam CT (CBCT) images. Material and methods: For 3 patients with lower and 3 with cranially located H&N tumours, virtual CTs (vCT) were generated by deformable registration of the planning CT (pCT) to the CBCT. Moreover, patient-specific look-up tables were used for scaling the CBCT intensities to the pCT HU range, obtaining a so-called CBCTLUT. IMRT and IMPT plans were generated on the pCT using RayStation. A Monte-Carlo planning tool was used to create proton SFUD plans for accurately probing the proton range. IMRT and IMPT dose recalculations on the vCT and CBCTLUT were analysed by means of a 3D gamma-index (3%, 3mm) and comparison of clinically relevant DVH parameters. A replanning CT (rpCT) acquired within 3 days of the CBCT served as reference. Results: The selected DVH parameters showed minor differences between rpCT, vCT and CBCTLUT in IMRT, but some clinically relevant deviations between CBCTLUT and rpCT in IMPT. Gamma-index pass-rates increased for the vCT (78-94%) compared to the CBCTLUT (67-84%) for lower H&N cases in IMPT. In IMRT only one patient showed an increased pass-rate (from 88 to 96%). For the cranial cases, similar pass-rates were found for different CTs in IMPT and IMRT. The SFUD-based proton ranges showed an enhanced agreement of vCT and rpCT, with 79-92% of the depth dose profiles agreeing within 3mm. For the CBCTLUT, only 62-80% of the profiles fulfilled this criterion. Conclusions: vCT and CBCTLUT are suitable options for dose recalculation in adaptive IMRT. In the scope of IMPT, the vCT approach is superior. Acknowledgements: This work was supported by the BMBF (01IB13001, SPARTA) and the DFG Cluster of Excellence MAP.

Friday June 12, 2015

9:30-9:40: Lucas Persoon, Maastricht, The Netherlands

Is integrated transit planar EPID dosimetry able to detect geometric changes in lung cancer patients treated with volumetric modulated arc therapy (VMAT)

Lucas C.G.G. Persoon1, Mark Podesta1, Lone Hoffmann2, Abir Sanizadeh1, Ben-Max de Ruiter1, Sebastiaan M.J.G.G. Nijsten1, Ludvig P Muren2, Esther G.C. Troost1, Frank Verhaegen1. 1 Department of Radiation Oncology (MAASTRO), GROW – School for Oncology and Developmental Biology, Maastricht University Medical Centre, Maastricht, the Netherlands 2 Department of Medical Physics, Aarhus University Hospital, Aarhus, Denmark

Introduction: Geometric changes are frequent during the course of treatment of lung cancer patients. This may potentially result in deviations between the planned and actual delivered dose. Integrated transit planar EPID dosimetry (ITPD) is a fast method for absolute in-treatment dose verification. The aim of this study was if ITPD could detect geometric changes in lung cancer. Methods and Materials: Over 400 patients treated with VMAT following daily CBCT-based setup, were visually inspected for geometrical changes on a daily basis. 46 patients were subject to changes and had a re-CT and an adaptive treatment plan. The ITPDs were calculated on both the initial planning CT and the re-CT and compared with a global gamma (γ) evaluation (criteria: 3%\3mm). A treatment fraction failed when the percentage of pixels failing in the radiation fields exceeded 10%. Dose-volume histograms (DVHs) were compared between the initial plan vs. the plan re-calculated on the re-CT. DVH metrics analyzed were ΔD98%, ΔD95%, ΔD5%, for the clinical target volume and ΔD2%, ΔD0.5cc, ΔDmax, for the mediastinum. When a DVH metric exceeded 4%, it was considered significant and this was compared to the γ fail-rate from the ITPDs. Results: The reason for adaptation in the 46 patients were: change in atelectasis (40%), tumor regression (17%), change in pleural effusion (17%) or other causes (26%). The ITPD threshold method detected 76% of the changes in atelectasis, while only 50% of the tumor regression cases and 42% of the pleural effusion cases were detected. Only 10% of the cases adapted for other reasons were detected with ITPD. The method has a 17% false-positive rate. No significant correlations were found between changes in DVH metrics and γ fail-rates. Conclusion: This retrospective study showed that most cases with geometric changes caused by atelectasis could be captured by ITPD, however for other causes ITPD is not sensitive enough to detect the clinically relevant changes.

Friday June 12, 2015

9:40-9:50: Andreas Gravgaard Andersen, Aarhus, Denmark

A Method to Evaluate the Robustness of Single Beam Proton Plans for Pelvic Lymph Node Irradiation with Respect to Inter-Fractional Motion

Andersen AG(1), Casares-Magaz O(1), Muren LP(1), Toftegaard J(1), Bentzen L(2), Bassler N(3), Thörnqvist S(4) and Petersen JBB(1). (1) Department of Medical Physics, (2) Department of Oncology, Aarhus University Hospital, (3) Department of Physics and Astronomy, Aarhus University, Aarhus, Denmark; (4) Section of Medical Physics, Haukeland University Hospital, Bergen, Norway

Aim This study addresses the robustness of single beam proton plans for irradiation of the pelvic lymph nodes (LN) with respect to inter-fractional motion. More specifically, we have explored whether there are certain beam directions that are less influenced by anatomical variations, and whether these are specific for each patient or apply for a patient population. Material and Methods The method is based on patient data sets consisting of a planning CT (pCT) as well as multiple repeated CT (rCT) scans, each with the volumes outlined according to the PROPEL trial performed at Aarhus University Hospital. For either the left or right LNs we optimized single beam proton plans using the spot scanning treatment planning system TRiP with PyTRiP, i.e. for every 5º gantry angles. Isotropic margins from the Clinical Tumor Volume (CTV) to the Planning Target Volume (PTV) of 0, 3, 5 and 7mm were investigated. To assess physical dose, the optimized fluence maps for the pCT for each beam were applied onto the all rCTs, recalculating the dose on the LN CTV and relevant volumes of interest. The variation in the water equivalent path length (WEPL) was calculated by creating beams eye view WEPL maps and taking the mean distance for all beam angle configurations: [0º, 360º] for gantry and [-90°, 90°] for couch, both in 5° steps. Results Dose coverage decrease with as much as 18% and 2% in volume for the D99% and D95% was observed, respectively, for the CTV (right LN side) when using 7mm margin, while decreasing 10-100% for the D99% and 5-90% for the D95% when using 0mm margin. Angles with the least dose to rectum, bladder and normal tissue, were found to correlate with those of less WEPL variation between 190º and 200º and around 320º for the right LN volume. Conclusion We have established a method to quantify the robustness to inter-fractional motion of single beam proton plans treating the pelvic lymph nodes from different gantry/couch angle combinations.

Friday June 12, 2015

9:50-10:00: Per Poulsen, Aarhus, Denmark

Calculation of interplay effects caused by liver tumor motion during scanning proton therapy in a commercial treatment planning system

Poulsen PR (a), Worm ES (b), Høyer M (a), Grau C (a), Petersen JBB (b). (a) Institute of Clinical Medicine, Aarhus University, Aarhus, Denmark and Department of Oncology, Aarhus University Hospital, Aarhus, Denmark. (b) Department of Medical Physics, Aarhus University Hospital, Aarhus, Denmark.

Introduction: Target motion during scanning proton therapy may severely distort the target dose distribution. In this study, we establish a method to calculate dose delivered to moving targets in scanning proton therapy by a commercial treatment planning system (TPS), and use it to investigate interplay effects for a number of liver SBRT patients with known tumor motion. Methods: Scanning proton plans from a commercial TPS (Eclipse, Varian Medical Systems) were exported as dicom files and manipulated by an in-house developed computer program that incorporated tumor motion into the plans by shifting each proton spot from its planned position in beam's eye view to its position in tumor's eye view. Depth motion and variations in source-surface-distance were modeled as beam energy modifications. The manipulated plans were re-imported into the TPS, where dose calculation resulted in the motion including target dose. The method was first tested with static target shifts in a digital water phantom with known ground truth dose for the shifted target and then used to investigate interplay effects in scanning proton treatments for four liver SBRT patients with known tumor motion measured by x-ray imaging during (photon) treatments. A total of 240 treatment deliveries were simulated, covering two optimization types (SFO and IMPT), two spot scan directions, and 1-10 paintings. The dosimetric impact of the interplay effects was quantified as D5-D95 for the GTV. Results: The liver tumor motion resulted in substantial interplay effects that were on average – but not for each case – reduced with increased repainting. IMPT was slightly less robust to motion than SFO. No systematic effect of the scan direction was observed. Conclusions: A method to investigate the dosimetric impact of tumor motion during scanning proton therapy by a commercial TPS was developed, validated in a water phantom, and applied for liver SBRT treatments using patient-measured intra-treatment tumor motion.

Session 8: Radiotherapy in Europe 2020

Friday June 12, 2015

10:30-10:50: Josep M. Borras, Barcelona, Spain

The need for radiotherapy in Europe 2020: not only data but also a cancer plan

Borras, JM. Department of Clinical Sciences, University of Barcelona, Barcelona, Spain

The need for planning radiation oncology equipment and staffing is necessary in public health care systems in Europe. In order to do this, we need three different inputs of data: the evidence-based indications for radiotherapy, the incidence of cancer and stage at diagnosis by each cancer type, both using population based data from cancer registries. In this paper we discuss the availability of these data and the implications for the estimation of the proportion of new cancer patients that would need a radiotherapy treatment, at least once during the course of the disease. Depending on the frequency of cancers and stage at diagnosis, it has been estimated that between 47 and 53 of incident cases among European countries would require external beam radiotherapy. It is argued that these are the optimal proportions of cancer patients should be considered optimal, but a more realistic policy target could be set at 80% or higher of the optimal proportion.. This realistic target also takes into account the inherent uncertainties in the assessment of evidence, and other factors that influences clinical decision-making in cases of multi-morbidity or patient preferences. Other factors are associated to problems that should be dealt in the framework of a cancer plan, such as the accessibility, preference bias in physician evaluation of the indication or shortage of resources and impact of reimbursement system. Finally, it is argued that a cancer plan is the framework for achieving the policy targets of the appropriate coverage of the evidence based indications for radiation oncology forecast.

Friday June 12, 2015

10:50-11:10: Christoffer Johansen, Copenhagen, Denmark

Patient-reported outcome measures

Johansen C. Danish Cancer Society Research Center, Copenhagen, Denmark

Patient Reported Outcomes (PRO) may serve as a new instrument informing the clinical decision proces and is probably a part of standard care of both cancer patients and patients in treatment for other chronic disorders within the next 5 to 10 years. This talk will put PRO into the context of Case Report Forms, Quality of Life scores and other patient reports used as proxies for well being or patients subjective experiences. The new phenomena related to PRO is, that for the first time, PRO will be used as a response from patients which will be included in the decision taken by clinicians. Thereby PRO present a challenge for clinicians as subjective information usually have been interpreted as inferior to objective observations, e.g., clinical examination, imaging or obtained by chemical analysis of blood/urine samples. Including PRO into decision making also becomes a difficult issue for patients as they gradually may become aware that responses to PRO questionnaires may contribute to these decisions. Several PRO scales have been developed and the terminology in these scales are now standardised in the so called PRO-CTCAE 'language', illustrating the drive to establish an instrument which may be used in all clinical settings. The presentation will cover these aspect of PRO.

Friday June 12, 2015

11:10-11:30: Vincenzo Valentini, Rome, Italy

Can automation in radiotherapy reduce costs?

Valentini V. Radiation Oncology Department, Gemelli-ART, Rome, Italy

The term automation refers to the use of various control systems for operating equipment or processes with minimal or reduced human intervention. Computerized automation can encompass all aspects of the radiotherapy process (Electronic Medical Record, image transfer and storage, treatment simulation and planning, treatment administration and treatment dosage verification) and can be used with the aim of optimizing patient services (processing of patientdata and care coordination) and individual practitioner (physician,dosimetrist, therapist, etc.) tasks. In recent years the economics of health care has been a topic of increasingly interest with competing demands on limited financial resources. Cost-effectiveness analysis is presented in the research literature as a methodology to help decision-makers allocate scarce resources by comparing the relative costs and outcomes (effects) of two or more courses of action. Computerized automation can impact on healthcare costs in many different ways. The most obvious one is by speeding up conventional tasks, meaning that more tasks could be completed in a typical work day. In the radiation oncology area, that allows to potentially increase the productivity for radiotherapy providers, decrease the waiting time for oncology patients, and reduce the need for investment in new radiotherapy units for payers. Computerized automation has also the potential to improve the quality and safety of patient treatments. A model to evaluate the economic impact of the introduction of a computerized automation tool somewhere in the radiotherapy chain for a typical radiotherapy provider is herein presented.

Friday June 12, 2015

11:30-11:50: Yolande Lievens, Ghent, Belgium.

Cost calculation: a necessary step towards widespread adoption of advanced radiotherapy technology.

Lievens Y1, Borras JM and Grau C. 1 Radiation Oncology, UZ Ghent, Ghent, Belgium.

Radiotherapy costs are an often-underestimated component of the economic assessment of new radiotherapy treatments and technologies. That the radiotherapy budget only consumes a finite part of the total cancer and health care budget does not relieve us from our responsibility to balance the extra costs to the additional benefits of the new, more advanced, but typically also more expensive treatments we want to deliver. Yet, in contrast to what is the case for oncology drugs, literature evidence remains limited, as well for economic evaluations comparing new radiotherapy interventions as for cost calculation studies. Even more cumbersome, the available costing studies in the field of radiotherapy fail to accurately capture the real costs of our treatments due to the large variation in cost inputs, in scope of the analysis, in costing methodology. And this is not trivial. Accurate resource cost accounting lays the basis for the further steps in health technology assessment leading to radiotherapy investments and reimbursement, at the local, the national and the worldwide level. In the presented paper we review some evidence from the existing costing literature and discuss how such data can be used to support reimbursement setting and investment cases for new radiotherapy equipment and infrastructure.

Poster discussion groups

(4 min presentation + max 6 min discussion for each poster – taking place next to the posters)

Group 1 Functional imaging in RT: PET
Kathinka Pitman, Oslo
Linda Wack, Tübingen
Daniel Warren, Oxford
Azadeh Abravan, Oslo
Marta Lazzeroni, Stockholm
Espen Rusten, Oslo
Mikkel Vendelbo, Aarhus
Morten Busk, Aarhus

Group 2 Functional imaging in RT: MRI
Anna Li, Oslo
Catarina D. Fernandes, Amsterdam
Kathrine R. Redalen, Lørenskog
Oscar Casares-Magaz, Aarhus

Group 3 In-room imaging
Jenny Bertholet, Aarhus
Lone Hoffmann, Aarhus
Mariwan Baker, Herlev
Mai L. Schmidt, Aarhus
Esben Worm, Aarhus
Maria Najim, Sydney
Ulrik V. Elstrøm, Aarhus
Lotte Lutkenhaus, Amsterdam

Group 4 Image analysis
Søren Haack, Aarhus
Martin Nielsen, Aalborg
Turid Torheim, Ås
Sara Carvalho, Maastricht
Ruta Zukauskaite, Odense
Jonathan Sykes, Sydney
Giske F. Opheim, Herlev
William (Bill) Nailon, Edinburgh

Group 5 Outcome and modelling
Anne W. Larsen, Aarhus
Christina M. Lutz, Aarhus
Anne Ramlov, Aarhus
Christina D. Lyngholm, Aarhus
Ferenc Lakosi, Liége
Emely Lindblom, Stockholm
Yasmin Lassen, Aarhus
Jørgen Johansen, Odense

Group 6 Planning challenges: Photons
Ditte S. Møller, Aarhus
Susanne Rylander, Aarhus
Marius R. Arnesen, Oslo
Bernt L. Rekstad, Oslo
Gitte Persson, Copenhagen
Stine Korreman, Roskilde
Anders T. Hansen, Aarhus
Patrik Sibolt, Roskilde

Group 7 Particle therapy challenges
Eirik Malinen, Oslo
David Hansen, Aarhus
Maria F. Jensen, Aarhus
Ellen M. Høye, Aarhus
Vicki T. Taasti, Aarhus
Anne I. S. Holm, Aarhus
Ida Mølholm, Lyngby
Shirin Rahmanian, Heidelberg

Group 8 Delivery solutions
Sidsel Damkjær, Næstved
Tine B. Nyeng, Aarhus
Rune Hansen, Aarhus
Annette Boejen, Aarhus
Jakob Toftegaard, Aarhus
Toke Ringbæk, Marburg
Alina Santiago, Marburg
Caroline Grønborg, Aarhus

Poster abstracts

Poster Discussion Group 1

Poster #1

Kathinka Elinor Pitman, Oslo, Norway

Variability of dynamic 18F-FDG-PET data in breast cancer xenografts

Pitman KE (1,2) , Rusten E (1,2), Kristian A (3), Malinen E (1,2). 1Department of Physics, University of Oslo, Oslo, Norway 2Department of Medical Physics/ 3Department of Tumour Biology, Oslo University Hospital, Oslo, Norway

Abstract Introduction: A murine breast cancer xenograft model was employed to evaluate inter- and intra-variability of various parameters derived from dynamic positron emission tomography with [18F]fluorodeoxyglucose as tracer (FDG-PET). Materials and Methods: 17 female athymic nude foxn1/nu mice with bila¬terally implanted triple-negative basal-like ductal carcinoma (MAS98.12) breast cancer xenografts underwent a dynamic PET scan over an hour after injection of ~10MBq FDG. Inter-animal data were obtained from the entire animal cohort, while intra-animal data were fro¬m four mice receiving an additional scan after one or two days. Standardised uptake values (SUVmax, SUVmean and SUVmedian) were estimated for all tumours and livers at different time points. Tumour uptake was analysed with a kinetic two-compartment model for estimation of pharmacokinetic parameters. The coefficient of variation (CV) was calculated for all PET-derived metrics. Results: The CV for SUVmean and SUVmedian was typically 10-20% for the tumours, depending on the time post injection and group (intra vs inter). The CV for SUVmax was mostly higher, both for tumour and liver. The variability in the pharmacokinetic parameters ranged from 23 to almost 150%. Conclusions: SUVmean and SUVmedian show less variability than SUVmax. Still, pharmacokinetic tumour metrics show much greater variability than the SUV based metrics. However, it is generally not known which of these metrics that best represents cancer aggressiveness and their use may still depend on the research questions addressed.

Poster #2

Linda Wack, Tübingen, Germany

Comparison of [18F]-FMISO, [18F]-FAZA and [18F]-HX4 for hypoxia PET imaging – a simulation study

Wack LJ(1), Mönnich D(1), van Elmpt W(2), Zegers CML(2), Troost EGC(2), Zips D(3), Thorwarth D(1). (1)Section for Biomedical Physics, University Hospital Tübingen (2)Department of Radiation Oncology (MAASTRO), GROW – School for Oncology and Developmental Biology, Maastricht, The Netherlands (3)Department of Radiation Oncology, University Hospital

A method for non-invasive assessment of hypoxia is positron emission tomography (PET) using dedicated radiotracers. Currently, several nitroimidazole-based hypoxia PET tracers are available, such as FMISO, FAZA, and HX4. The purpose of this study was to assess the image contrast of different hypoxia PET tracers. Tissue oxygenation was simulated on 5 vessel maps derived from tumor xenografts. The partition and diffusion coefficients for the tracers in tumor tissue were taken from literature or simulated using dedicated models and software. Blood activities for 20 to 45 different time points were derived from multiple clinical dynamic PET scans by selecting a region of interest in the heart or a major blood vessel. The data were fitted to an exponential function to determine clearance rate (CR) and the average input function for each tracer. PET signals after 2 and 4h post injection (pi) were simulated in hypoxic and normoxic tissue areas of 1x1mm2, presenting with median partial O2 pressure of 2.5±0.1mmHg and 35±2mmHg, respectively. Contrast was defined as the ratio of activity in hypoxic vs normoxic tissue areas. HX4 and FAZA presented with a higher CR (11.78*10-5 s-1 and 4.27*10-5 s-1 vs 1.90*10-5 s-1, $p<0.05$) than FMISO, but HX4 had a larger standard deviation (5.75*10-5 s-1 vs 1.55*10-5 s-1, $p=0.047$). At 2h pi, mean HX4 contrast (1.52) was slightly superior to FAZA and FMISO (both 1.34). 4h pi, HX4 and FAZA showed increase in mean contrast of 43% (HX4) and 5% (FAZA) compared to FMISO. HX4 had a higher inter-patient range in contrast (1.87-2.73 vs. 1.54-1.64, $p=0.025$). Mean contrast for each tracer varied 4-5% due to different vascular patterns found inside the tumor areas. At the late time point preferred in clinical studies, HX4 showed the highest contrast between hypoxic and normoxic tissue areas, whereas contrast for FAZA was similar to FMISO. However, FMISO may lead to more reliable clinical results as the range in contrast observed is lower than for HX4.

Poster #3

Daniel Warren, Oxford, United Kingdom

A predictive model of three-dimensional hypoxia distributions in tumours

Warren, D R and Partridge, M. CRUK/MRC Oxford Institute for Radiation Oncology, University of Oxford, Oxford, United Kingdom

INTRODUCTION: Hypoxia has been implicated as a major source of radioresistance in a number of cancers. Imaging studies typically show a heterogeneous distribution within the gross tumour volume, and image-derived hypoxia regions have been proposed as targets for dose painting. However, characteristic distances for oxygen diffusion in tissue (~100µm) are smaller than the resolution of PET imaging (~5mm), thus a broad distribution of pO2 values is expected within each PET voxel, increasing the complexity of radiosensitivity calculations. The purpose of this work is to assess the extent to which microscopic pO2 distribution can be inferred from voxel-scale measurements. MATERIAL AND METHODS: A MATLAB simulation is presented where blood vessels are represented by the intersection of infinite cylinders and a 1mm^3 domain (10^6 voxels), with spatial distribution, orientations and radii sampled from user-defined probability density functions. The vessel map is used as a source term for 2D and 3D diffusion equations with oxygen consumption, which are solved to steady-state by finite difference methods. RESULTS AND CONCLUSIONS: Significantly different pO2 distributions are observed in the 2D and 3D simulations for the same source distribution. The 2D simulations do not properly reproduce the expected pO2 histograms. For 100 randomly generated 3D source maps with vessel densities of 100, 150 and 200 vessels/mm^3, predicted hypoxic fractions range between 16–26%, 1–8% and 0–2% respectively, which is consistent with published experimental data. A monotonic, quasi-linear increase in hypoxic fraction is seen with decreasing vascularisation over a biologically relevant range (mean tissue pO2 1–12 mmHg). Vessel density is not the only determinant of hypoxic fraction; work is in progress to quantify the effect of vessel radius and oxygen tension, and to model perfusion of misonidazole, which will enable the prediction of histologically-defined hypoxia and 18F-MISO PET images.

Poster #4

Azadeh Abravan, Oslo, Norway

Correlation between normal tissue dose and 18F-FDG-PET uptake for non-small cell lung cancer patients receiving thoracic radiotherapy and erlotinib

Abravan Azadeh 1, Knudtsen Ingerid Skjei 1, 2, Eide Hanne 3, Brustugun Odd Terje 3, Helland Åslaug 3, Malinen Eirik 1, 2. 1: Department of Physics, University of Oslo, Oslo, Norway 2: Department of Medical Physics, Oslo University Hospital, Oslo, Norway 3: Department of Oncology, Oslo University Hospital, Oslo, Norway

Introduction Cytotoxic effects in organs at risk (OARs) are dose limiting factors for both radio-therapy (RT) and targeted-therapy. Medical imaging such as 18FDG-PET/CT may be employed to study the response patterns in normal tissues and to identify cytotoxic effects of treatment. Methods 22 patients with advanced stage non-small cell lung cancer, participating in a phase II trial on combined radiation and erlotinib therapy, were included. The patients were examined by 18F-FDG-PET/CT at three sessions; prior to, one week into, and six weeks after fractionated radiotherapy (3Gy x 10). Nine patients received fractionated RT only, while 13 patients received erlotinib and fractionated RT. For each patient, lungs, heart, esophagus, and bone marrow were delineated in CT images. The FDG-uptakes within volumes, represented by standardized uptake values (SUVs), were extracted. The RT dose matrix was co-registered with the PET/CT image series. SUVmean was calculated in dose bins of 0.5 Gy to identify the association between SUV and RT dose. The effect of erlotinib was also investigated. Results A linear relationship was identified between SUV and RT dose in many OARs at both mid- and post-therapy, considering all patients. A strong positive correlation between lung SUV and RT dose was identified at mid-therapy. However, the FDG-uptake was significantly higher (16%) in the erlotinib-receiving group. At post-therapy, patients receiving erlotinib again had a significantly elevated FDG-uptake in lung but the association with RT dose was absent. For other OARs no significant differences were identified by separating patients based on erlotinib treatment. Conclusions Normal tissue glucose metabolism correlated with RT dose during the first week of treatment. Erlotinib increased the FDG uptake in the lung compared to RT only. This study indicates that more detailed follow-up of lung toxicity in patients undergoing erlotinib therapy is required.

Poster #5

Marta Lazzeroni, Stockholm, Sweden

Evaluation of early response in H&N cancer patients based on effective radiosensitivity derived from repeated FDG-PET scans

Lazzeroni M (1), Uhrdin J (2), Sonke J-J (3), Hamming-Vrieze O (3), Dasu A (4) , Toma-Dasu I (1,5). 1 Onc Path Dept,Karolinska Institute Stockholm (SE),2 RaySearch Laboratories AB Stockholm (SE),3 Dept Rad Oncol, The Netherlands Cancer Institute Amsterdam (NL),4 Dept Rad Phys, Linköping University (SE),5 Med Rad Phys Dept, Stockholm University (SE)

Treatment failure for advanced head and neck (H&N) cancers is often due to poor locoregional control and it is important to early identify the patients with poor response at risk of local recurrence. The aim of this study was to evaluate the feasibility of applying a previously developed method for assessing the early responsiveness of tumours during radiotherapy for H&N. Ten patients undergoing concurrent chemoradiotherapy were imaged with FDG-PET before the start and during the 2nd week of treatment. A systematic voxel based analysis was performed on the 2 registered PET images and an operational parameter, the effective radiosensitivity αeff, was determined at voxel level based on uptake variations and delivered dose distribution. The average and negative fractions of αeff values were derived within the primary GTV. The analysis was feasible and not affected by the location and complex shape of H&N targets and their changes during the first 2 weeks of treatment. The range of average αeff in the primary GTVs was -0.017-0.026 Gy-1 while the range of the negative fraction of αeff was 10.4-71.2%. A stratification of the patients was attempted by applying criteria based on average αeff >0.004 Gy-1 and negative fraction of αeff <40% previously determined for complication free survival at 2 years for concurrent chemoradiotherapy in lung cancer. Results indicate that 50% of the cases had a simultaneous average αeff >0.004 Gy-1 and a negative fraction of αeff <40%. The voxel based method used for tumour response assessment appears feasible for H&N cancers to stratify the patients according to their apparent response at the time of the 2nd PET investigation. The study will include more patients and the correlation with outcome will be further investigated when results at a relevant clinical endpoint will become available to determine thresholds to discriminate between responders and non-responders corresponding to the higher survival expected from this trial.

Poster #6

Espen Rusten, Oslo, Norway

Early radiotherapy response monitoring of anal carcinoma with 18F-FDG-PET

Rusten E, Rekstad BL, Undseth C, Hernes E, Guren MG, Malinen E. Department of Physics, University of Oslo, Oslo, Norway. Department of Medical Physics / Department of Oncology / Department of Radiology and Nuclear Medicine, Oslo University Hospital, Oslo, Norway

Introduction Anal carcinoma is a rare cancer, and the curative treatment is chemoradiotherapy. Although survival rates are quite high, some patients need salvage surgery due residual disease, and 15-20% develop locoregional recurrence. It is important to identify early markers of therapy-resistant disease in order to further tailor treatment and improve outcome. In this study, 18F-FDG-PET is used to assess early changes in tumor metabolism two weeks into radiotherapy. Materials and methods Eleven patients with anal carcinoma from a prospective clinical trial were included. Patients received fractionated radiotherapy to a total dose of 54 Gy or 58 Gy with concomitant Mitomycin C and 5-fluorouracil. 18F-FDG-PET images were acquired before treatment (pre) and two weeks into treatment (mid). The primary tumor was delineated in each image series. The maximum standardized uptake value (SUVmax) in the tumor was extracted. Cohort based median and range was calculated. A Wilcoxon signed rank test was used to evaluate changes in SUVmax from pre to mid treatment. Results All patients had FDG-PET-positive tumor. The median SUVmax pre treatment was 11.4, with a range of [6.0, 23.5]. Mid treatment, the corresponding values were 8.0 and [5.4, 12.4]. The reduction in SUVmax from pre to mid treatment was highly significant ($p<0.01$) for the current cohort. The median relative change in SUVmax was 28 %, and seven patients showed a partial metabolic response (> 25 % reduction in SUVmax) . Conclusions Anal carcinomas appear highly FDG-PET-avid. A high proportion of patients show a metabolic response already two weeks into radiotherapy. The remaining non-responders may be at risk of locoregional failure. More patients will be included in this prospective study, and the PET responses will be related to outcomes.

Poster #7

Mikkel Vendelbo, Aarhus, Denmark

PET-based assessment of tumor IGF1- and insulin receptor expression and its linkage to anti-receptor treatment response

Vendelbo MH (1), Busk M (2), Bender DA (1), Iversen AB (2), Jessen N (3,4,5), Frøkiær J (1), Morsing A (1). 1) Department of Nuclear Medicine and PET center, 2) Department of Experimental Clinical Oncology, 3) Research Laboratory for Biochemical Pathology, 4) Department of Molecular Medicine, Aarhus University Hospital

Background: IGF1- and Insulin receptors (IGF1R and IR) are increased in various cancers. Receptor stimulation leads to enhanced glucose consumption and protein synthesis and thus tumor growth through the Akt/mTOR pathway. Increased expression of IGF1R has been linked to radioresistance, and IGF1R is an emerging target in radiotherapy. The IGF1R and IR inhibitor OSI906 has shown promising results and is undergoing clinical testing. Aim: We set out to investigate if IGF1R and IR inhibition is associated to decreased Akt/mTOR activation and glucose uptake in cancer cells, and to develop a PET detectable probe for IGF1R and IR based on chemical modification of OSI906. Methods: OSI906 was used to detect Insulin and IGF1 sensitive cancer cells. Effect of inhibition was assessed with 18F-FDG uptake, measurements of glycolysis and phosphorylations on Akt and mTOR in stimulated and non-stimulated conditions. Furthermore, we are currently assessing the specificity of [11C]-methyl-OSI906 in tissue samples. Results: Metabolic in vitro assays based on 18F-FDG and extracellular flux analysis revealed that both insulin and IGF stimulated glucose uptake and lactic acid formation in most cell lines. These changes were effectively inhibited by OSI906. The most pronounced effect was detected in SW948 colon cancer cells and in accordance with metabolic data, Akt and mTOR phosphorylation could be stimulated by IGF1 and insulin, and this stimulation was effectively inhibited by OSI906. Non-radioactive methyl-OSI906 (backbone for the PET tracer) was able to block receptor stimulation and we are currently assessing the specificity of [11C]-methyl-OSI906. Conclusions: Present results demonstrate that IGF1R and IR inhibition reduce Akt/mTOR signaling, glycolysis and 18F-FDG uptake in SW948 cells. Furthermore, [11C]-methyl-OSI906 may detect cells responsive to IGF1R and IR inhibition monotherapy or combination therapy with radiotherapy, which could allow for rational individualized therapy.

Poster #8

Morten Busk, Aarhus, Denmark

Pre-clinical assessment of the robustness and reliability of PET-based identification and quantification of tumor hypoxia

1Busk M, 1Iversen AB, 2Jakobsen S, 1Overgaard J, 1Petersen JB, 2Munk OL, 2Frøkiær J and 1Horsman MR. 1) Department of Experimental Clinical Oncology, Aarhus University Hospital, Aarhus, Denmark (AUH); 2) PET centre, AUH, Aarhus, Denmark

Background. Tumor hypoxia is linked to poor prognosis, but personalized hypoxic intervention with radiosensitizers (e.g., nimorazole) or dose escalation to hypoxic tumor volumes may improve outcome. Hypoxia-selective PET tracers like FAZA is available, but inherent weaknesses of PET in general (low resolution) and hypoxia PET in particular (low image contrast due to slow tracer retention and clearance) may compromise the quantitative accuracy and reproducibility of hypoxia PET. Methods. To assess the severity of this problem, UMSCC47 (human Head and Neck), SiHa (human cervix) or SCCVII (murine head and neck) tumors were established in mice. Subsequently, mice were administered FAZA and scanned on two consecutive days using a high-resolution (~1 mm) Mediso nanoPET/MRI. Scans were performed at two different post-injection (PI) time points to mimic the image contrast obtainable clinically (1.5h PI) and a much better contrast (3h PI), which can only be obtained in rodents due to rapid clearance of unbound tracer in organisms with high metabolic rates. On the next day, mice were administered FAZA and the hypoxia marker pimonidzole and scanned again (at 1.5h or at 1.5 and 3h) followed by tumor dissection, cryosectioning and high-resolution analysis of tracer distribution (autoradiography) and hypoxia (pimonidazole) on multiple tissue sections covering the whole tumor volume. Results/discussion. Using PET scans and invasive tissue analysis, the following questions are addressed during our ongoing work: 1) do target definition differ substantially at a clinical relevant contrast at 1.5h and a superior contrast at 3h at a high (1 mm, animal scanner) and low (4 mm, clinical scanners) resolution, respectively? 2) is target definition reproducible on consecutive days and how do robustness of target definition depend on different quantification measures? To what extent do PET images at a clinical relevant contrast reflect the voxel-wise true distribution of hypoxic cells?

Poster Discussion Group 2

Poster #9

Anna Li, Oslo, Norway

Hypoxia imaging with dynamic contrast enhanced MRI and focal brachytherapy of cervical cancers

Anna Li (1,2), Erlend Andersen (2,3), Christoffer Lervåg (4), Cathinka H. Julin (5), Heidi Lyng (5), Taran P. Hellebust (1,2), Eirik Malinen (1,2). 1) Dep. of Physics, University of Oslo, Norway. 2) Dep. of Medical Physics, Oslo University Hospital, Norway. 3) Sørlandet Hospital Trust, Norway. 4) Dep. of Cancer Therapy, Ålesund Hospital,Norway. 5) Dep. of Radiation Biology, Oslo University Hospital,Norway

Purpose: To derive a novel method to segment dynamic contrast enhanced magnetic resonance (DCEMR) images of patients with locally advanced cervical cancers (LACC), to investigate the relation between segmented tumor subvolumes and a previously published hypoxia gene signature, and to perform brachytherapy planning based on the segmented images. Materials and methods: Pharmacokinetic ABrix maps were derived from DCE-MR images taken prior to chemoradiotherapy of 78 patients with LACC. A logistic regression procedure was used to segment the tumor volume fraction from the ABrix maps that showed the strongest association with patient survival, denoted biological target volume (BTV) fraction. A hypoxia gene score was calculated from the gene signature and correlated against the BTV fraction. Brachytherapy planning based on the ABrix maps was performed, for 23 patients. Two planning approaches were investigated: (1) a conventional uniform and (2) a non-uniform targeted approach. Results: The segmented BTV fraction was significantly associated local and locoregional control ($P<0.025$) and the hypoxia gene score ($P=0.002$). Comparing brachytherapy approaches 1 and 2, it was possible to escalate the dose to the BTV with 0.4 Gy per brachytherapy fraction in median (range: [0, 3.8]). Some tumors could not be dose escalated without violating the dose constraints to the organs at risk. Conclusions: A method to segment the most aggressive tumor region was presented. The segmented region may be targeted with hypoxia guided brachytherapy to improve treatment outcome.

Poster #10

Catarina Dinis Fernandes, Amsterdam, The Netherlands

Characterising irradiated prostate tissue in radio-recurrent PCa patients using mp-MRI and histopathology

Fernandes, C.D., Ghobadi, G., de Jong, J., Dinh, C., van Houdt, P.J., Smolic, M., van der Poel, H.G., van der Heide, U.A. Department of Radiation Oncology, The Netherlands Cancer Institute, Amsterdam, The Netherlands

Aim: Multi-parametric MRI (mp-MRI) is not yet standard in diagnosing radio-recurrent prostate cancer (PCa) as the interpretation of images is complicated by the presence of radiation effects. Although patients only sporadically receive a salvage radical prostatectomy (SRP) we have collected a dataset of 7 radio-recurrent PCa patients who underwent a mp-MRI (T2w, DWI- and DCE-MRI) prior to SRP. We aim to characterise imaging of prostate tissue after radiotherapy (RT), using pathology as ground truth. Materials/Methods: Central whole-prostate histopathology slices were selected and the best corresponding slices on T2w MRI were visually identified. Images and histopathology slices were then registered using 2D deformable registration. Tumour regions were delineated on scanned histopathology slices by an experienced uropathologist and propagated to imaging. Signal intensity (SI) of T2w images was normalised to skeletal muscle. Median and distribution range values (Q10%-Q90%) were calculated for T2w, ADC, Ktrans and kep in tumour and other prostate regions, and then averaged per region. Sagittal T2w MRI was used for peri-urethral (PU) zone delineation. Results: Median T2w (normalized SI) was similar between tumour 2.33[1.71-3.20] and non-tumour tissue 2.25[1.35-3.26]. The PU zone had the highest T2w median 2.81[1.98-3.89]. The median ADC (x10-3mm2/sec) value was lower for tumour 1.09[0.83-1.36] than non-tumour 1.20[0.83-1.49]. The PU zone had the highest median ADC value 1.40[1.15-1.65]. The Ktrans median (min-1) was higher for tumour 0.24[0.14-0.50] than non-tumour 0.16[0.09-0.34], while the PU zone had the highest value 0.41[0.31-0.55]. The kep median (min-1) was 0.46[0.28-0.82] for tumour, 0.33[0.20-0.50] for non-tumour, and 0.47[0.39-0.59] for the PU zone. Conclusion: Tumour in the PU zone is hard to identify using Ktrans and kep. T2w and ADC may provide a better distinction and aid the diagnosis of recurrent tumour after RT in this particular prostatic region.

Poster #11

Kathrine Røe Redalen, Lørenskog, Norway

Quantitative diffusion-weighted MRI of rectal cancer is strongly influenced by the choice of b-values

Bornstein M, Negård A, Holmedal SH, Meltzer S, Borthne AS, Ree AH, Redalen KR. Department of Oncology, Akershus University Hospital, Lørenskog, Norway. Department of Radiology, Akershus University Hospital, Lørenskog, Norway. Institute of Clinical Medicine, University of Oslo, Oslo, Norway.

Introduction: The apparent diffusion coefficient (ADC) is calculated from diffusion-weighted MRI (DWI) acquired with at least two degrees of diffusion-weighting, i.e., b-values, most commonly by a simplified monoexponential model. Recognising the lack of consensus on optimal b-value selection for ADC calculation in rectal cancer, we aimed to examine how different b-value combinations in the monoexponential model affect resulting ADCs. ADC calculated by a biexponential model, accounting for contributions from blood perfusion to the diffusion signal, was used as the reference ADC. Materials and methods: DWI with seven b-values (b = 0, 25, 50, 100, 500, 1000 and 1300 s/mm2) was acquired from six rectal cancer patients enrolled in the prospective study OxyTarget (NCT01816607) on a 1.5T Philips Achieva MRI scanner. Two experienced radiologists contoured whole-tumour ROIs. ADCs were calculated from 15 different b-value combinations in the monoexponential model as well as by the biexponential model incorporating all b-values. Results: Significant variability in tumour ADCs was detected for the different b-value combinations. Using all seven b-values in the monoexponential model overestimated mean tumour ADC by 85% ($P<0.001$) compared to the reference ADC. The ADCs were significantly reduced when excluding low b-values (0, 50 and 100 s/mm2). The b = 0 s/mm2 is commonly included in ADC calculation; this study shows its inclusion results in a substantial overestimation. The combination of b = 500 and 1300 s/mm2 resulted in a deviation of only 0.7% compared to the reference ADC. Conclusion: In rectal cancer, tumour ADC calculated using the monoexponential model is strongly influenced by the choice of b-values. By eliminating the contribution from perfusion ($b \leq 100$ s/mm2) the uncertainty in the ADC calculation is significantly reduced. Quantitative inter- and intratumour comparisons should not be performed if the ADCs are calculated using DWI with different b-value combinations.

Poster #12

Oscar Casares-Magaz, Aarhus, Denmark

Biomechanical image-based rectal properties following radiotherapy of prostate cancer

O. Casares-Magaz1, M. Thor2, D. Liao3, J. Frøkjær4, P. Kræmer5, M. Høyer5, K. Krogh6, A. M. Drewes7, V. Moiseenko8, J. Deasy2 and L. Muren1.

INTRODUCTION: Biomechanical properties of the rectum may disclose key components of organ function and hence be associated with morbidity after RT. The aim of this study was therefore to explore biomechanical properties for the rectum in patients with prostate cancer treated with RT. More specifically, we present a method to measure changes in thickness and elasticity of the rectal wall using MRI. MATERIAL AND METHODS: Four patients previously treated with RT for prostate cancer underwent an MRI session with step-wise rectal balloon inflation (from 0ml to a maximum tolerable volume, in 50ml steps). MRIs were acquired using Dixon sequences at each inflation step, and a probe was inserted inside the balloon to monitor the internal rectal pressure. The rectal walls were defined from the recto-sigmoidal junction to 3 cm from the distal anal canal surface. Biomechanical properties were calculated from the pressure measurements and the MRI-segmented rectal walls and included strain, stress, stiffness and wall thickness. Pearson's correlation (Pr) was applied to investigate potential relationships between properties. RESULTS: The integral rectal pressure ranged from 1.3 to 4.6kPa with the largest values observed for the maximum tolerable volume (ranged from 150 to 250ml). The population median (range) of the rectal strain, stress, and stiffness was 0.12 (0.07-0.34)kPacm2, 3.7 (0.6-22.2)kPacm2, and 26.3 (3.0-221.2). Corresponding values for the rectal wall thickness were 2.9 (2.2-3.9)mm. Biomechanical properties were modest correlated (Pr<0.60), except between strain/stress and stiffness (Pr=0.97). Further work will correlate these properties with dose/volume parameters. CONCLUSION: We presented a method to measure various biomechanical properties of the rectal wall. The findings could provide guidance in future rectum outcome modelling, where at most only the rectal volume is accounted for, in order to better understand the complex rectal dose-volume response relationship.

Poster Discussion Group 3

Poster #13

Jenny Bertholet, Aarhus, Danemark

Targeting accuracy in image-guided stereotactic liver radiation therapy with and without time resolved rotation corrections

J. Bertholet, W. Fledelius, E.S. Worm, M. Høyer, P.R. Poulsen. Department of oncology, Aarhus University Hospital, Denmark

Purpose: Image-guided liver SBRT often relies on markers implanted near the tumor. The localization accuracy is known to decrease with increased marker-target distance. This may be partly due to rotations and could therefore be improved using rotational correction. The aim of this study was to calculate time resolved translation and rotations of liver markers constellations and investigate if rotational corrections can improve the targeting accuracy in liver SBRT. Method: 29 patients with three implanted markers received SBRT in 3-6 fractions. The markers were retrospectively segmented on CBCT projections and their 3D trajectories were estimated by a probability based method. For each CBCT scan, the time-resolved translation and rotation of the marker constellation were calculated. The mean vector AB from Marker A to Marker B was calculated for each marker pair and used to estimate the position of Marker B in three scenarios: (1) as Marker A's mean position plus AB, i.e. no time-resolved estimation; (2) as Marker A's time-resolved position plus AB; and (3) as Marker A's time-resolved position plus AB corrected with the time-resolved rotation of the marker constellation. The rotation correction used either the calculated angles (3A) or angles estimated using the correlation between rotations and the superior-inferior (SI) marker position (3B). The targeting accuracy was quantified as the root-mean square error (rmse) for each CBCT. Results: The 3D mean targeting rmse was 3.2mm (Scenario 1), 0.9mm (Scenario 2), 0.6mm (Scenario 3A), and 0.7mm (Scenario 3B). The time with 3D rmse below 1mm was 4% (1), 75% (2), 92% (3A), and 82% (3B). The 3D rmse correlated significantly with marker-marker distance. Conclusion: Rotational correction improves targeting accuracy in liver SBRT. The needed time-resolved rotation angles for the correction may be estimated from the SI marker position by utilizing patient-specific pre-determined correlations between rotations and translations.

Poster #14

Lone Hoffmann, Aarhus, Denmark

Positional stability of fiducial markers in oesophageal cancer patients during radiotherapy treatment

Hoffmann, L (1) Nyeng, TB (1) Andersen MH (2) and Nordsmark, M (2). (1) Department of Medical Physics, Aarhus University Hospital, Denmark (2) Department of Oncology, Aarhus University Hospital, Denmark

Introduction. Large interfractional anatomical changes are observed in oesophageal cancer patients (pts) at the daily treatment fractions due to e.g. oesophageal peristalsis and abdominal filling. The aim of the present study was to investigate the usability of Olympus and Boston Scientific fiducial markers for verification of interfractional positional changes of the primary tumour. Materials and methods. Fourteen consecutive pts were treated with chemoRT for oesophageal cancer. The median gross tumour volume GTV was 43cm3 (9-141cm3) and the median cranio-caudal extend was 7cm (2-10cm). The pts were setup according to daily online kV CBCT imaging. In 12 pts, markers were implanted at the cranial and caudal border of GTV and in two pts only one marker was implanted. The interfractional shifts between each marker and the GTV soft tissue match were recorded retrospectively from the daily CBCTs. Results: Fourteen markers were visible at the planning CT (54%). Four markers disappeared before the fifth treatment fraction and were excluded. Thus, ten marker positions were recorded. Only three markers (12%) were visible at the last CBCT scan. The mean 3D interfractional displacement between the marker and GTV was 6.7mm with systematic/random errors of 3.0/7.3mm. Thus, large positional differences between the marker and the GTV were observed. In two pts, 3D deviations above 5mm were seen for all fractions. Overall, no preferential direction was observed for the displacements. However for the individual pts, the displacements were primarily seen in one direction. The deviation between the GTV and the marker may have more explanations such as migration of the marker, deformation of the tumour or both. Conclusion: Olympus and Boston Scientific markers have a tendency to migrate and disappear during the RT treatment. Fifty-four percent of the implanted markers were visible at planning CT and only 12% were visible at the end of the RT course.

Poster #15

Mariwan Baker, Herlev, Denmark

Using Real-time Four-dimensional Ultrasound Imaging to Determine Prostate Displacement during Transabdominal Ultrasound Image-guided Radiotherapy

Mariwan Baker1,2, and Claus F. Behrens1. 1: Department of Oncology, Radiotherapy Research Unit, Herlev Hospital, University of Copenhagen, Herlev, Denmark 2: Center for Nuclear Technologies, Technical University of Denmark, DTU Risø Campus, DK-4000 Roskilde, Denmark

Transabdominal ultrasound (US) imaging is currently available for localizing the prostate in daily image-guided radiotherapy (IGRT). The aim of this study was to determine the prostate induced displacements during such transabdominal US imaging. The prostate displacement was monitored using a novel transperineal 4D US system. Materials and Methods Nine prostate cancer patients, mean age 69 years (58/80), were US scanned in the CT room utilizing the Clarity transperineal 4D monitoring system (Clarity®, Elekta, Stockholm, Sweden). The patients were asked to comply with a moderate bladder-filling protocol. After US-CT fusion, the prostate volume was delineated and used as reference for weekly US imaging in the treatment room. Prior to treatment, kilovoltage (kV) images was acquired for prostate alignment by utilizing implanted gold fiducial markers. Immediately after treatment delivery the transperineal 4D US monitoring system was set up. During real-time tracking of the prostate, a conventional 2D probe was applied to simulate a transabdominal US scan. Thus the prostate displacements induced by the 2D probe pressure were recorded for the three orthogonal directions. During the simulation, also superfluous probe pressure was applied. In total 40 monitoring curves with applied 2D probe was recorded. Results The overall mean value (±1SD) of the probe induced displacements of the prostate was [mm]; anterior (+)-posterior (AP): (-0.3±1.2), inferior (+)-superior (IS) (0.1±0.9), and left (+)-right (LR): (0.2±0.8). The largest displacement was -2.9 mm and 2.1 mm in posterior and inferior directions, respectively. Conclusion The novel 4D US system was capable in tracking and recording the prostate positional displacements. Proper education of the staff is necessary for safe implementation of the system. The study showed that the prostate induced displacements due to applied transabdominal US IGRT are small and in most cases clinically irrelevant for prostate radiotherapy.

Poster #16

Mai Lykkegaard Schmidt, Aarhus C, Denmark

Time-resolved differential motion of tumor and lymph nodes during conebeam computed tomography (CBCT) of lung cancer patients

Mai L Schmidt,1,2, Marianne Knap,1, Torben R Rasmussen,3, Birgitte H Folkersen,3, Lone Hoffmann,4, Ditte S Møller,4, Per R Poulsen,1,2. 1: Department of Oncology, Aarhus University Hospital, DK. 2: Institute of Clinical Medicine, Aarhus University, DK. 3: Department of Pulmonology, Aarhus University Hospital, DK. 4: Department of Medical Physics, Aarhus University Hospital, DK

Introduction: The accuracy of radiotherapy delivery to lung cancer patients is challenged by the motion of the tumor (T) and the lymph node (LN) targets caused by respiratory and cardiac motion. In this study the differential time-resolved three-dimensional (3D) internal motion was investigated from CBCT scans acquired throughout the treatment course for lung cancer patients. Material and Methods: Six patients with Visicoil markers implanted by EBUS bronchoscope in the T and/or LN targets received IMRT in 30-33 fractions. Before each fraction a setup CBCT scan with ~675 projections was acquired during a full gantry rotation. The CBCT scans were used for daily online soft tissue match on T. Offline, the Visicoil positions were segmented in each projection image using a semi-automatic template-based algorithm. The 3D Visicoil trajectories were estimated from the segmented positions by a probability-based method. Results: The motion of in total 19 Visicoils during 185 setup CBCT scans for 6 patients were segmented. The motion was largest in the cranial-caudal (CC) direction, mean 8.3mm (range 4.6-14.1mm) compared to left-right (LR): 2.3mm (1.6-3.6mm) and anterior-posterior (AP): 4.1mm (2.1-6.6mm). The most caudal Visicoils had substantially larger CC motion than the more cranial ones; e.g. one patient had a Visicoil in the primary tumor (12R) with a CC motion of 14.1mm (10.1-17.8mm) compared with the Visicoil in LN station 4R with a CC motion of 6.5mm (4.7-10.6mm). Frequency analysis showed that the caudal Visicoils only had a respiratory induced motion, with no cardiac motion, whereas the more cranial ones had considerable cardiac induced motion. Conclusion: Highly detailed time-resolved internal 3D motion was determined throughout lung IMRT using standard imaging equipment. Variations between the different targets were observed, while the most caudal targets motion were governed by respiration, the more cranial LNs had substantial cardiac induced motion.

Poster #17

Esben Worm, Aarhus, Denmark

Is a delay between marker insertion and planning CT needed in fiducial marker guided liver SBRT?

Worm ES (a), Bertholet J (b), Høyer M (b), Fledelius W (b), Hansen AT (a), and Poulsen PR (b,c). Departments of (a) Medical Physics and (b) Oncology, Aarhus University Hospital, Aarhus, Denmark. (c) Institute of Clinical Medicine, Aarhus University, Denmark.

Introduction In fiducial marker guided liver SBRT it is crucial that the geometric marker-to-tumor relationship remains constant from the time of planning CT to treatment. To minimize the risk of marker migration it is often recommended to add a delay of several days between marker insertion and CT. However, a delay prolongs the RT planning process which, to avoid tumor progression, should be kept short. The aim of this study was to investigate whether the time lapse between marker insertion and CT plays a role for marker stability in the liver. Methods 29 patients each had 3 gold markers implanted for three-fraction liver SBRT at a conventional LINAC. A 4DCT was acquired for treatment planning. CBCT-guidance was used for patient setup. All markers were retrospectively segmented in the 4DCT and in all projections of the CBCT acquired at first treatment fraction. For the CBCT projections, the segmentations provided the 3D marker trajectories during CBCT by a probability based method. For each marker-pair (n=87) the difference between the mean marker-pair vector in the 4DCT and the same mean marker-pair vector in the CBCT defined the marker-marker prediction error. Such an error may arise from liver deformations, rotations, and marker migration. Spearman's rank test was used to test for correlation between marker-marker prediction error and time lapse between marker insertion and 4DCT. Results The median [10th–90th percentile] time lapse between marker insertion and 4DCT was 2 days [1-9 days]. The mean [10th–90th percentile] 3D marker prediction error was 2.0mm [0.7-3.5mm]. No correlation was found between the marker prediction error and number of days between marker insertion and 4DCT (Tau=-0.04, p=0.70). Conclusion We found no indication for a delay of several days between marker insertion and CT. However, marker prediction errors of several mm were observed. Preferentially, three markers or more should be inserted to address such uncertainties at patient setup

Poster #18

Maria Najim, sydney, Australia

Retrospective review to assess volumetric and dosimetric change in organs at risk (OAR) during IMRT/VMAT treatment for HN cancer

Dr M Najim, A/Prof M Veness, Dr L Perera, Dr J Sykes, L Bendall. Department of Radiation Oncology Westmead, Sydney University

To document anatomical and dosimetric change during a course of IMRT/VMAT for patients with HN cancer. Materials and Methods Retrospective review of 20 patients who underwent comprehensive IMRT/VMAT treatment from 2013-14. OAR were contoured on initial planning CT scans, and weekly CBCT scans. Volumes were assessed at end of treatment and compared with initial volumes. Cumulative dose was recorded for OAR and compared with that from the initial DVH. Results: 17 male, 3 female patients Mean age 61 years (43-76) 9 exsmokers, 3 current smokers, 8 nonsmokers. Majority of patients were T1-2, N2 stage. Most patients lost weight throughout their treatment. Mean weight loss was -4.7% (=2.8 to -15.5%). Cumulative dose and volume to OAR did not significantly change from baseline, except in the PG Mean volume reduction in the PG was 24.4% (0-53.6%) This was observed in 80-90% of patients, and more pronounced in the contralateral PG (-27% c/w -22%). Mean PG volume loss was 0.7%/treatment day (0-1.5%). Most of the volume change occurred between fraction 15-20, after which the mean change in PG volume plateaued. PG shifted medially in all patients throughout treatment. Mean shift in PG was 3.4mm (2-6.7mm) Mean increase in PG dose was 19.5% (-6.7 to 61%). These changes again were more pronounced in the contralateral PG (23.4% c/w 15.7%). Again, these changes were more pronounced between fraction 15-20. Conclusion: There was no significant change in volume or cumulative dose to OAR except in the PG During the course of treatment there was significant volumetric change in the PG. This was associated with a shift in the PG medially, and an increase in the cumulative dose compared to that initially planned. These changes were more pronounced between fractions 15 to 20. These results have lead to a prospective study which is currently underway, which will also focus on clinical outcomes.

Poster #19

Ulrik Vindelev Elstrøm, Aarhus, Danmark

Cone-beam CT-based Dose Calculation in Radiotherapy of Head and Neck Cancer

Elstrøm U.V.1; Hvid C.A.2; Muren L.P.1,2; Petersen J.B.B.1; Grau C.2. 1) Aarhus University Hospital, Dept. of Medical Physics, Aarhus C, Denmark. 2) Aarhus University Hospital, Dept. of Oncology, Aarhus C, Denmark

The implications of anatomical changes during a course of radiotherapy for head and neck (H&N) cancer can potentially be reduced through image-based adaptive RT (ART) strategies. In-room imaging modalities like cone-beam CT (CBCT) provides images that potentially can be useful in ART. Developments in CBCT calibration and reconstruction have resulted in improved image quality. The aim of this study was to directly compare treatment planning calculations based on optimised CBCT vs. conventional CT scans in a series of H&N cancer patients. The study included thirteen patients with locally advanced H&N cancer treated with IMRT that had both a conventional CT and a high-quality CBCT acquired on the same day, halfway through the treatment course. The CBCT projections were reconstructed twice, using both the standard clinical method as well as an experimental reconstruction algorithm. Delineated structures on CT were propagated to the CBCT scans using deformable image registration. The original treated IMRT plan was re-calculated on both the CT and the two CBCTs, and key dose/volume-parameters for the plans were compared. There was a significant reduction in volume from CT to CBCT for all volumes investigated for both reconstruction methods, although most pronounced with the standard clinical reconstruction, with the mean difference ranging from 2 to 13%. The mean doses to target volumes and the parotid glands were higher for CBCT (with at most 1.7%), yet with a significant difference between the reconstruction methods for the targets. The maximum doses on the mandible and spinal cord decreased with at most 1.9% using CBCT-based dose calculation. The differences in dose/volume-parameters for both targets and critical normal tissues from CT- vs. CBCT-based planning were found to be within a clinically acceptable range. Improved CBCT image quality diminishes the discrepancies to CT. The results of this study open a potential for CBCT-based ART for patients with H&N cancer.

Poster #20

Lotte Lutkenhaus, Amsterdam, The Netherlands

A comparison of two adaptive strategies for radiotherapy of urinary bladder cancer using biological models

Lutkenhaus, L.J., Vestergaard, A., Bel, A., Høyer, M., Hulshof, M.C.C.M., Casares-Magaz, O., Petersen, J.B., Muren, L.P. Department of Medical Physics, Aarhus University Hospital, Aarhus, Denmark.

Introduction: In adaptive radiotherapy for bladder cancer, a library of plans is created. Prior to every treatment fraction, the daily cone beam CT (CBCT) scan is used to select the smallest plan covering the bladder. Currently, no consensus exists regarding the best adaptive strategy. The aim of this study was to compare two strategies in terms of normal tissue complication probability (NTCP) model predictions. Methods: With strategy A, bladder contours from the first four CBCTs were used to create a library of three plans, corresponding to a small, medium and large bladder. Patients were treated with an empty bladder, and received 70 Gy to the bladder tumor, 60 Gy to the non-involved bladder and 48 Gy to the lymph nodes (the two latter with simultaneous integrated treatment). With strategy B, the libraries of five plans were created using interpolated bladder volumes between a full and empty bladder, obtained from two pre-treatment CT scans. Patients were treated with a full bladder. They received 55 Gy to the bladder tumor and 40 Gy to the bladder and lymph nodes, using simultaneously integrated plans. A total of 20 patients were available for analysis, ten from each institution (results for the first six are presented below). To calculate NTCPs, dose distributions for all plans as calculated on the planning CT scan were summed based on the number of times each plan was selected. Using this, the equivalent uniform dose (EUD) and corresponding NTCP were calculated for bowel and rectum, with parameters from literature (Foroudi Radiat Oncol 2012). Results: We found a considerable difference in mean EUD both for the bowel (48 Gy for strategy A vs. 38 Gy for strategy B) and for the rectum (43 and 48 Gy, respectively). Maximum NTCP found was 4% for late bowel obstruction. Conclusion: The two strategies lead to different doses to the bowel and rectum. In further analysis we will explore the differences in NTCP, as well as in tumor control probabilities.

Poster Discussion Group 4

Poster #21

Søren Haack, Aarhus, Denmark

Diffusion Weighted MRI during Radiotherapy of Locally Advanced Cervical Cancer – Treatment response assessment using different segmentation methods

Haack S (1,2), Tanderup K (2), Kallehauge JF (3), Mohamed SM (2,4), Lindegaard JC (4), Pedersen EM (5), Jespersen SN (6,7). 1) Dept of Clin Engineering, 2) Dept of Oncology, 3) Dept of Med Physics, 5) Dept of Radiology, Aarhus University Hosp, 6) CFIN/MindLab, 7) Dept of Physics & Astronomy, Aarhus University, Aarhus, DK, 4) Dept of Radiotherapy, NCI, Cairo University, Egypt

Introduction Diffusion weighted MRI (DW-MRI) and the derived Apparent Diffusion Coefficient (ADC) value has potential value for monitoring tumor response to radiotherapy (RT). However, the method used for segmentation of volumes with reduced diffusion will influence both the size of the volume as well as the observed distribution of ADC values. This study evaluates 1) different segmentation methods, and 2) how they affect assessment of tumor ADCs during RT. Materials and methods Eleven patients with locally advanced cervical cancer underwent MRI three times during RT: prior to start of RT (PRERT), two weeks into external beam RT (WK2RT), and one week prior to brachytherapy (PREBT). Volumes on DW-MR images were segmented using three semi-automatic segmentation methods: “cluster analysis”, “relative signal intensity” (SD4) and “region growing”. Segmented volumes were compared to the gross tumor volume (GTV) identified on T2 weighted MR images using the Jaccard Similarity Index (JSI). ADC values from segmented volumes were compared and changes of ADC during RT were evaluated. Results A significant difference between the four volumes (GTV, DWIcluster, DWISD4 and DWIregion) was found ($p < 0.01$), and the volumes changed significantly during treatment ($p < 0.01$). There was a significant difference in JSI among segmentation methods at time of PRE-RT ($p < 0.016$), with region growing having the lowest JSI (0.35 ± 0.1). There was no significant difference in mean ADC when comparing the ADC values of tumor volume between the three different segmentation methods at same treatment time, but the mean tumor ADC increased significantly ($p < 0.01$) for all methods when compared across treatment time. Conclusion The volume size of segmented tumor with hyper-intense intensities on DW-MR images depends significantly of segmentation method used. Evaluation of mean ADC was robust and did not depend on segmentation method.

Poster #22

Martin Nielsen, Aalborg, Denmark

A new method to validate CT-CT deformable image registration using an auto-segmented bronchial branch point grid

Nielsen,M.S; Østergaard,L.R; Carl,J. Department of Medical Physics, Aalborg University Hospital, Aalborg, Denmark

Introduction: Identification of registration inaccuracies in thoracic 3D CT-CT image registration, using automatically defined anatomical landmarks, generated by segmentation of the airway bronchial tree. Materials and methods: Five lymphoma patients were CT scanned three time within a period of 18 months, with the initial CT defined as the reference scan. For each patient, the two successive CT scans were registered to the reference CT, using three different image registration algorithms (demon, b-spline and affine). The image registrations were evaluated using Dice Similarity Coefficients (DSC) for the overall patient volume (body) and the total airway volume (lungs). In addition, the internal airway (bronchial volume) was segmented using a constrained wavefront propagation method. Extraction of the bronchial branch points provided a grid of anatomical landmarks. Deviation of corresponding landmarks, between registered images, were used to quantify inaccuracies with respect to both misalignment and geometric location within the patient. Results: The DSC and bronchial branch deviations revealed registration discrepancies among the three tested algorithms. The mean DSC (Lungs) for respectively demon, b-spline and the affine algorithms were 0.960, 0.973 and 0.914. The analogous median bronchial branch deviations were 1.6, 1.1 and 4.2 [mm] for the three tested algorithms. An overall median branch deviation of 1.7 [mm] was found significant different ($p = 0.0018$) for bronchial branch points superior in the lungs, relative to the branch point in the middle and lower lung segment of 2.0 [mm]. The maximum bronchial branch point deviations (16 mm) were found within the demon and the b-spline registrations. Conclusions: Bronchial branch points as validation of thoracic image registration agreed with DSC measures. Additionally, the bronchial branch points identified local registration errors up to 16 mm within the deformable demon and b-spline algorithms.

Poster #23

Turid Torheim, Ås, Norway

Cluster analysis of DCE-MRI pharmacokinetic parameter maps is related to locoregional and metastatic relapse for cervical cancer patients

Torheim, T (1); Groendahl, A R (1); Andersen, E K F (2); Kvaal K (1); Lyng H (3); Malinen E (1,4); Futsaether C. M (1). 1: Dept. of Mathematical Sciences and Technology, Norwegian University of Life Sciences, Ås, Norway 2: Dept. of Medical Physics, Oslo University Hospital, Oslo, Norway 3: Dept. of Radiation Biology, Oslo University Hospital, Oslo, Norway

Introduction: Dynamic contrast enhanced magnetic resonance imaging (DCE-MRI) allows us to examine the microenvironment of tumours. Material and methods: 81 patients with locally advanced cervical cancer underwent pre-chemoradiotherapy DCE-MRI. Based on these images, we calculated the relative signal increase (RSI), and constructed Brix (Abrix, kep, kel) and Tofts (Ktrans, ve) parameter maps. We grouped the voxels in these parameter maps by k-means cluster analysis, and estimated the difference in survival for patients with different volume fraction of each cluster by log-rank tests. The distribution of the clusters within each tumour was investigated. In addition, we examined the gene expression profiles for 67 of the patients. Results: K-means analysis based on the Tofts model resulted in three voxel clusters. Each cluster was significantly related to treatment outcome, either locoregional control or metastasis. For k-means analysis based on the Brix parameter maps, we identified one cluster that was significantly related to progression-free survival. Conclusions: The main separation between the Tofts clusters was given by the ve parameter, the extravascular extracellular volume fraction of the voxel. Our analysis indicated that this parameter was more important for treatment outcome than the influx rate Ktrans.

Poster #24

Sara Carvalho, Maastricht, The Netherlands

The impact of region of interest definition on PET textural features of involved lymph nodes in NSCLC – a separate region per node or a combined one?

Ralph T.H. Leijenaar, Wouter van Elmpt, Esther G.C. Troost*, Cary Oberije, Philippe Lambin. *Helmholtz Zentrum Dresden-Rossendorf, OncoRay, Universitätsklinik Carl Gustav Carus der TU Dresden, Germany

NSCLC patients often present with metastatic lymph nodes that have a tendency to disease progression and formation of distant metastases. Initial results showed that common imaging descriptors of the PET positive lymph nodes have a higher prognostic value than of the same metrics from the primary tumor (presented work). Hypothesizing that textural information of lymph nodes, would also hold prognostic value, we first investigated whether these features, for patients presenting more than one involved lymph node, were comparable if derived from each lymph node separately, or from a single structure combining all the involved ones. We included 279 stage I-III NSCLC patients with nodal involvement referred for radical (chemo)radiotherapy. Out of these, 188 had two or more independent structures referring to the involved nodes. A proportionally allocated sub-cohort of 23 patients, in regard to the nodes structures compared to the original cohort, was randomly selected. In total, 19 textural features derived from run length grey level (RLGL, n=8), grey level co-occurrence (GLCM, n=10), and grey level size zone matrices (GLSZM, n=1), were extracted for both the combined structure and the independent nodes. An Intraclass correlation (ICC) analysis was performed. Fifteen textural features presented an ICC above 0.70 (range 0.71 – 0.85) between total structure and independent nodes, with 10 features with an ICC above 0.80. The only feature with an extremely low ICC (-0.025) was the only GLSZM feature still in the analysis. For comparison purposes it is worthwhile mentioning that a similar approach for common metrics (maximum, peak and mean SUV) presented with an ICC above 0.77. Approximately one third of our cohort presented a single structure corresponding to the involved lymph nodes. For the remaining 67%, a single textural feature extracted from the combined structure provides a satisfactory generalization for the involved lymph nodes.

Poster #25

Ruta Zukauskaite, Odense, Denmark

Comparison of local rigid and deformable image registration in head and neck cancer

[1] Zukauskaite R; [1,2]Brink C; [2,3]Hansen CR; [4]Johansen J; [5]Grau C; [4]Eriksen JG. [1] University of Southern Denmark, Institute of Clinical Research, Odense, Denmark; [2] Laboratory of Radiation Physics, Odense University Hospital, Denmark [3] Institute of Medical Physics, School of Physics, University of Sydney, Sydney, Australia; [4]Dept. of Oncology, Odense University Hospital, Denmark

This study investigates the accuracy of RIR and DIR in head and neck cancer (HNSCC), when used to identify the recurrence point of origin (PO) in relation to primary radiotherapy treatment. Methods Twenty patients treated with definitive IMRT for HNSCC were retrospectively and randomly included in the study. For each patient a planning CT (pCT) and a diagnostic recurrence CT (rCT) scans were used (CT voxels 3x1x1 mm). The recurrences were delineated on rCT and a likely PO of the recurrence was identified by two independent observers as well as the mass mid-point (MMP). These points were afterwards transferred to pCT using both local RIR, adapting images manually by bony structures or organs containing air, and DIR using the freeware tool Elastix (http://elastix.isi.uu.nl/). The difference in PO transformation (PODIR-PORIR) was calculated to quantify the changes between DIR and RIR and related to observer placement of PO.Differences in patient weight before treatment and at recurrence were computed, hypothesizing that it might affect the difference in PO transformation between DIR and RIR. Results In total 29 loco-regional recurrences were found in 20 patients. Standard deviations (SD) of the differences between DIR and RIR were 4 and 4.5 mm for two observers and 4 mm for MMP. Sixteen patients (80%) lost weight in the period between treatment and recurrence. One patient lost 19 kg weight that resulted in 20 mm difference between DIR and RIR. If the results were analyzed without this patient, SD would be 2.8 and 3.1 mm for two observers and 3.0 for MMP, which is close to a voxel size. DIR did not change the distance in PO between observers or MMP and neither were affected by weight loss (p=0.5) or recurrence volume (p=0.4). Conclusions The results show that automatic DIR is at least as accurate as manual RIR and of the order of one voxel, when used for transformation between rCT and pCT. The higher reproducibility of DIR is desirable over the subjective manual RIR.

Poster #26

Jonathan Sykes, Sydney, Australia

Performance evaluation of head and neck contour adaptation with cone beam CT using commercial software systems

Bendall L1,2, Najim M1, Stensmyr R1, Flower E1,2, Yau S1, Thwaites DI2, Sykes JR1,2. 1 Radiation Oncology, Sydney West Regional Oncology Network, Sydney, Australia; 2 Institute of Medical Physics, University of Sydney, Australia

Introduction Re-planning during head and neck radiotherapy, to account for changes in anatomy, is resource intensive. Contour adaptation between CT and CBCT scans can be automated using deformable image registration algorithms, with potential to help with the decision of when plan adaptation is required. In this study two commercial systems were evaluated for CT-CBCT adaptation of head and neck contours and compared to CT-CT contour adaptation. Methods Manual delineation of normal tissue structures was performed for twenty head and neck patients on a planning CT (CT1), a re-plan CT (CT2) and a CBCT acquired immediately prior to CT2. All contouring was performed by a single clinician. Five CT and five CBCT scans were contoured twice to assess clinician contouring uncertainty. Deformable image registration and contour adaptation was performed between CT1 and CT2, and between CT1 and CBCT using two commercial systems (A and B). The automatically generated contours were compared with the manual contours using the Haussdorff distance (HD) and the normalised Dice Index (nDSC). Results The mean standard deviation of Haussdorff distance (sHD) for clinician contouring uncertainty on CT (and its range) was 1.5(1.3-2.9)mm for the nine normal tissue structures. sHD was significantly greater for both systems A and B, 4.0(3.2-5.3)mm and 4.7(3.7-6.1)mm respectively. Clinician uncertainty was very similar using CBCT, but sHD increased significantly for system A to 4.9(3.6-6.9) for CT-CBCT, while system B performed equally well with CBCT as with CT. Maximum HD distances between pairs of structures were typically (5%-95%) between 5mm and 15mm, indicating that all contours require some editing before clinical use. Conclusion Automatic contours adapted from CT1 to CT2 using deformable image registration using two commercial systems have greater uncertainty than inherent intra-clinician uncertainty. An increase in uncertainty was observed for one system when using CBCT.

Poster #27

Giske Fiskarbekk Opheim, Herlev, Denmark

How different delineation strategies affect parameter estimation in diffusion MRI study of treatment response in brain metastases

(1,2)Opheim G.F., (3)Johannesen H.H., (2)Mahmood F. (1)Dept. of Biomedical Eng., Technical University of Denmark, Copenhagen. (2)Radiotherapy research unit, Dept. of Oncology, Herlev Hospital, Denmark. (3)Dept. of Radiology, Herlev Hospital, Denmark.

Introduction. Diffusion weighted MRI (DW-MRI) is widely used in treatment response studies in radiotherapy. Nevertheless, no standard method for delineating the region of interest (ROI) exists in DW-MRI studies. Here we present two existing ROI delineation methods and one new ROI delineation method based on non-linear transformation, and evaluate the differences between the corresponding estimates of the apparent diffusion coefficients (ADC). Materials and methods. Ten metastases from five patients, prescribed a dose of 30 Gy in 10 fractions, were analysed. A 1T Philips MR system was used to acquire two sets of DW-MRI (8 b-values, 0-800 s/mm^2) and T2W-MRI: pre-treatment and end-treatment (at 10th fraction). Three ROI delineation methods were used. Method 1: ROIs drawn individually on all DW images, based on T2W information. Method 2: Pre-treatment ROIs based on T2W information were copied to end-treatment DW images (same ROIs). Method 3: End-treatment ROIs based on T2W information were non-linearly transformed into a new ROI using pre-treatment ROI based on T2W information. ADC values were estimated with mono-exponential fit using mean signal values from ROIs. Differences in ADC estimates between methods were evaluated using Pearson product-moment correlation test. Results. Method 1 and 2 only agreed on two out of ten metastases, both showing a reduction in the ADC. For the remaining eight metastases method 1 and 2 showed opposite outcomes (increase/decrease). There was a positive correlation between ADC estimates although not very strong, rho=0.67 (p=0.036). Conclusions. These preliminary results indicate a critical dependency of the estimated ADC values with the selected ROI delineation method. This further implies that comparisons between treatment response studies should take into account the methods used for ROI delineation. Unfortunately, results from method 3 were not ready to be included.

Poster #28

William (Bill) Nailon, Edinburgh, Scotland

Identifying Focal Prostate Cancer by Image Analysis

Feng Y, Cheng K, Montgomery D, Welsh D, McDonald K, Lawrence J, Forrest L, McLaughlin S, Argyle D, McLaren DB, Nailon WH. University of Edinburgh, NHS Lothian, School of Veterinary Studies - University of Edinburgh, Heriot-Watt University, University of Wisconsin

Introduction: Prostate cancer is now the only solid organ cancer in which therapy is commonly applied to the whole gland. With the availability of multi-parametric magnetic resonance (MR) imaging it is now possible to identify cancer foci within the prostate gland. One of the main challenges in adopting focal-therapy is in confidently mapping cancer foci defined on MR images onto computerised tomography (CT) images, which are essential for radiotherapy planning. Materials and Methods: Prostate cancer patients (n=15) previously treated at the Edinburgh Cancer Centre (ECC) were selected for this study. All patients underwent MR scanning for the purpose of diagnosis and staging. Patients received 3 months of androgen deprivation hormone therapy followed by a radiotherapy planning CT scan. Focal prostate lesions were identified on MR scans by a radiologist and a novel image analysis approach was used to map the location of the focal lesion from MR to CT. The image analysis algorithm was based on a B-spline image registration method combined with a method for identifying scale-invariant features on the MR and corresponding CT. An experienced radiation oncologist defined the location of the focal lesion on the planning CT images and rated the contours produced by the image analysis algorithm. Results: On 13 of the 15 cases the algorithm was deemed to show clinically acceptable estimates of the location of the focal disease on CT. Standard rigid registration was found to produce unacceptable estimates of the focal lesion on CT. Using the image analysis-defined contours radiation boosts were planned to each focal lesion. Conclusions: These preliminary results demonstrate the potential of image analysis for reliably identifying focal disease within the prostate for adaptive radiotherapy and boosting focal regions. This work is being extended to investigate the potential of this technique in identifying focal disease on cone-beam CT for adaptive radiotherapy.

Poster Discussion Group 5

Poster #29

Anne Winther Larsen, Aarhus, Denmark

Influence of PET-staging on outcome in limited disease small-cell lung cancer treated with definitive chemoradiotherapy

Winther-Larsen A, Khalil AA and Knap MM. Department of Oncology, Aarhus University Hospital, Aarhus, Denmark

Introduction: Positron emission tomography/computed tomography (PET/CT) is now recommended as part of staging in small-cell lung cancer (SCLC) patients (pts) if limited disease (LD) is suspected. However, only few studies have evaluated the effect of PET-staging on clinical outcome in LD-SCLC. Material and methods: At our institution, 147 consecutive LD-SCLC pts underwent definitive chemoradiotherapy (chemoRT) from 2007-2013. PET/CT was performed for staging in 102 pts. RT was delivered as either 45 Gy in 30 fractions (fx) twice daily (N=130) or 46-50 Gy in 23-25 fx (N=17). Chemotherapy was etoposide combined with either carboplatin (N=97) or cisplatin (N=49) given concomitant (N=129) or sequential (N=18) with RT. Disease free survival (DFS) and overall survival (OS) for PET-staged and non-PET-staged pts were calculated by Kaplan-Meier method and compared by log-rank test. Multivariate analysis was conducted by Cox proportional hazard model. Results: With a median follow up time of 42.2 months (mth), we found a significant longer median OS (30.6 mth) in the PET-staged group compared with the non-PET-staged (17.1 mth; p=.001). Furthermore, a prolonged median DFS of 17.3 versus 11.6 mth (p=.017) was found. Both results remained significant in a multivariate analysis (OS: adjusted hazard ratio (AHR) 0.39, p=.005; DFS: AHR 0.54, p=.01). Incidence of distant failures was lower in the PET-staged pts (41% versus 71%; p=.001) while no difference in the incidence of loco-regional failures was seen (24% versus 29%; p=.49). Other independent factors for longer OS were having received prophylactic cranial irradiation (AHR 0.46; p=.009) and lower N-stage (AHR 0.41; p=.016). Conclusion: LD-SCLC pts staged with a PET/CT showed a significantly longer OS and DFS independent of treatment and stage. A significantly lower incidence of distant failures was seen in the PET-staged pts. The data support PET/CT scans as an important tool before selecting LD-SCLC pts to definitive chemoRT.

Poster #30

Christina Maria Lutz, Aarhus, Denmark

The reliability of dose-response model selection

Lutz C.M.(1), Møller D.S.(2), Hoffmann L.(2), Khalil A.A.(1), Knap M.M.(1), Alber M.(1). (1) Department of Oncology, Aarhus University Hospital, Aarhus, Denmark; (2) Department of Medical Physics, Aarhus University Hospital, Aarhus, Denmark

Introduction Initiatives like QUANTEC were initiated to compile dose planning constraints from clinical outcome data, e.g. the mean lung dose (MLD) and the volume of the lung receiving 20Gy (V20) for pneumonitis. However, the data are tarnished by uncertainties in dose recording, patient heterogeneity and sample size and -variability. We tried to answer the question: if the dose response followed a mechanistic model, how reliably would it be identified from clinical data? Materials/Methods We simulated trial populations using a number of postulated dose-response models and real-life dose distributions of advanced lung cancer patients. Each patient was randomly assigned complication/no-complication based on the postulated model risks. This way, a great number of study populations were created, each of which represented a possible clinical study result. Each population was analyzed with a number of normal tissue complication probability (NTCP) models, and the best fitting model was selected. This was matched to the known postulated model to determine a recognition rate. As postulated models, the QUANTEC MLD best fit model and a V20 dose cutoff model were used. Results For the QUANTEC MLD model and the V20 model, the correct model parameter was selected in 11.5% CI[11.0;12.0] and 34.3% CI[33.6;35.0] of the simulated populations of 100 individuals, respectively. For a MLD and a V20 model with lower complication risks, these rates decreased to 7.6% CI[7.2;8.1] and 17.2% CI[16.7;17.7]. For a population size of 500, the recognition rates increased to 43.4% CI[42.6;44.1] and 78.6% CI[77.9;79.4]. However, for the lower complication incidence of the two models with lower risks this rate decreased again to 30.0% CI[29.4;30.7] and 46.5% CI[45.7;47.3]. Conclusion The postulated dose response was identified in 1-in-3 to 1-in-9 cases. This low success rate could explain the persistent difficulties to derive dose constraints from clinical data in large-volume effect organs.

Poster #31

Anne Ramlov, Aarhus, Denmark

Impact of lymph node dose on nodal control in patients with locally advanced cervical cancer.

Ramlov, A (1), Kroon P (2), Jürgenliemk-Schulz I (2), De-Leeuw A (2), Gormsen LC (3), Fokdal L (1), Tanderup (1) K, Lindegaard, J (1). 1. Department of Oncology, Aarhus University Hospital, Aarhus, Denmark. 2. Department of Radiotherapy, University Medical Center Utrecht, Utrecht, The Netherlands. 3. Department of Nuclear medicine and PET center, Aarhus University Hospital, Aarhus,

Introduction: Regional and distant metastases compromise overall survival in locally advanced cervical cancer despite local control rate > 90%. No consensus exists on the optimal dose needed to control regional nodal disease at time of diagnosis. Materials and Methods: 139 patients consecutively included in the EMBRACE study 2008-2013 were analyzed. Treatment consisted of external beam radiotherapy (EBRT), brachytherapy (BT) and weekly Cisplatin. Total dose delivered by EBRT and BT was determined and converted to EQD2. Treatment scans obtained at time of nodal recurrence were matched with the EBRT planning scan and the relation to boosted node and field border was determined. Results: 84 patients were node positive of which 8 were treated with lymphadenectomy. In total, 209 nodes in 76 patients were boosted. Median nodal boost dose was 62 Gy (range 53-69 Gy), nodal volume 1.5 cm3 (range 0.1-44.9 cm3), nodal SUVmax 5.5 (range 2.1-21.5). The dose for elective nodal irradiation was 43-47 Gy EQD2. After a median follow-up of 30 months (range 3-64 monts) 6 patients recurred within a boosted node. 203/209 of the boosted nodes were controlled. Using Wilcoxon rank sum test maximum FDG standard uptake value (SUVmax) was significantly higher in recurrent nodes (p=0.02). However, no significant relation for dose (p=0.48) or volume (p=0.14) was found. Nodal relapse in non-boosted elective nodal volumes was observed in 7 patients. Thirteen patients recurred just above the treatment field and of these, 9 patients had para-aortic nodes (PAN) as only site of relapse. Conclusion: Current treatment schedules secure high nodal control in both boosted nodes and in the elective nodal region. Nodal SUVmax was significantly higher in recurrent nodes. No dose-response relationship could be established due to very few recurrences. The majority of nodal relapses occur above the field in the PAN. The results are currently being used for design of the EMBRACE2 study.

Poster #32

Christina Daugaard Lyngholm, Aarhus, Denmark

Survival and recurrence pattern in the DBCG 89-cohort treated with Breast Conservation; focusing on age

C D Lyngholm[1], P M Christiansen[2], T E Damsgaard[3], J Alsner[1], T Laurberg[1], J Overgaard[1]. 1 Department of Experimental Clinical Oncology, Aarhus University Hospital, Aarhus, Denmark, 2 Breast and Endocrine Surgery Unit, Department P, Aarhus University Hospital, Aarhus, Denmark and 3 Deparment of Plastic Surgery, Aarhus University Hospital, Aarhus, Denmark

Introduction

Breast conserving surgery, followed by radiation therapy, has since the implementation during the late 1980's shifted the first choice of treatment away from mastectomy. Based on a large national cohort of Danish breast cancer patients, we set out to evaluate recurrence pattern and survival, particularly focusing on the significance of age, in patients treated with Breast Conserving Treatment (BCT) according to the DBCG-1989 trial (Danish Breast Cancer Cooperative Group).

Materials and methods

A national cohort of 1.902 Danish breast cancer patients treated according to the DBCG-89 TM-guidelines in the period of 1989-2000 were eligible to enter this study. Patients were almost evenly distributed into the age groups: below (950) and above 45 years (952). Through the national Pathology Data Bank, the Danish Cause of Death Registry and audits of medical records, patients were followed up until death or end of study at December, 2014, with data collected on date and localization of recurrence, date and diagnosis of other malignant disease, and date and cause of death.

Results

The median age was 46.1 years and median follow-up time was 15.4 years. At the end of follow-up 1214 patients (64%) were still alive. The following distribution of the events of interest were: 290 isolated Local recurrences, 12 isolated Regional recurrences, 98 isolated Contra-lateral Cancers, 340 isolated Distant Metastases, 156 other primary cancers than breast, and 475 breast cancer deaths. Time to a primary recurrence was on average 6.7 years with no difference between the age groups. Disease Specific mortality at 20 years was 26.6% (CI, 24.5% to 28.8%) for the cohort as a whole, with a significantly higher risk of dying from breast cancer in the younger patients HR 1.21 (CI, 1.01-1.45). The rate at which Local Recurrences occurred, was almost doubled in the younger patient group compared to the older (HR 1.93, CI, 1.52 to 2.46).

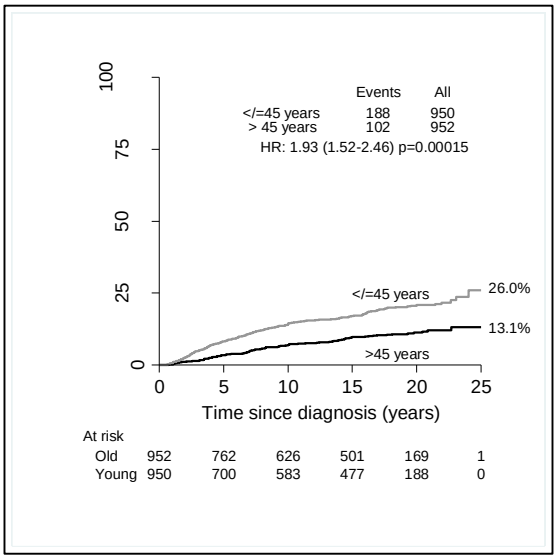

Conclusion

Long-term disease control after BCT in the DBCG-89 cohort reaches international levels. Young patient need special attention because of significantly higher frequencies of primary recurrences resulting in increased disease specific mortality compared to their older counterparts.

Poster #33

Ferenc Lakosi, Liège, Belgium

Clinical efficacy and toxicity of radio-chemotherapy and MRI-guided brachytherapy for locally advanced cervical cancer patients: a mono-institutional experience

Lakosi F., Nguyen P.V., Hermesse J., Jansen N., Werenne X., Warlimont B., Martin N., Gennigens C., Gulyban A., Siedel L., Kridelka F.#, Coucke P. Department of Radiation Therapy, University Hospital of Liège, Liège, Belgium

Purposes: To evaluate efficacy and toxicity of radio-chemotherapy (RCT) and MR-guided pulsed-dose-rate (PDR) adaptive brachytherapy (IGABT) for locally advanced cervical cancer (LACC). Materials and methods: Between 2007 and 2014 eighty-five patients with FIGO stage 1B1 N+ or ≥ 1B2 cervical cancer were treated with RCT+IGABT. The treatment consisted of a pelvic±paraaortic external beam radiotherapy (EBRT) (45-50.4 Gy±10 Gy boost to primary tumor and/or to pathologic lymph nodes) with concurrent cisplatin followed by 25-35 Gy of PDR IGABT in 30-50 pulses. The ratio of 3D-CRT/IMRT was 61/24 pts. Dose–volume parameters of HR-CTV, IRCTV and D2cc OARs (organs at risk) were reported. Local control (LC), cancer specific survival (CCS) and overall survival (OS) were analysed actuarially and morbidity crude rates were scored using CTCAEv3.0-4.0. Results: Mean follow-up was 36 months (range:6–94). The mean D90 and D98 for HR-CTV was 85.5±15.6 Gy and 77±8.1 Gy, while for IR-CTV was 69.3±4.6 Gy and 64.8±4.3 Gy respectively. The mean D2cc for OARs was the following: bladder: 77.8±10.3 Gy, rectum: 65.1±6.8 Gy, sigmoid: 64.3±13.4 Gy and intestine: 64.0±9.3 Gy. Three year LC, CSS and OS were: 96%, 87% and 84%. The 3-year regional-and distant controls were 90% and 79%. Node negative patients had significantly higher 3-year CSS (100 vs. 76%, $p<0.01$) and OS (95 vs. 73%, $p<0.01$) compared to node positive ones. Late Gr.≥3 morbidity was the following (events/pts): GI: 7/4 (4.7%), GU: 7/5 (5.8%), Sexual: 4/4 (4.7%). The frequency of Gr.≥3 haematological toxicities including anaemia/leukopenia/neutropenia/thrombocytopenia were 7%/28%/19%/3.5%, respectively. Conclusions: This large mono-institutional experience reinforces radio-chemotherapy and MRI-guided BT as optimal therapeutic approach for patients suffering LACC. This series will serve as a good basis to evaluate the added value of adaptive and/or bone marrow sparing RT techniques in the near future.

Poster #34

Emely Lindblom, Stockholm, Sweden

Radiobiological modelling of tumour response based on the 5 Rs of radiobiology in search for optimal radiotherapy treatment parameters for non-small-cell lung cancer

1) Lindblom E, 2) Dasu A, 1+3) Toma-Dasu I. 1) Med. Rad. Physics, Dept. of Physics, Stockholm Univ., Stockholm, Sweden, 2) Dept of Rad. Physics, Linköping Univ., Linköping, Sweden, 3) Med. Rad. Physics, Dept of Oncol. and Pathology, Karolinska Inst., Stockholm, Sweden

Introduction: Conventionally fractionated radiotherapy (CFRT) has proven ineffective in treating non-small-cell lung cancer. While more promising results have been obtained with stereotactic body radiotherapy (SBRT), hypoxic tumours might present a significant challenge to extremely hypofractionated schedules due to the decreased possibility for inter-fraction fast reoxygenation. A potentially successful compromise might be found in schedules employing several fractions of varying doses per fraction. In this modelling study, we have explored a wide range of fractionation schedules from single-fraction treatments to heterogeneous, multifraction schedules taking into account the 5 Rs of radiobiology: repair, redistribution, repopulation, reoxygenation and radiosensitivity. Materials & Methods: Tumours with heterogeneous oxygenation were simulated based on a previously derived model which was further developed to include the 5 Rs. Various treatments with respect to time, dose and fractionation were simulated for tumours with varying degree of hypoxia. Survival was calculated with the LQ model and local control was estimated as Poisson-based tumour control probability. Results: For well-oxygenated tumours, heterogeneous fractionation could increase local control regardless of reoxygenation pattern. While a heterogeneous fractionation scheme could achieve control rates superior to some of the other schedules only if reoxygenation was completely neglected for tumours with hypoxic foci, schedules employing 2-5 fractions predicted very similar D50s of 52.9-53.1 Gy if fast reoxygenation between fractions was assumed. For a larger number of fractions the D50 increased as a result of inter-fraction repair. Conclusions: For well-oxygenated tumours, heterogeneous fractionation schedules could increase local control rates substantially compared to CFRT. For hypoxic tumours, SBRT-like hypofractionated schedules might be optimal despite the increased risk of intra-fraction repair.

Poster #35

Yasmin Lassen, Aarhus, Denmark

Pseudoprogression after proton radiotherapy for pediatric low grade glioma

Lassen-Ramshad Y.1, Petersen J.B.B.2, Tietze A.3, Borghammer P4., Mahajan, A5, McGovern S.L.5. 1: Dept. of Oncology, Aarhus University Hospital (AUH), Denmark, 2: Dept. of Medical Physics, AUH, Denmark, 3: Dept. of Neuroradiology, AUH, Denmark, 4: Dept. of Nuclear Medicine, AUH, Denmark, 5: Dept. of Radiation Oncology, MD Anderson Cancer Center, USA

Introduction:Pseudoprogression in pediatric low-grade glioma may occur after photon radiation. Some functional imaging studies help to differentiate between pseudo- and real progression.We report the case of a 17-year old girl with lowgrade glioma in the left tectum, presenting with pseudoprogression 4 months after proton radiotherapy. Material and Methods:The patient was diagnosed with an inoperable, lowgrade astrocytoma in 2011. In 2014, a small area of enhancement on post-contrast T1-weighted images was noted, that was interpreted as tumor progression. She was treated with proton radiotherapy, 50.4 GyRBE in 28 fractions in the tumor region and a boost of 1.8 GyRBE in 1 fraction to the enhancing volume. Four months postradiotherapy, the patient developed diplopia and right-sided dysesthesia. MRI revealed progression of the enhancement and of high signal changes on T2-weighted series. The radiation dose plan was reviewed, and a perfusion-weighted MRI and 18Fluoro-Ethyl-Thyrosine(FET)-PET were performed. The girl was treated with corticosteroids. She was observed clinically and followed closely with MRI scans. Results: Review of the dose plan showed that the area of increasing enhancement was mainly located in the boost area. Perfusion-weighted MRI showed a small region with increased cerebral blood volume in this area, but it was difficult to interpret due to vascular structures in the vicinity. FET-PET revealed tracer uptake in this area with a tumor/background ratio of 2.24, suspicious for pseudoprogression. Subsequent MRIs showed decreasing T2 hyperintensity and contrast enhancement. The diplopia regressed completely, whereas the dysesthesia remained. A herpes zoster infection occurred. The corticosteroids treatment could be discontinued after six months. Conclusion: FET-PET was important for the diagnosis of pseudoprogression, subsequently confirmed by the clinical course. Treatment with high dose corticosteroids resulted in some clinical improvement.

Poster #36

Jørgen Johansen, Odense, Denmark

Validation of a normal tissue complication probability (NTCP) model for radiation-induced hypothyroidism in two independent cohorts

Rønjom MF, Brink C, Bentzen SM, Hegedüs L, Overgaard J,Petersen JB, Primdahl H, Johansen J. Odense University Hospital, Denmark; University of Southern Denmark, Odense, Denmark; University of Maryland School of Medicine, Baltimore, USA; Aarhus University Hospital, Aarhus, Denmark

Introduction. An NTCP model for radiation-induced hypothyroidism (HT) was previously derived in patients (cohort1) with squamous cell carcinoma of the head and neck (HNSCC) taking thyroid volume (Vthyroid), mean thyroid dose (Dmean), and latency into account. The purpose of this study was to validate the model in an independent cohort of patients treated with definitive radiotherapy (RT). Material and methods. An equal sized cohort (cohort2) of HNSCC was included with a baseline thyrotropin (TSH) assessment and a single TSH sample during follow-up after RT. HT was defined as TSH > 4.0 mU/l. Due to only one follow-up TSH assessment in cohort2, a new cohort (cohort1S) was sampled from cohort1. The time factor derived from cohort1 was fixed in a multivariable mixture model and applied for NTCP analysis. Results. Dmean and Vthyroid were significant risk factors for radiation-induced HT in all three cohorts. Comparing the NTCP models NTCP1 and NTCP2, the model from cohort1 (NTCP1) generated higher risk estimates of HT. However, taking the number of TSH assessments into account, NTCP1S and NTCP2 estimated the risk of HT equally. Conclusions. Dmean and Vthyroid were significant risk factors of radiation-induced HT in all cohorts. A direct comparison of the NTCP models was not possible due to the diversity of TSH sampling, however, when the number of TSH assessments taken into account, a good agreement between the models was observed with comparable risk estimates of HT between patient cohorts.

Poster Discussion Group 6

Poster #37

Ditte Sloth Møller, Aarhus, Denmark

Adaptive radiotherapy for advanced lung cancer ensures target coverage and decreases lung dose

Møller D. S. (1), Khalil A. A. (2), Knap M. M. (2), Holt M. I. (2), Alber M. (1), and Hoffmann L. (1). (1) Department of Medical Physics, Aarhus University Hospital, Aarhus, Denmark, (2) Department of Oncology, Aarhus University Hospital, Aarhus, Denmark

Introduction Locally advanced lung cancer lacks effective treatment options. Increased treatment precision and decreased treatment volume are mandatory for increasingly aggressive radiotherapy, e.g. dose escalation to metabolically active regions of the tumor. With adaptive radiotherapy (ART) the treatment plan is adjusted to physical changes like atelectasis, pleural effusion and positional or volumetric changes of the tumor. In this study, we evaluate the dosimetric effect of ART. Materials/Methods Smaller PTV margins, daily online tumor match, and ART intervention rules were implemented for lung cancer patients. Any systematic violation of geometrical acceptance criteria for normal tissue and tumor triggered evaluation. If the observed change led to either underdosage of tumor or overdosage of normal tissue a re-plan was created. The dosimetric consequence of a re-plan was found by recalculation of the original plan on the re-CT for the first 140 patients. For the first 50 patients, two additional CTs were acquired during the RT course and the treatment plans were recalculated to evaluate the actual delivered dose. This subgroup was compared to a control group (n=54) treated with larger margins and bone match set-up to evaluate the benefit of ART in terms of reduced lung dose. Results Thirty-two patients (23%) had at least one re-plan. Twenty-two adaptations corrected for a decrease in V95%PTV (mean 8%, max 19%) and V95%CTV (mean 2%, max 10%), while six corrected for an increase in heart dose (D10cc mean 10 Gy, max 18 Gy). In patients with no re-plans, 94% had less than 1% decrease in CTV coverage on the additional CT-scans. Compared to a control group, the ART patients showed a decrease in PTV from 569 cm3 to 398 cm3, and consequentially a decrease in mean lung dose from 14.1 Gy to 12.6 Gy. Conclusions The implementation of tumor match and ART secures high treatment precision and decreases the mean lung dose, thereby paving the way towards dose escalation.

Poster #38

Susanne Rylander, Aarhus C, Denmark

A comparison study for US- and MR based dose planning in high-dose-rate interstitial prostate brachytherapy

Rylander S, Buus S, Bentzen L, Tanderup K. Department of Clinical Medicine, Aarhus University Hospital, Aarhus, Denmark

Introduction The purpose was to compare dose planning for US- and MR-based high-dose-rate (HDR) brachytherapy (BT) and to evaluate the dosimetric impact to target and organs at risk (OAR) caused by the contouring- and needle reconstruction uncertainties on US. Materials and Methods US- and MR images were acquired post needle insertion for 10 BT fractions for 5 patients treated with combined EBRT and BT. Contouring of the prostate target (CTVp) and OAR, needle reconstruction and dose optimization were performed in OncentraProstate (Elekta). Planning objectives for US- (PlanUS) and MRI dose plans (PlanMR) were; CTVp D90%>100%=8.5 Gy, CTVp+3 D90%>95% (CTVp+3=CTVp plus a 3 mm margin, constrained to rectum and bladder), urethra V10Gy<3.5%, rectum D2cc<75%. The dosimetric uncertainties in PlanUS were evaluated by performing US/MR registration followed by needle position corrections according to needle visualization on axial MRI. The resulting target- and OAR dose (PlanUS-corr) were evaluated on MR-prostate- and US-OAR contours, respectively. Results The mean prostate volume was 31±6 cm3 on US- and 30±9 cm3 on MR images. The mean D90% to targets in PlanUS (CTVp=108±6%; CTVp+3=96±8%) were not significantly different from PlanMR (CTVp=106±6%; CTVp+3=95±7%) (p=0.1, 0.3, respectively). However, the target dose in PlanUS-corr was lower, by a mean of 4±6% to CTVp and 6±10% to CTVp+3 as compared to PlanUS . The mean D2cc rectum was reduced by 4±10% with PlanMR as compared to PlanUS and PlanUS-corr. The mean V10Gy-urethra was significantly higher in PlanUS-corr by 13±18% (p=0.02) as compared to PlanUS. Conclusions Prostate target volumes on US and MRI were not significantly different and the planned target doses were comparable for the US- and MR plans. The MR plans achieved a lower rectal-dose as compared to US. After needle position corrections in the US plans, the resulting doses were lower to MR based targets and higher to urethra as compared to initially planned.

Poster #39

Marius Røthe Arnesen, Oslo, Norway

Dose painting by numbers in a standard treatment planning system using inverted dose prescription maps

Arnesen M.R.(a,b), Rekstad B.L.(a), Knudtsen I.S.(a,b), Eilertsen K.(a), Dale E.(c), Bruheim K.(c), Helland Å.(c), Hellebust T.P.(a,b), Malinen E.(a,b). a) Department of Medical Physics, Oslo University Hospital, Oslo, Norway. b) Department of Physics, University of Oslo, Oslo, Norway. c) Department of Clinical Oncology, Oslo University Hospital, Oslo, Norway

Introduction Dose painting is a method to increase tumor control by delivering an inhomogeneous dose with a prescription based on medical images reflecting tumor aggressiveness. In dose painting by numbers (DPBN), each tumor voxel is prescribed a dose according to the value in the medical image voxel. However, planning of DPBN is not possible in commercial treatment planning systems today. Here, a straightforward method for DPBN with a standard treatment planning system (TPS) is presented. Materials and methods DPBN tumor dose prescription maps were generated from FDG-PET-images applying a linear relationship between image voxel value and dose. The mean tumor dose (Dmean) was held fixed and the minimum dose (Dlow) kept equal to the conventional dose. From this, an inverse DPBN prescription matrix was created and imported into a standard TPS where it was defined as a mock pre-treated dose. Using inverse optimization for the summed dose and striving for a homogeneous dose within the tumour, a DPBN dose distribution was thus created. The procedure was tested using VMAT planning in Eclipse (Varian Medical Systems) for three different cases; cervix, lung and head and neck. The treatment plans were compared to the prescribed DPBN dose distribution by 3D gamma analysis with 2% /2mm criteria. Treatment delivery was verified with Portal Dosimetry on a Varian Clinac iX. Results By setting Dmean to 120% of Dlow, a maximum dose Dhigh of 149%, 140% and 151% was prescribed for the cervix, lung and head and neck case respectively. DPBN distributions were well obtained within the tumor whilst normal tissue doses were within the constraints for all three cases. Gamma pass rates of 89%, 93% and 99%, respectively, were found. According to portal dosimetry, all DPBN plans could be successfully delivered. Conclusions: The presented methodology enables the use of currently available treatment planning systems for DPBN planning and may therefore pave the way for clinical implementation.

Poster #40

Bernt Louni Rekstad, Oslo, Norway

Anal carcinoma - a candidate for FDG-PET guided high-dose simultaneously integrated boost

Rekstad BL (a), Rusten E (a,b), Undseth C (c), Arnesen MR (a,b), Hellebust TP (a,b), Holmboe L (d), Guren MG (c), Malinen E (a,b). (a) Department of Medical Physics, Oslo University Hospital, Oslo, Norway (b) Department of Physics, University of Oslo (c) Department of Oncology, Oslo University Hospital (d) Department of Radiology and Nuclear Medicine, Oslo University Hosptial

Introduction Chemoradiotherapy is the standard of care for anal carcinoma. Complete tumour regression occurs in 80-90%, the main cause of relapse are local recurrences occuring in 15-20%. As anal carcinomas are FDG-PET-positive, we wanted to investigate a dose escalation to the FDG-PET-positive part of the tumour in order to increase local control, and without a substantial increase in the dose to organs at risk. Materials and methods Six anal carcinoma patients from a prospective clinical trial were included in this treatment planning study. FDG-PET-CT images at baseline were co-registered with the treatment planning CT. The PET-positive part (GTV-t-PET) of the gross tumour volume (GTV-t) was contoured by an oncologist. For each patient a set of two simultaneously integrated boost (SIB) VMAT plans were created, with two full arcs, delivered by 27 fractions: A standard SIB plan (VMATstd) with total dose 48.6 Gy / 54.0 Gy / 57.5 Gy to elective lymph nodes, lymph node metastases and tumour respectively, and a PET-guided dose escalation plan with an additional dose level of 65.0 Gy to GTV-t-PET (VMATpet). Results The median volume of GTV-t-PET was 5.4 cm3 (range 0.8 – 62.6 cm3), which was 14.4% (range 4.0 – 37.7%) of the GTV-t. The median dose to the GTV-t-PET was increased from 58.4 Gy with VMATstd to 65.7 Gy with VMATpet. The intestinal cavity D2cm3 increased slightly from 56.3 Gy to 57.6 Gy. The mean intestinal dose did not differ. The bladder D2cm3 increased from 56.3 Gy to 56.6 Gy, and mean bladder dose increased from 46.6 Gy to 47.4 Gy. The mean dose to the genitals increased from 39.7 Gy to 40.8 Gy. Conclusions The dose to the PET-positive volume can be increased considerably with an additional simultaneous boost, with only a small effect on OAR doses. The increased dose to OARs depended on size and localization of the GTV-t-PET. Further investigation including adaptive strategies and a larger number of patients should be performed.

Poster #41

Gitte Persson, Copenhagen, Denmark

Deep Inspiration Breath-Hold Radiotherapy for Lung Cancer - Can Dose to Heart and Mediastinal Structures be Decreased?

Persson GF, Rydhög JS, Aznar M, Maraldo MV, Nygård L, Costa J, Berthelsen AK, Specht L, Josipovic M. Dept. of Oncology and Dept. of Clinical Physiology, Nuclear Medicine and PET, Rigshospitalet, Copenhagen University Hospital, Denmark

Introduction: When thoracic radiotherapy (RT) doses are escalated, toxicity from mediastinal structures has been shown to be a limiting factor (Cannon et al. JCO 2013). In this study, we examined if deep inspiration breath-hold (DIBH) in combination with volumetric modulated arc therapy (VMAT) can decrease the estimated dose to lungs, heart, central bronchi and esophagus compared to free breathing (FB) RT. Materials and methods: 17 patients with stage III NSCLC referred for RT were CT scanned in both FB (4DCT) and visually guided voluntary DIBH before radical RT. Lungs, heart, central bronchi, trachea, and esophagus were contoured, as were heart subvolumes: coronary arteries and valves. Three dimensional conformal and volumetric modulated arc therapy (VMAT) plans were computed using FB and DIBH scans. VMAT plans were optimized using constraints for target and lung dose. Only results comparing VMAT FB and DIBH plans are reported here. Student's t-test for correlated samples was used. Results: GTV sizes were slightly smaller in DIBH (mean 119 vs 132 cc, $p=0.01$). Lung volume increased in DIBH by median 64% (range 35-108%, $p<0.0001$) compared with FB. Average mean lung dose was 2.7 Gy lower and average lung V5 was 9.6% lower in DIBH ($p<0.0001$). Mean heart dose, -esophageal and -tracheal dose were all significantly lower in DIBH, as was maximum esophageal dose. No significant differences were found for mean and maximum bronchial dose or doses to heart subvolumes. Conclusion: DIBH VMAT decreased the estimated mean doses to both heart, lungs and esophagus compared to FB VMAT. Possibly, the dose could be further reduced, had the mediastinal structures been included in the VMAT optimization process. Combining DIBH and VMAT may open possibilities for dose escalation to target volumes or subvolumes, while ensuring a high precision in dose delivery.

Poster #42

Stine Korreman, Roskilde, Denmark

Loss of TCP by geometrical uncertainties in dose painting strategies

Korreman, SS. Department of Science, Systems and Models, Roskilde University, Roskilde, Denmark

Dose painting strategies aim to increase tumour control probabillity (TCP) by escalating dose to subvolumes in the target which are more radioresistant as identified by functional imaging. Dose painting by numbers (DPBN) strategies apply a dose prescription function at voxel level mapping a range of doses to the target based on the range of intensities in the functional image. In standard radiotherapy with uniform target dose, geometrical errors are counteracted by the introduction of a treatment field margin, in order to conserve TCP. This cannot be done for DPBN, and geometrical errors therefore potentially have a large detrimental effect on the TCP. Thereby, the gain in TCP achieved by applying the DPBN strategy in the first place is compromised. This study uses a simple standard TCP model, transferred to dose painting delivery, to estimate loss of TCP introduced by geometrical errors. As a ”rule of thumb” for such a model, a positional uncertainty resulting in ~12% volume receiving <90% of prescription dose, gives a 3% TCP reduction (for γ50=1.8). The dose painting plan in [Korreman et al Acta Oncologica vol 49 2010] is an example of a high resolution DPBN case for a functional hypoxia image obtained a by [61Cu]Cu-ATSM PET/CT-scan. Here, a ~15% decrease in volume receiving <90% of intended dose, was found for a 2 mm systematic shift, corresponding to a 4-5% TCP reduction. This figure is well in accordance with other literature on geometrical uncertainty effects of dose painting. Lower resolution dose painting is less prone to TCP deterioration by positional error, but on the other hand also have lower TCP gain in the first place compared to uniform dose prescription.

Poster #43

Anders Traberg Hansen, Aarhus, Denmark

Exploring the optimal dose-prescription strategy for liver SBRT including the effects of target motion

Hansen A.T. (a), Poulsen P.R. (b,c), Høyer M. (b), Worm E.S. (a). Departments of (a) Medical Physics, (b) Oncology, Aarhus University Hospital, Aarhus, Denmark and (c) Institute of Clinical Medicine, Aarhus University, Denmark

Introduction In lever SBRT it is typical to prescribe a lower dose at the PTV rim than in the tumor center. During SBRT treatment, motion may deteriorate the tumor dose. The aim of this study was to explore the optimal dose prescription strategy, including the effects of intra-treatment motion. Methods and Materials Three patients received 3-fraction liver SBRT. The 3D motion of an implanted gold marker was monitored throughout treatment by fluoroscopic kV and MV imaging. Retrospectively, four VMAT treatment plans were made for each patient, all with a mean GTV dose of 18.8Gy per fraction, while the PTV was covered by 50%, 67% (our standard), 80%, and 95% of this dose, respectively. The PTV margin was 5mm (LR,AP) and 10mm (CC). Using a NTCP-model, the50%, 80% and 95% plans were re-normalized to give the same NTCP for radiation induced liver disease (RILD) as the standard 67% plan. The D99 and mean GTV dose of the four iso-toxic plans were calculated, both without tumor motion and with the observed 3D motion, using a validated method for motion-including dose reconstruction. Results The absolute mean tumor displacement during treatment was 2.9±3.1mm. The planned GTV mean dose of the four iso-toxic plans was on average 21.4 (50% plan), 18.8 (standard 67% plan), 17.0 (80% plan) and 15.1Gy (95% plan), respectively. With intra-treatment motion this decreased to 20.2, 18.4, 16.7 and 14.9Gy, respectively. In mean, the planned D99 was 20.6, 18.2, 16.6, and 14.7Gy, respectively, which decreased to 16.7(-19%), 16.1 (-12%), 15.2 (-8%), and 13.7(-7%) Gy with intra-treatment motion. Conclusions The dose level at the PTV rim had a large effect on the NTCP for RILD. Using a low dose at the PTV rim (50%, 67%), where the probability of tumor location is low, allowed for a higher GTV dose for iso-toxic conditions. Although these plans experienced larger GTV dose reductions, their GTV dose remained superior to the 80% and 95% plans when intra-treatment motion was included.

Poster #44

Patrik Sibolt, Roskilde, Denmark

Adaptation requirements due to anatomical changes in free-breathing and deep-inspiration-breath-hold for standard and dose escalated radiotherapy of lung cancer patients

Sibolt P.(1,2), Ottosson W.(2), Behrens C.F.(2), Larsen C.(2), Sjöström D.(2). (1)Center for Nuclear Technologies, Technical University of Denmark, DTU Risø Campus, DK-4000 Roskilde, Denmark. (2)Radiotherapy Research Unit, Department of Oncology, Herlev Hospital, University of Copenhagen, DK-2730 Herlev, Denmark.

Introduction Radiotherapy of lung cancer patients is subject to uncertainties related to heterogeneities, anatomical changes and breathing motion. Use of deep-inspiration-breath-hold (DIBH) can reduce the treated volume, potentially enabling dose escalated (DE) treatments. This study is designed to investigate the need for adaptation due to anatomical changes, for both standard (ST) and DE plans in free breathing (FB) and DIBH. Materials & Methods Tumor shrinkage (TS) and pleural effusion (PE) was simulated for three different tumor locations in a CIRS thorax phantom. PE was systematically simulated by adding fluid in the dorsal region of the lung and TS by isotropic reduction of the tumor diameter. Similar changes were simulated in patients, CT imaged both in FB and DIBH. The effect of TS was also investigated for DE treatment plans. Additionally, the effect of atelectasis change was studied. Simulations were carried out by density alterations and re-calculations. Results PE and TS phantom simulations resulted in the following maximum deviations of the <D> to the GTV-T: (i) 3 cm PE resulted in a 1.3% reduction for the centrally located tumor, and (ii) TS to 1 cm diameter resulted in a 3.1% increase for an anterior tumor location. For the clinical cases, TS simulations resulted in maximum increase of <D> to GTV-T of 2.3 Gy (3.4%) and 2.6 Gy (3.9%) for ST plans, and 3.1 Gy (3.3%) and 2.8 Gy (2.9%) for DE plans, for FB and DIBH, respectively. A large atelectasis reduction during treatment increased the GTV-T <D> with 2.4% and 0.2% for FB and DIBH, respectively. Conclusions This study indicates, by simulations in phantom and patients, that an adaptive procedure needs to be considered as anatomical changes appear in the thoracic region. Comparable relative dose deviations due to introduction of TS, PE and atelectasis were demonstrated for all the treatment techniques investigated. However, DE plans are subject to greater deviation in terms of absolute <D> to the GTV-T.

Poster Discussion Group 7

Poster #45

Eirik Malinen, Oslo, Norway

Dose or 'LET' painting – what is optimal for hypoxic tumors?

Malinen E, Søvik Å. Department of Physics, University of Oslo, Oslo, Norway. Department of Medical Physics, Oslo University Hospital, Oslo, Norway. Department of Monitoring and Research, Norwegian Radiation Protection Authority, Østerås, Norway.

Introduction Dose painting is a concept that may increase the tumor control probability (TCP). In particle therapy, the linear energy transfer (LET) is a parameter that also may be modulated. For hypoxic tumors, it may be beneficial to redistribute the LET so that that the oxygen effect is minimized. The purpose of the present study was to estimate the TCP for dose and LET painting of hypoxic tumors. Materials and Methods Particle therapy with protons, lithium ions and carbon ions was considered. Tumor images tentatively depicting hypoxia were used as input. Optimal dose prescription maps were obtained by optimizing TCP under dose and/or LET redistribution. TCPs were compared to those resulting from conventional radiotherapy with no dose or LET painting. The therapeutic gain at a given iso-effect was calculated. Treatment adaptation during therapy in response to changes in the spatial hypoxia distribution was also considered. Results Both dose and LET painting gave higher TCPs compared to conventional radiotherapy, irrespective of particle type. The therapeutic gain from LET painting, dose painting and combined dose+LET painting was 1.08/1.44/1.46, 1.23/1.35 /1.23 and 1.26/1.27/1.32 for protons, lithium ions and carbon ions, respectively. Thus, the highest gain is obtained for dose painting with protons. Combined dose+LET painting gives only a marginally increased effect compared to dose painting only. The importance of treatment adaptation diminished for particles heavier than protons. Conclusion Dose painting is expected to give a higher tumor control probability than LET painting, in particular for protons. For heavier ions, LET painting may also give an enhanced tumor effect compared to conventional particle therapy. Dose painting may still be preferred for carbon ions, as required dose gradients are moderate. Also, adaptive dose painting with carbon ions seems to be of less importance.

Poster #46

David Hansen, Aarhus, Denmark

A simulation study comparing proton CT and dual energy CT for stopping power estimation

Hansen DC, Seco J, Sørensen TS, Petersen JBB, Wildberger JE, Verhaegen J, Landry G. Medical Physics, Aarhus University Hospital, Aarhus, Denmark: Radiation Oncology, MGH, Boston, USA; Clinical Medicine, Aarhus University, Aarhus, Denmark,Radiation Oncology, MUMC, Maastricth, the Netherlands; Medical Physics, LMU, Munich, Germany

Introduction: Accurate stopping power estimation is crucial for dose planning in particle therapy, and the uncertainties in stopping power are currently the largest contributor to the clinical dose margins. These uncertainties primarily come from the fact that x-ray CT Hounsfield units in the planning CT have no direct correlation to particle stopping power. This can cause both random and systematic errors. Dual energy x-ray CT (DECT) and proton CT (PCT) have both been proposed as improved methods for obtaining patient stopping power maps. The purpose of this work is to compare the performance of these two methods as well as the state-of-the-art single energy CT (SECT) method. Methods: Two phantoms were scanned with DECT and SECT with a DECT scanner (Siemens Medical), at a CT dose index (CTDI) of 30mGy. PCT scans were obtained from Monte Carlo simulations. Setup and detectors were modeled based on the PCT scanner at Loma Linda University, USA, including detector and electronic noise. The scans were done at a CT dose equivalent index (CTDEI) of 10mSv. Stopping power maps were calculated for all three scans, and compared with the ground truth stopping power. In addition, a sensitivity study of the stopping power accuracy of PCT was made by artificially increasing the detector noise. Results: Both DECT and PCT consistently gave better stopping power estimates than the standard CT method, reducing the root-mean-square error from 1.6% to 0.93% and 0.26% respectively, and the maximal error to 1.7% and 0.51% from 2.6%. For the sensitivity study, PCT did better than DECT at noise levels up to 10%, giving a maximal error of 0.9%, but increasing to 2.4% when 20% noise was added to the data. Conclusion: In conclusion, DECT gives an improved stopping power estimate and is commercially available and should be adopted clinically. While PCT is not yet ready for clinical use, our results indicate that it would provide an additional improvement to particle therapy.

Poster #47

Maria Fuglsang Jensen, Aarhus, Denmark

Flexible spot scanning patterns improve dose quality and -robustness in intensity-modulated proton therapy (IMPT) treatment planning

Jensen, M.F.(1), Petersen, J.B.B.(2), Alber, M.(1). (1) Department of Oncology, Aarhus University Hospital, Aarhus, Denmark (2) Department of Medical Physics, Aarhus University Hospital, Aarhus, Denmark

Introduction: Currently, the majority of intensity-modulated proton therapy (IMPT) plans are created with a regular spot scanning pattern and optimized for a homogeneous dose in each individual field (a single field uniform dose (SFUD) plan). This has proven to be the most robust approach as compared to an IMPT plan, where only the combined dose from all fields is homogeneous. The IMPT plan on the other hand, can have a much better normal tissue sparing. Methods/Materials: In this study we improve both the scanning pattern and the optimization method. We introduce an algorithm which can place the proton spots along a contour and we impose a smoothing algorithm directly on the beam weights, which allows us to optimize on all fields simultaneously and get a robust plan. We have implemented the algorithms in the multi-criteria dose planning system, Hyperion, which has a proton pencil beam dose engine. Results: Allowing the spots to be placed freely, leads to many advantages, such as improved conformity and normal tissue sparing. Also, in order to do dose painting, the dose and therefore the proton spots would need to follow some contour or well defined structure within the target. Technically, the magnetic scanning system in a pencil beam gantry is already able to handle these irregular grids. The new concept of spot weight smoothing allows us to perform a robust optimization, and find solutions that lie between the highly modulated IMPT plans and the extremely homogeneous SFUD plans. The degree of smoothing is tunable and therefore the robustness can match the uncertainties for a given diagnosis area. These results will be illustrated in a set of clinical cases. Conclusions: Using spot patterns that are adapted to a contour leads to a large variety of planning possibilities such as dose painting, precise placement of dose gradients and improved conformity. Smoothing the spot weights during optimization allows us to optimize and tune the level of robustness in a dose plan.

Poster #48

Ellen Marie Høye, Aarhus, Denmark

Improving the stability of a radiochromic deformable 3D dosimeter

Høye E M, Balling P, Drasbæk J B, Muren L P, Petersen J B B, Yated E, Skyt P S. Dept of Oncology, Aarhus University Hospital, Denmark; Dept of Physics and Astronomy, Aarhus University, Denmark

Intro: 3D dosimetry is important for verification of radiotherapy (RT) planning and delivery, in particular for complex techniques. A radiochromic silicone-based 3D dosimeter, which can be deformed during irradiation, was recently developed. The dosimeter has excellent dose response that fades quickly, and we have therefore investigated methods for improving its stability. Material & Methods: Dosimeters containing 0.26 % (w/w) leuco-malachite-green (LMG) dye, 1 % (w/w) chloroform and 9 % (w/w) curing agent (CA) were prepared with a range of bismuth neodecanoate (BiNeo) concentrations from 0 to 0.08 % (w/w), which has previously been found to increase the stability of a similar dosimeter. The CA concentration was also varied from 5 to 9 % (w/w) in dosimeters without BiNeo, and with 0.26 % (w/w) and 1.5 % (w/w) LMG dye and chloroform, respectively. The dosimeters were irradiated in a standard setup to doses from 0 to 30 Gy and read out using a spectrophotometer both prior to and several times after irradiation, in order to find the change in optical density (ΔOD) as a function of time. The dose-dependent ΔOD was fitted to a linear expression with the slope giving the dose response. Results: The dose response was stable over the first seven days after irradiation for dosimeters with 0.08 % (w/w) BiNeo, but also (59 ± 2) % lower compared to a batch without BiNeo. Decreasing the CA concentration from 9 to 5 % (w/w) increased the dose response by (24 ± 3) %, while the time constant of the observed exponential fading increased from (1.6 ± 0.2) days to (5.1 ± 0.3) days. Read out of a 3D dosimeter requires transmission of a laser beam through it, and thus the pre-irradiation OD is critical. This initial OD increased by (156 ± 3) % and (38 ± 1) % when adding 0.08 % (w/w) BiNeo and 5 % (w/w) CA, respectively. Conclusion: The stability of a new radiochromic, deformable 3D dosimeter can be greatly improved by including low concentrations of BiNeo or by reducing the CA concentration.

Poster #49

Vicki Trier Taasti, Aarhus C, Denmark

A new approach for stopping power ratio calibration in proton beam therapy using spectral CT

Taasti V. T.1, Hansen D. C.1, Muren L. P.2, Grau C.1, Petersen J. B. B.2. 1: Department of Oncology, Aarhus University Hospital, Aarhus, Denmark. 2: Department of Medical Physics, Aarhus University Hospital, Aarhus, Denmark.

Background Precise range determination of protons is required to release the full potential of proton therapy. The range calculations are based on proton stopping power ratios (SPRs), today determined through a calibration relation with the CT-numbers from an x-ray CT scan. However, there is no simple correspondence between these quantities, and large range uncertainty margins are therefore required, diminishing the advantage of proton therapy compared to conventional photon therapy. In this study we have developed a new general method for calibrating CT-numbers to SPR from dual energy CT (DECT) or spectral CT scans, independent of the number of energy spectra. The method does not require the energy spectrum of the CT scanner, but relies on calibration scans of a phantom with known elemental composition. Methods CT images of the Gammex 467 calibration phantom were acquired at a Dual Source CT scanner (Siemens Somatom Definition Flash) using a number of energy spectra. The calibration phantom contains 13 tissue mimicking inserts with known SPRs. The new approach for CT calibration was compared to previously published methods for DECT to investigate if it reduces the uncertainty in the SPR calculation. For testing the performance of the various calibrations, one insert at a time was excluded from the calibrations and then the calibration parameters of each method were used for calculating the SPR of this insert. Results In general, our method showed an improvement in the SPR calculation when the number of energy spectra was increased from two to four – the mean error was reduced from 1.2% to 0.6%. The mean SPR error for the 13 tissue inserts with two energy spectra was comparable to that obtained using the DECT calibrations presented by other groups. Conclusion Our new calibration approach with more than two energy spectra was found to improve the accuracy of SPR calculation, potentially opening for reduction of range uncertainty margins.

Poster #50

Anne Ivalu Sander Holm, Aarhus, Denmark

Dose escalation IMRT and IMPT study using FET-PET in high-grade gliomas – initial experiences

Holm, A.I.S.2, Seiersen, K.2, Lassen-Ramshad, Y.1, Borghammer, P.3, Petersen, J.B.B.2, Lukacova, S.1. 1Aarhus University Hospital, Oncology Department, Aarhus, Denmark, 2Aarhus University Hospital, Department of Medical Physics, Aarhus, Denmark 3Aarhus University Hospital, Department of Nuclear Medicine & PET Centre, Aarhus, Denmark

Introduction: We investigated the impact of amino-acid 18F-fluoro-ethyl-tyrosine (FET) positron emission tomography (PET) on target definition and treatment planning of high-grade gliomas versus the current standard using MRI alone. Furthermore, the possibility of dose escalating the FET-PET active area by either IMRT or IMPT was addressed. Materials and methods: A 40-year old patient with radically resected anaplastic astrocytoma was scanned using FET-PET/CT and MRI (T1 and T2/fluid attenuated). CTV-MR(60 Gy) and CTV-MR(46 Gy) were defined as tumor cavity plus 1 cm and 2 cm, respectively. CTV-MR(46 Gy) included the surrounding edema and was adapted to anatomic barriers. CTV-FET(60 Gy) was defined from the postoperative FET-PET imaging and covered the volume within a tumor-to-brain ratio cut-off value of FET uptake ≥ 2,1. PTVs were generated by adding 3 mm uniformly. The standard 5 field IMRT plan was compared to an IMRT plan on CTV-FET(60 Gy), and to both IMRT and IMPT dose escalation plans. The homogeneity of PTV(46 Gy) were defined by V(1.07×46Gy) and the resulting dose distributions were evaluated by means of dose-volume histograms. Results: The CTV-FET(60 Gy) volume was considerably smaller than the corresponding CTV-MR(60 Gy) volume. Thus, the mean doses to the surrounding organs at risk were decreased (2.4%-6.7%). Furthermore, the volume of the brain receiving doses higher than 60 Gy was considerably reduced (72 cc to 17 cc). It was possible to dose escalate CTV-FET(60 Gy) with no accompanying decrease in PTV(46 Gy) homogeneity or increase in the dose to the organs at risk. The technical obtainable maximum and mean doses were 93 Gy and 68 Gy with IMRT and 156 Gy and 97 Gy with IMPT. Conclusion: For this patient FET-PET based target delineation reduced the 60 Gy target volume, which in turn yielded modest dosimetric benefits, with regards to normal tissue sparring. Furthermore, dose escalation of the CTV-FET(60 Gy) using IMRT or IMPT was found feasible.

Poster #51

Ida Mølholm, Lyngby, Denmark

The dosimetric impact of an MRI contrast agent in photon and proton radiotherapy

Finnerup E1, Mølholm I1, Edmund JM2 and Mahmood F2. 1Dept. of Electrical engineering, Technical University of Denmark. 2Radiotherapy Research Unit, Dept. of Oncology, University of Copenhagen, Herlev, Denmark.

Introduction: The increased use of MRI for target delineation in radiotherapy shows a promising potential for adaptive treatments and online image guidance using e.g. the MRI-Linac with a MRI contrast agent. In this study, we investigate the dosimetric impact of a Gd-based MRI contrast agent in intracranial targets during photon and proton beam irradiation. Materials and methods: Delineations of 30 brain metastases from 12 patients with Gd contrast enhanced T1W MRI scans were transferred to the co-registered CT scans. Gd concentrations in the metastases were estimated from an MRI and CT scan of a Biresin cylindric phantom with 5 inserts of known Gd Dotarem solutions (8.4, 4.2, 0.83, 0.17, 0.08 mg/mL) and a saline reference (0 mg/mL). Histograms of MRI intensities in the phantom and patients were normalized to the saline reference and the cerebrospinal fluid of the ventricles, respectively. The phantom/patient peak-to-peak distance was compared and a Gd concentration and CT number assigned to patient CT scan. Clinical photon and 3-field proton plans were re-calculated with the assigned CT numbers in the metastases (Eclipse v. 11) and the difference in D90% (dD90) noted. The phantom CT- concentration curve was further linearly extrapolated to estimate the dosimetric effect of the Gd concentration in the metastases up to 200 mg/ml. Results: A non-significant dosimetric effect (dD90 < 1%) was found in both the photon and proton plans for the estimated patient concentrations (0.08-8.4 mg/ml). At concentrations > 100 mg/ml, the decrease in dD90 is > 1.2% for protons while the dD90 < 1% for photons up to 200 mg/ml. Conclusions: At clinical Gd concentrations, no dosimetric effect was found for both the photon and proton irradiations. For simulated Gd concentrations > 100 mg/ml a significant effect could be observed for the proton irradiations.

Poster #52

Shirin Rahmanian, Heidelberg, Germany

Toward a New Microscopic Dosimetry of Ion therapy

Rahmanian S, Niklas M, Abdollahi A, Jäkel O ,Greilich S. Department of Medical Physics in Radiation Oncology, German Cancer Research Center (DKFZ), Heidelberg, Germany

Introduction: Ion beam radiotherapy offers an important advantage over conventional photon radiotherapy due to the highly localized energy deposition of ions leading to an enhanced relative biological effectiveness (RBE). However, the energy deposition is marked by large fluctuation on a microscopic scale and needs to be taken into account for reliable prediction of the clinical effect. Current dosimetric measurements used in radiotherapy are not sufficient to quantify energy deposition at such microscopic levels and thus a dosimteric system capable of assessing such variation at a sub-cellular level is highly desired. Materials & Methods: Fluorescent Nuclear Track detector (FNTDs) based on Al2O3:C,Mg crystals combined with laser scanning microscopy allow for high resolution detection of particle tracks including information on 3D track trajectories, (charge composition) and pattern of energy deposition. FNTDs coated with cells (Cell-Fit-HD) were irradiated at Heidelberg Ion Therapy Center with carbon ions in order to study the cellular energy deposition pattern of carbon ions near the Bragg peak. Results: The cellular hit statistics obtained from the Cell-Fit-HD readout were translated into relevant dosimetric quantities. Different sources of variations including fluctuation in fluence, energy loss straggling, nucleus size distribution and chord length distribution in the nucleus were analyzed to measure the uncertainties in the calculated quantities. Conclusion: The track structure information gained from the FNTD technology in addition to the analysis of factors influencing energy deposition of ions at subcellular scales, in terms of magnitude and significance, can pave the way toward constructing a biologically relevant dosimetry system for ion therapy.

Poster Discussion Group 8

Poster #53

Sidsel Damkjær, Næstved, Denmark

Improved dose coverage of internal mammary nodes using deep inspiration breath hold for right-sided breast cancer radiotherapy

Damkjær SMS, Nielsen MEK, Kadkhoda ZT, Leth MJ, Jensen NKG, Logadottír Á, Lassen SA. Department of Radiation Oncology, Næstved Sygehus, Næstved, Denmark

Purpose: Including the internal mammary nodes(IMN) in the CTV of adjuvant radiotherapy of breast cancer(BC) patients increases survival[1]. Right-sided BC patients are often treated in free breathing (FB) and occasionally part of the IMN is left untreated to be able to avoid exceeding the dose constraint of the ipsilateral lung. The deep inspiration breath hold (DIBH) technique is routinely used for left-sided BC patients. Here, we investigate if right-sided BC patients benefit from DIBH in terms of IMN dose coverage. Method: Ten right-sided BC patients (four lumpectomy and six mastectomy patients) with locoregional lymph node involvement were CT scanned in DIBH and FB. The delineations were retrospectively evaluated to ensure uniformity especially regarding IMN. Treatment plans of 50 Gy in 25 fractions were created according to Danish national guidelines. Dose indices from DIBH and FB plans were compared using the Wilcoxon signed rank-sum test. Results: A statistically significant increase was seen in the volume of the IMN receiving 90% or more of the prescribed dose (<V90%,IMN,FB>=59% and <V90%,IMN,DIBH>=88%, $p<0.03$). For the ipsilateral lung the volume receiving 20Gy or more, V20Gy,lung, was significantly decreased (<V20Gy,lung,FB>=34% and <V20Gy,lung,DIBH>=29%, $p<0.006$). For eight patients the V90%,IMN increased using DIBH and for nine the V20Gy,lung decreased with DIBH. For two patients V90%,IMN was higher for FB compared to DIBH (max difference 3.4%, both above 90%), however, V20Gy,lung was decreased by at least 6.5% in both DIBH plans. There were no significant differences in the dose coverage of the breast($p>0.19$) or dose to the heart and cardiac arteries($p>0.13$). Conclusion: On average, right-sided BC patients treated in DIBH have improved dose coverage of the IMN. If sufficient IMN coverage can be achieved in FB, patients still benefit from a decrease in ipsilateral lung dose without compromising target coverage.
[1]: Acta Oncol 2014;53:1027-1034.

Poster #54

Tine Bisballe Nyeng, Aarhus, Denmark

Dosimetric evaluation of interfractional shifts in oesophageal cancer patients

Nyeng, TB (1), Nordsmark, M (2) and Hoffmann, L (1). (1) Department of Medical Physics, Aarhus University Hospital, Denmark (2) Department of Oncology, Aarhus University Hospital, Denmark

Introduction. Some oesophageal cancer patients (pts) undergoing chemoRT treatment show large interfractional anatomical changes during the treatment course. These changes may modify the dose delivered to the target and organs at risk (OARs). The aim of the present study was to investigate the dosimetric consequences of anatomical changes over a treatment course. Materials and methods. Twenty three consecutive pts were treated with chemoRT for oesophageal and gastro-esophageal junction cancer and set up according to daily cone-beam-CT scans (CBCTs). The median gross tumour volume (GTV) was 45cm3 (9-235cm3). The median clinical target volume (CTV) was 283cm3 (98-692cm3) and the median cranio-caudal extent was 13cm (8-20cm). All patients had an additional CT scan around fraction ten, which was deformably registered to the planning-CT. GTVs, CTVs and OARs were transferred to the additional CT and corrected by an experienced physician. Treatment plans were recalculated and dose to targets and OARs were evaluated. Pts were re-planned if V95% coverage of CTV decreased >1% or PTV decreased by >3%. Results: The median decrease in V95% coverage of CTV was 0.2% (0-35%) and coverage of PTV 3.0% (0-41%). In five pts (22%) CTV V95% decreased more than 1% and in another five pts PTV V95% decreased more than 3%. All these pts had their treatment plan adapted. The largest discrepancies were caused by interfractional baseline or amplitude shifts in diaphragm position (4 pts). Mediastinal (4 pts), oesophageal (2 pts) and bowel filling changes (2 pts) caused the remainder of the changes. For pts selected for adaptation, the discrepancies were confirmed by inspecting the daily CBCTs. In 30% of all pts, heart V30% increased more than 2% (max 5%). Only minor charges in lung dose or liver dose were seen. Conclusion: Target coverage throughout the course of chemoRT treatment is compromised for some pts due to interfractional anatomical changes. Dose to the heart may increase as well.

Poster #55

Rune Hansen, Aarhus, Denmark

Calypso-guided MLC tracking on a TrueBeam accelerator

Hansen R., Ravkilde T., Worm E.,Toftegaard J., Grau C., Macek K., Poulsen P. Department of Oncology, Aarhus University Hopsital, Aarhus, Denmark

Purpose: MLC tracking is a promising method for real-time target motion compensation, and a number of studies with prototype MLC tracking systems have demonstrated the ability to mitigate motion-induced dose errors. However, to get MLC tracking into routine clinical practice a more integrated system is needed. This study provides the first characterization of the prototype MLC tracking system included in the research part of the Varian TrueBeam 2.0 accelerator. Methods: The MLC tracking system latency was determined as the time lag between sinusoidal target motion and the center of a circular beam as recorded by continuous MV portal imaging during MLC tracking with prediction turned off. The same measurements were done for the backup jaws. The geometric tracking accuracy was determined as the 2D distance in portal images between a target following eight representative trajectories (prostate and lung) and the circular MLC aperture. The dosimetric tracking accuracy was quantified by measuring the dose of low and high modulation VMAT plans to a moving Delta4PT phantom that reproduced the same eight trajectories and comparing this dose with a static reference dose (2%/2mm gamma evaluation). A linear Kalman filter prediction was used to account for the tracking system latency in the accuracy experiments. Results: The mean tracking system latency was 145ms (SD=7.4ms) for MLC tracking and 143ms (SD=17ms) for the tracking backup jaws. Compared to non-tracking, MLC tracking reduced the mean root-mean-square geometric targeting error from 2.7mm to 0.5mm (parallel to MLC leaves) and from 2.4mm to 1.1mm (perpendicular). Dosimetrically, MLC tracking reduced the motion induced gamma failure rate from 30.0% to 9.4% (prostate) and from 41.2% to 3.4% (lung) on average. Conclusions: TrueBeam MLC tracking performance was thoroughly investigated for the first time. The system has similar geometric and dosimetric performance as previously reported for prototype MLC tracking systems.

Poster #56

Annette Boejen, Aarhus, Denmark

A learning program qualifying radiation therapists to manage daily online adaptive radiation treatment

Boejen A1, Vestergaard A2, Hoffmann L2, Ellegaard MB1 , Rasmussen AM1, Moeller D2, Muren LP2, Grau C1. 1: Aarhus University Hospital, Department of Oncology, Aarhus C, Denmark, 2: Aarhus University Hospital, Department of Medical Physics, Aarhus C, Denmark

Introduction: Successful and cost-effective implementation of image guided adaptive radiotherapy (ART) requires Radiation Therapists (RTTs) with skills to manage daily online ART. The aim of this study was to show that RTTs in large scale can be qualified to manage daily online ART safely and with limited increase in treatment time. Material and methods: Fourteen RTTs were involved in the learning program for selection of the smallest treatment plan that covers the entire bladder from a predefined library of three plans. Twenty nine RTTs were involved in primary lung tumour match followed by evaluation of tumour and lymph nodes positions and anatomical changes. Lectures, e-learning (LäraNära AS) and seminars with hands-on exercises based on retrospective patient (pt) data were scheduled in a Learning Centre (VERTUAL, VMS). All RTTs had to pass a test. RTTs worked in pairs and their 16 plan selections were compared to two expert results. For lung, the RTTs worked individually and match as well as anatomical changes in 12 fractions (fx) were compared to two expert results. Retrospective expert evaluation was performed for 22 bladder cancer pts and 50 lung cancer pts treated with online ART. The increase in treatment time was monitored. Results: In the bladder project, all RTTs passed the test in plan selection. Review of 22 bladder cancer pts (555 fx) revealed 11 fx(2%) with a marginal wrong choice of treatment plan, 3 fx(0,5%) where couch corrections were not performed. In the lung project, 22 RTTs (76%) passed the first ART test, 7(24%) had additional learning and test. The evaluation of deviations noted by the RTTs after clinical start showed that 54 scored deviations were correct, 17 deviations were missed, 9 scored deviations were incorrect.The treatment time increased with 5 min/fx for bladder and 4 min/fx for lung Conclusion: It was possible to qualify RTTs in large scale to manage daily online ART safely and with a moderate increase in treatment time.

Poster #57

Jakob Toftegaard, Aarhus, Danmark

Design improvement for TrueBeam MLC tracking investigated with an MLC tracking simulator

J. Toftegaard, R. Hansen, T. Ravkilde, K. Macek, P. R. Poulsen. Aarhus University Hospital, Aarhus C, Denmark and Varian Medical Systems, Imaging Laboratory GmbH, Baden-Daettwil, Switzerland

Purpose: MLC tracking is a promising method for intrafraction tumor motion management by real-time adaptation of the MLC aperture to the moving target. However, limitations in MLC adaptation leads to residual dosimetric errors. Here, we investigate the dosimetric benefits of potential tracking system improvements by performing large-scale simulations with an MLC tracking simulator. Materials/Methods: The Varian TrueBeam MLC tracking system, using Calypso as target localization system (25Hz) was used as reference for the simulator. Both the accelerator and simulator performs three steps every 10ms. 1) Predict target position, 2) fit MLC shape to the estimated target position, and 3) adjust MLC leaves to the fitted MLC shape. Residual MLC adaptation errors were quantified by the over- and under-exposed MLC aperture area (Au+Ao). The simulated gantry and MLC dynamics were benchmarked against tracking experiments. The simulator was tested with the following design improvements: A) halving the prediction error (localization), B) halving the MLC leaf width (MLC fitting), C) dynamic alignment of the collimator with the preferred target motion direction (MLC fitting), and D) doubling acceleration and maximum speed of the MLC (leaf adjustment). Each improvement were compared with the current system and tested for a significant decrease in Au+Ao. A high and a low modulated plan for both prostate and lung were simulated with 160 lung and 187 prostate traces. Results: For lung, the mean Au+Ao was on average reduced by A) 13.5%, B) 4.2%, C) 28.1%, D) 5.77% and all 50.9% by the tested tracking system improvements. For prostate, Au+Ao was reduced by A) 2.4 %, B) 10.1 %, C) 18.8%, D) 5.20% and all 30.3%. All reductions were significant with a p-value below 0.01. Conclusion: All system modification simulated gave significant reductions of the tracking error. The largest improvement was seen for dynamic collimator rotation, which does not require any hardware modification.

Poster #58

Toke Ringbæk, Marburg, Germany

Planning evaluations of new 2D ripple filters in carbon ion treatment plans using TRiP98 and Monte Carlo code SHIELD-HIT12A

Ringbæk T P (1,2,3), Weber U (1), Santiago A (3,4), Simeonov Y (1), Fritz P (5), Wittig A (4), Bassler N (2,6), Engenhart-Cabilic R (4) and Zink K (1,4). 1)Technische Hochschule Mittelhessen, Gießen, 2)Department of Experimental Clinical Oncology Aarhus, 3)Philipps-University Marburg, 4)University Hospital Gießen-Marburg, 5)St Marien-Krankenhaus Siegen, 6)Department of Physics and Astronomy Aarhus

A ripple filter (RiFi) is a passive energy modulator that enlarges the bragg peak (BP) width proportionally to the maximum RiFi-thickness so larger energy steps can be applied in scanned particle beam treatments to significantly reduce the treatment time. First generation RiFis, used at European treatment centers, have a 3 mm maximum thickness and 1D groove shapes with a flat non-modulating base layer. A new second generation RiFi with 2D groove shapes has been developed using stereolithography with thicknesses up to 6 mm and no base layers. Treatment plans for 2, 3 and 4 fields were prepared using the standard 1D 3 mm RiFi and 4 and 6 mm 2D RiFis for spherical PTVs as well as for stage I NSCLC tumor cases, which were treated with photon SBRT under high-frequency jet ventilation, which largely reduces tumor motion. Energy step sizes were set to the respective RiFi thicknesses. The planning objective is minimum 95% prescribed dose to 98% of the PTV. TRiP98 was used for treatment planning with facility-specific physical kernels made with the Monte Carlo code SHIELD-HIT12A. CT-images, contours and planned dose distributions are displayed with PyTRiP. DVHs, dose distributions and dosimetric indexes were used for plan evaluation. Plan homogeneity and conformity are found to be slightly better for thinner RiFis but satisfactory plans can be made for all. Spiked structures in the dose distribution caused by larger energy steps are observed at PTV edges for some 6 mm RiFi cases, requiring more fields to reach the planning objectives. Performance increases with penetration depth since straggling and scattering effects blur out inhomogeneities and further broaden the BPs. The new RiFi design produces for studied cases in general results comparable to the standard RiFi. 2D 4 mm RiFis lower the irradiation time by 33% and can easily be implemented in systems already utilizing the standard design. Two-field 6 mm RiFi plans are still faster than three-field 3 mm RiFi plans.

Poster #59

Alina Santiago, Marburg, Germany

Interfractional local changes in the radiological depth correlate with dosimetric deterioration in particle beam therapy for stage I NSCLC patients under jet ventilation

Alina Santiago1*, Peter Fritz2, Werner Mühlnickel2, Rita Engenhart-Cabillic1, and Andrea Wittig1.

1. Philipps University Marburg and University Hospital Giessen and Marburg, Department of Radiotherapy and Radiation Oncology, Marburg, Germany; 2. St Marien-Krankenhaus, Department of Radiotherapy, Siegen, Germany; *Corresponding Author

Current strategies for image guidance usually rely on anatomic landmarks or fiducial markers. However, particle dose distributions are highly sensitive to anatomy changes, and even under a correct geometric tumor repositioning substantial dosimetric deviations may occur. For this reason dedicated image-guidance solutions are needed to tackle these specific problems. The aim of this work is to develop methods to quantify anatomical discrepancies depicted by repeated CT imaging and to test their ability to predict clinically relevant dosimetric deviations. Software tools have been developed which allow voxel-based calculations of the changes in the water equivalent path length (WEPL) in specific beam directions inside selected regions of interest. We tested these methods on available datasets of stage I NSCLC patients for which planning and localization CT under high frequency jet ventilation as tumor fixation method were available. Proton and carbon ion plans were made and we analyzed the deviations in target coverage between planning and delivery times and correlated them with the corresponding changes in the WEPL. Proton plans for 12 patients were prepared assuming fixed beam lines at 0° and 45°. The decrease in the V95%(GTV) between plan and recomputation was in median 0.1 percentual points (pp), range 0 to 8.9 pp. For two patients the decrease was unacceptably high: 4.5 and 8.9 pp, presenting the higher differences in the mean absolute value of the WEPL at the beam directions of 4.7 and 3.3 mm (water equivalent), respectively. With new two-field plans at 0° and 90°, the decrease in the V95%(GTV) could be reduced to 1.3 and 0.0 pp, reflected also in lower WEPL differences of 3.3 and 1.5 mm, respectively. Preliminary results show that local WEPL differences after co-registration of the planning and the localization CT correlated significantly with the decrease in dosimetric indexes and helped to detect the two problematic cases in this patient series.

Poster #60

Caroline Grønborg, Aarhus C, Denmark

Population-based vs patient-specific margins for intra-fractional motion in adaptive bladder radiotherapy

Grønborg C[1], Vestergaard A[1], Høyer M[2], Pedersen EM[3], Petersen JBB[1], Jesper Kallehauge[1] and Muren LP[1]. 1: Dept of Medical Physics, Aarhus University Hospital, Aarhus, Denmark 2: Dept Oncology, Aarhus University Hospital, Aarhus, Denmark 3: Dept of Radiology, Aarhus University Hospital, Aarhus, Denmark

Introduction: The bladder is an appealing target for adaptive radiotherapy (ART) strategies due to inter-fractional motion, but it may also display intra-fractional changes. The aim of this study was to calculate population-based and patient-specific margins for intra-fractional changes using repeat volumetric magnetic resonance imaging (MRI). Materials/methods: 9 patients treated in a phase II clinical plan selection ART trial for bladder cancer were included. They underwent pre-treatment and weekly repeat MRI series (mDixon; voxel size: 0.9×0.9×1.5 mm; scan time: 40s) acquired at t=0, 2, 4, 6, 8, 10min. The bladder CTV was delineated in all scans and described using spherical coordinates. Population-based 2D margin maps were derived by adapting a conventional margin recipe for bladder (Meijer et al, IJROBP 2003), characterising the intra-fractional changes (t=0min to t=10min) in terms of systematic and random errors. Patient-specific intra-fractional margins were explored by using the bladder expansions occurring in the first two series. A linear model was used to fit the radial changes as a function of time, focusing on expansions larger than 5mm. The margin was defined as the upper 95% confidence limit of the linear coefficient times the relevant intra-fractional time (here 10min). Results: The population-based margins are: superior/anterior 14mm, posterior 9mm and inferior/left/right 5mm. Margins specific for each patient could be derived from the linear model (ranging up to 12 mm; R^2 in the range: 0.33-0.68). Conclusions: This is the first study to present both population-based and patient-specific margins for intra-fractional motion for the bladder. The population-based margins were large in superior and anterior directions, and are a concern in particular when pursing on-line re-planning. We also found that the large intra-fractional margins required for some patients can be identified and estimated from limited data.

General Poster Display

Poster #61

Ahmad Ali, Cairo, Egypt

MIM: A New Auto-Contouring and Deformable Registration Software for Adaptive Lung Radiation Therapy

Ali A.S.a, Nyeng T.B. b, Moller D.S. b, Hoffmann L. b , Khalil A.A.c. a) Department of Clinical Oncology, Cairo University, Cairo, Egypt b) Department of Medical Physics and c) Department of Clinical Oncology, Aarhus University, Aarhus, Denmark

Introduction: The practicality of adaptive radiotherapy depends on the use of suitable automation algorithms that allow for accurate and fast adaptation. The aim of this study was to assess MIM software and compare it to a commercially available model in terms of organs at risk (OAR) and gross target volume (GTV) delineation. Material and Methods: 20 consecutive lung cancer patients underwent auto-contouring of the OAR on the planning CT by MIM atlas-based segmentation algorithm, followed by a timed correction. This was compared to the time required for manual delineation on Varian Eclipse program. After that, they underwent deformable registration (DFR) of the GTV on rescans by MIM and Eclipse SmartAdapt software. Assessment of the degree of overlap between manually delineated GTV and those auto-contoured by DFR of both software algorithms was done by means of the DICE co-efficient. Results: The MIM auto-contouring software mean correction time was longer than manual delineation time for the heart 3:35±0:44 vs. 2:48 ±0:33min (p=0.001), and esophagus 6:56±1:28 vs. 2:50 ±0:37min (p=0.002). Similar results were seen in trachea and bronchi. On the other had it was shorter for the lungs 0 vs. 3:33±0:48min (p=0.001) and spinal cord 0:02±0:08 vs. 0:42±0:33min (p=0.001). In terms of DFR there was no significant difference between either software and manually delineated target volumes in terms of accuracy measured by the DICE co-efficient for GTV-T: 0.85±0.12 vs. 0.88±0.10 (p=0.335) and GTV-N : 0.78±0.05 vs. 0.78±0.13 (p=0.969). However, MIM was shown to be less time consuming as it performed DFR in a single step through the workflow option compared to Eclipse SmartAdapt which carries out the same process in 3 steps. Conclusion: MIM OAR auto-contouring algorithm did not reduce delineation time, due to non-optimal atlas segmentation. However, its DFR software is comparable to Eclipse SmartAdapt in terms of GTV delineation accuracy, and has been shown to be more time-saving.

Poster #62

Mette Winther, Aarhus, Denmark

Evaluation of miR-21 and miR-375 as prognostic biomarkers in esophageal cancer

Winther M, Alsner J, Tramm T, Baeksgaard L, Holtved E, Nordsmark M. Dept. of Exp. Clinical Oncology, Aarhus University Hospital, Aarhus, DK. Dept. of Pathology, Aarhus University Hospital, Aarhus, DK. Dept. of Oncology, Rigshospitalet, Copenhagen, DK. Dept. of Oncology, Odense University Hospital, Odense, DK.

Introduction: MicroRNAs (miRs) have been shown to be associated with prognosis in esophageal cancer, suggesting a role for miRs to help guide treatment decisions. Especially, miR-21 and miR-375 have been investigated as prognostic markers. However, results have been contradicting. The aim of this study was to evaluate the prognostic potential of miR-21 and miR-375 in esophageal squamous cell carcinomas (ESCC) and esophageal adenocarcinomas (EAC) in order to improve patient selection for chemoradiotherapy (CRT). Materials and methods: Pre-therapeutic tumour specimens from 195 patients with loco-regional esophageal cancer treated with neoadjuvant or definitive (CRT) or perioperative chemotherapy were analysed. Expression levels of miR-21 and miR-375 were quantified using Affymetrix GeneChip miRNA 1.0 Array. The Cox proportional hazards model was performed to assess the correlation of miR-21 and miR-375 with disease-specific survival (DSS) and overall survival (OS). Median expression levels of miR-21 and miR-375 were used as cut off. Results: For miR-21, a trend towards a poorer DSS and OS was shown for ESCC patients with induced miR-21 expression. To further elucidate this correlation, miR-21 expression was divided into tertiles. High levels of miR-21 significantly correlated with shortened DSS and OS (HR: 2.00 (95%CI: 1.89-3.37) and HR: 1.89 (95% CI: 1.19-2.99)). Similarly, a significant association between high miR-21 expression and DSS was observed for patients with EAC (HR: 2.57 (95%CI: 1.11-5.93)) and a trend towards a poorer OS for patients with induced miR-21 expression was shown. Multivariate analyses identified miR-21 as an independent prognostic marker for both DSS and OS in ESCC, but not in EAC. For miR-375, no correlations with DSS or OS were observed in ESCC or EAC. Conclusions: In this study, miR-21 was identified as an independent prognostic biomarker in patients with ESCC but not EAC. miR-375 did not serve prognostic value in neither ESCC nor EAC.

Poster #63

Alexandr Kristian, Oslo, Norway

Dynamic 18F-FDG PET of breast cancer xenografts and correlation with treatment outcome

Kristian A, Revheim ME, Qu H, Mælandsmo G, Engebråten O, Malinen E. Oslo University Hospital, Oslo, Norway. University of Oslo, Oslo, Norway.

Introduction: Treatment outcome of breast cancer is dependent on tumor perfusion and tumor burden, among others. Dynamic 18F-FDG-PET (D-PET) allows for 4D studies of glucose distribution in tissue. The purpose of this study was to utilize D-PET for assessment of perfusion and glucose metabolism in patient-derived breast cancer xenografts (BCX) and investigate whether D-PET image parameters correlate with chemotherapy outcome. Materials and methods: Three basal-like and three luminal-like xenograft lines were inoculated bilaterally in mammary fat pads in athymic nude mice. D-PET (1 hour scan) was performed with 18F-FDG as tracer. Pharmacokinetic analysis was done to estimate transfer rates between the vascular, non-metabolized, and metabolized compartments. Mice were then randomized in four groups, receiving either vehicle, paclitaxel, doxorubicin or carboplatin. Tumor doubling time (DT) was calculated. Correlations between DT and pharmacokinetic parameters were estimated using Spearman's correlation. Results: The pharmacokinetic rate constants varied significantly between the different BCXs ($p<0.05$), indicating distinct vascular and metabolic tumor profiles. In each BCX group, variations in rate constants were small. DT was significantly increased for all the models and all treatments ($p<0.05$). However, some of cytotoxic drugs showed moderate effect on DT, while others increases DT more than 10-fold. The rate constants were mostly not significantly correlated to DT. However, for paclitaxel treatment, DT showed a tendency towards negative correlation with rate parameters. This may be due to higher treatment resistance of hypoperfused tumors. Conclusions: The different xenograft lines have different vascular and glycolytic D-PET parameters. The parameters showed little intra-xenograft variation, indicating that D-PET is a robust technique. Poor outcome following paclitaxel treatment may be predicted by pharmacokinetic rate constants.

Poster #64

Anne Winther Larsen, Aarhus, Danmark

Loco-regional failures in limited disease small-cell lung cancer patients treated with definitive chemoradiotherapy

Winther-Larsen A1, Hoffmann L2, Moeller DS2, Khalil AA1 and Knap MM1. 1) Department of Oncology, Aarhus University Hospital, Aarhus, Denmark. 2) Department of Medical Physics, Aarhus University Hospital, Aarhus, Denmark

Background: Radiotherapy (RT) for patients (pts) with limited disease small-cell lung cancer (LD-SCLC) has improved in the last decades. The number of distant metastases has declined considerably mainly due to improved staging procedures. However, loco-regional failure (LRF) remains to be a significant problem. This study was conducted to evaluate the pattern of first failure in a cohort of LD-SCLC pts treated with definitive chemoRT. Material and methods: From 2007-2013, 147 consecutive LD-SCLC pts underwent definitive chemoRT. RT was delivered as either 45 Gy in 30 fractions (fx) twice daily (N=130) or 46-50 Gy in 23-25 fx (N=17). Chemotherapy was etoposide combined with either carboplatin (N=97) or cisplatin (N=49) given concomitant (N=129) or sequential (N=18) with RT. Pattern of first failure and survival were retrospective evaluated. Disease free survival (DFS) and overall survival (OS) were calculated by Kaplan-Meier method. The impact of covariates (age, sex, performance status, TNM-stage, dose and schedule of RT, chemotherapy, and dosimetric parameters) on development of LRF was tested by logistic regression. In pts with LRF, clinical target volume (CTV) was compared to Cone Beam computed tomography (CBCT) scans if available. Results: With a median follow-up time of 42.2 months, the site of first failure was LRF in 37 pts (25%) and distant in 74 pts (50%). Sixteen pts had isolated LRF. 1-year DFS was 52% and 31% at 3-year. 1-year OS was 74% and 34% at 3-year. Having T3 or T4 disease was the only factor being independent correlated to development of LRF (p=0.05). Daily CBCT scans were available in 20 pts, and the CTV was in-field for all fx in 14 pts (70%), marginal covered in 3 pts (15%) and partly out-of-field in 3 pts (15%). Conclusion: LRF was seen in 25% of LD-SCLC pts treated with definitive chemoRT. In pts with LRF, the CTV was predominantly in-field for all fx. Reduction of LRF might be achieved with dose-escalation in pts with high T-stage.

Poster #65

Kirsten Legaard Jakobsen, Herlev, Denmark

Soft tissue vs. bony anatomy registration in an adaptive plan selection protocol for bladder cancer

Jakobsen K.L. (1), Lindberg H. (1), Petersen J.B.B (2) , Muren L.P. (2), Høyer M.(2), Vestergaard A. (2).
(1): Herlev Hospital, University of Copenhagen, Department of Oncology, Herlev, Denmark
(2): Department of Medical Physics and Department ofOncology, Aarhus University Hospital.

PURPOSE: In radiotherapy of urinary bladder cancer, deformations of the bladder is a major challenge. Our institutions are therefore running a clinical trial of adaptive radiotherapy (ART) using plan selection where the bladder on each treatment session is treated with the smallest possible PTV. We treat patients based on bony anatomy registration although set-up based on the bladder might be favourable. The increased patient focus on the importance of having an empty bladder every day might reduce the difference between soft tissue vs. bony anatomy based registrations. In this study we compare this difference for patients treated in vs outside the adaptive protocol. MATERIALS AND METHODS: The study included the first ten patients from our institution included in the bladder ART trial and nine patients treated before enrolling patients. The difference between bony anatomy vs soft tissue registration was compared on CBCTs. For the bony anatomy registration, the patients were aligned on the whole pelvic bones except the moveable part of the femoral heads. For the soft tissue match the registration volume was narrowed to 1 cm from the bladder. The difference between these strategies was assessed by calculating the vector length of the difference in Cartesian coordinates. RESULTS: Patients treated in the ART trial have a stronger correlation between soft tissue and bony anatomy registration. The mean vector length was 2 mm for the ART patients and 4 mm for the non-ART patients. The difference in the vector and the vertical direction are statistically significant ($p<0.05$) while the longitudinal and lateral differences were not statistically significant ($p>0.4$). CONCLUSIONS: For patients treated with ART the difference between a bony anatomy and a soft tissue registration is in the order of 2 mm compared to 4 mm for bladder patients treated outside the ART protocol. This difference is possibly due to the increased patient-awareness to the bladder emptying instruction.

Poster #66

Mirjana Josipovic, København, Denmark

Image quality and registration uncertainty in image guided deep inspiration breath hold radiotherapy of lung cancer

Josipovic M, Persson GF, Westman G, Bangsgaard JP, Specht L, Aznar M. Dept. of Oncology, Section for Radiotherapy, Rigshospitalet, Copenhagen, Denmark

Introduction: We investigated the impact of deep inspiration breath hold (DIBH) and tumor baseline shifts on image registration uncertainty and image quality in image guided radiotherapy (IGRT) for locally advanced lung cancer. Materials and methods: The 15 patients included were referred for free-breathing (FB) radiotherapy with daily CBCT as image guidance. At fractions 2, 16 and 31 (of 33) additional CBCT in DIBH was obtained. Both CBCTs from these fractions were off-line rigidly registered (on tumor) to the planning day's FB and DIBH CTs. All registrations were performed twice to evaluate the intraobserver uncertainty. To assess the image quality, CBCTs were scored by a single observer on degree of streak artifacts, and visualization of tumor, bronchi, lung vessels and fissures. Tumor baseline shift between consecutive DIBHs is ≤2 mm for 70% of cases1. We simulated tumor baseline shifts (1,2,5 mm) between three consecutive DIBHs while acquiring a DIBH CBCT of a CIRS Thorax phantom. A cylindric 9 mm high nodule with half-sphere (radius 9 mm) on top was inserted in the phantom, emulating a lung tumor. Results: Intraobserver uncertainty in image registration was small (mean <1mm, SD 2-3 mm). 3D registration uncertainty in FB on days 16 and 31 increased compared to DIBH ($p<0.05$), presumably due to tissue changes combined with image artifacts. DIBH CBCT scored higher than FB for all image quality parameters. Simulated tumor shifts ≤2mm did not impact image quality considerably, while 5mm shift smeared out the nodule, with only the middle part keeping density comparable to that of CT. Conclusions: Image registration uncertainty in DIBH is stable throughout the treatment. Improved image quality in DIBH CBCT strengthens the potential of DIBH IGRT for locally advanced lung cancer, also in presence of smaller tumor shifts from consecutive DIBHs.
1 - Josipovic et al. ESTRO 2015

Poster #67

Noha Jastaniyah, Riyadh, Saudi Arabia

A volumetric analysis of GTVD and CTVHR as defined by the GEC ESTRO recommendations in FIGO stage IIB and IIIB cervical cancer patients treated with IGABT in a prospective multicentric trial (EMBRACE)

Noha Jastaniyah, * Kenji Yoshida, § Kari Tanderup, ‡ Jacob Lindegaard, ‡ Alina Strudza, † Firuza Patel,¶ Primoz Petric, ‖ Barbara Segedin, # Christine Haie-Meder, ** Rachel Cooper, †† , Susovan Banerjee, Richard Pötter †. *King Faisal Specialist Hospital and Research Center, Riyadh, Saudi Arabia †Kobe University Graduate School of Medicine, Kobe, Japan ‡Aarhus University Hospital, Aarhus, Denmark §Medical University of Vienna, Vienna, Austria ¶Post Graduate Institute

Purpose: To quantify the gross tumor volume at diagnosis (GTVD) and high-risk clinical target volume (CTVHR) at brachytherapy (BT) and describe subgroups with different response patterns to chemoradiotherapy in patients with cervical cancer treated with image-guided adaptive brachytherapy (IGABT). Additionally, to evaluate the feasibility of IGABT achieving adequate target coverage in these groups. Methods and Materials: Patients with FIGO stage IIB and IIIB cervical cancer enrolled in the EMBRACE study were analyzed. GTVD and CTVHR were defined as per the GEC ESTRO recommendations. Patients were classified into six groups (G1-G6) reflecting response to CRT and tumor burden at BT using the following criteria: 1) volume of GTVD (≤40 cm3 vs. >40 cm3); 2) the ratio of CTVHR to GTVD ; 3) the extent of residual parametrial disease at BT. The clinical, pathological and treatment characteristics were then analyzed. Results: A total of 481 patients were evaluated. The mean (SD) GTVD and CTVHR were 43.6 (32.8) cm3 and 31.6 (16.1) cm3, respectively. In G1 (n=55), mean GTVD and CTVHR were 12.6 cm3 and 23.7 cm3. In G2 (n=78), mean GTVD and CTVHR were 47.5 cm3 and 25.3 cm3. In G3 (n=123), mean GTVD and CTVHR were 23.9 cm3 and 29.9 cm3. In G4 (n=147), mean GTVD and CTVHR were 73.4 cm3 and 38.5 cm3. In G5 (n=75), mean GTVD and CTVHR were 79.4 cm3 and 59.5 cm3. The mean GTVBT D100 in G1-5 was 103.1 Gy, 91.8 Gy, 93.5Gy, 88.3 Gy and 87.1 Gy. The mean CTVHR D90 in G1-5 was 95.1 Gy, 92.1 Gy, 92.6 Gy, 87.6 Gy and 88.4 Gy. The use of interstitial needles was progressively higher among the groups (mean 0, 0, 2, 3, 6 in G1-5, P< 0.001). Conclusions: In patients with stage IIB and IIIB disease, intra-stage heterogeneity and overlap between the groups exist. Based on initial tumor volume and residual disease at BT, five major groups are described. IGABT can accommodate the different variants of tumor regression but considerable variation in the dose to the target exists.

Poster #68

Taran Paulsen Hellebust, Oslo, Norway

Influence of rectum and bladder filling and position on the motion of the central clinical target volume for cervical cancer patients

Hellebust TP 1,2 , Djupvik LH 1, Rekstad BL 1, MArnesen R 1,2, Skipar K 3, Nakken E 3, Bruheim K 3, Malinen E 1,2. 1 Department of Medical Physics, Oslo University Hospital, Oslo, Norway, 2 Department of Physics, University of Oslo, Oslo, Norway, 3 Department of Oncology, Oslo University Hospital, Oslo, Norway

Introduction The benefit of IMRT for cervical cancer patients will largely be determined by the margin that is used on the central CTV (CTV-C). Several studies have shown that the bladder filling can influence the shape and the position of the CTV-C. The influence of rectum filling as well as the position of the rectum and bladder has not been analysed to the same extent and is addressed in the following study. Materials and Methods Pre-treatment MR and CT images acquired on separate days from 18 cervical cancer patients were retrospectively analysed. Prior to the MR study the patient was asked to void and the rectum was emptied. Prior to the CT acquisition the patient followed our clinical drinking protocol to have comfortable full bladder, while no protocol was used for the rectum. The image sets were co-registered for every patient and the CTV-C, bladder and rectum was delineated on both sets. The CTV-C included GTV, cervix, entire uterus, parts of vagina and the parametria. To evaluate the change in the volume and position of the structures the Jaccard similarity coefficient, JSC, for corresponding structures in the MR and CT images were calculated (JSC=intersection volume/union volume). Additionally, the relative change of the centre of mass (COM) was calculated. Results The mean JSC for the CTV-C was 0.48 [range: 0.16-0.77]. A linear regression between the JSC for the CTV-C and the JSC for rectum and bladder showed R2 of 0.22 and 0.16, respectively. The COM for the CTV-C moved in average 9.6 mm from CT to MR. The corresponding figures for the rectum and bladder were 5.5 and 11.1, respectively. A linear regression showed no correlation between the COM for the CTV-C and the bladder, while a R2 of 0.23 was found for the rectum. Conclusions Our data indicate that rectum filling and position also are influencing the CTV-C and should be taken into account. Studies including dosimetry and repeated imaging during treatment are ongoing in our clinic.

Poster #69

Jacob Lilja-Fischer, Aarhus, Denmark

Response evaluation of the neck in oropharyngeal cancer: value of MRI and influence of p16 in selecting patients for post-radiotherapy neck dissection.

Lilja-Fischer JK (1,2), Jensen K (3), Nielsen VE (2). Dept. of Experimental Clinical Oncology (1), Dept. of Otolaryngology - Head & Neck Surgery (2), Dept. of Oncology (3). Aarhus University Hospital, Denmark.

Introduction: Residual neck disease after radiotherapy in advanced oropharyngeal squamous cell carcinoma (OPSCC) is associated with increased mortality, and some patients may benefit from post-radiotherapy neck dissection (PRND). Aim of the present study was to assess the value of magnetic resonance imaging (MRI) and other clinical characteristics in selecting patients for PRND. Materials and methods: Retrospective cohort study. Consecutive patients with N+ OPSCC were included. Results: A total of 100 patients from a three-year period were included. Neck response was evaluated with MRI. Sixty patients were suspicious for residual neck disease, and were offered surgery. Only 7 of these patients had histologic evidence of carcinoma. Salvage was successful in 4 patients. Cumulative neck failure after 3 years was 14 % (8.4 – 24 %), and did not differ significantly among patients with positive compared to negative MRI (p = 0.47, log-rank test). Applying neck failure as gold standard, sensitivity and specificity of MRI was 69 % and 41 %, respectively, positive and negative predictive value was 15 % and 90 %. Analysis of receiver operating characteristic curves in 191 individual lymph nodes showed, that a short axis ≥ 10 mm should be classified as suspicious. Furthermore, T-stage and p16-status were associated with increased risk of neck recurrence. However, patients with p16+ disease had significantly larger lymph nodes after treatment, and so imaging based on lymph node size results in many false positives. Conclusion: These results suggest that lymph node size, T-stage as well as p16-status could be used in selecting patients for PRND in OPSCC. Yet, anatomical imaging may be inappropriate for evaluating neck response in patients with p16+ disease, since enlarged lymph nodes often do not indicate residual neck disease. Other clinical characteristics or imaging modalities may be more predictive.

Poster #70

Jasmin Mahdavi, Lyngby, Danmark

Dosimetric effect of unwanted air gaps under bolus in volumetric modulated arc therapy (VMAT).

Mahdavi J.M. 1,3, Petersen T.H. 1,3, Sjölin M.2, Sibolt P. 2, Behrens C.F. 2, Beierholm A.R. 4, Mahmood F. 2. 1 Department of Electrical Engineering, DTU, Lyngby, Denmark. 2 Department of Oncology, Herlev Hospital, Herlev, Denmark. 3 Faculty of Health and Medical Sciences, University of Copenhagen, Copenhagen, Denmark. 4 DTU Nutech, DTU, Lyngby, Denmark.

Introduction: In radiotherapy, tissue equivalent material (bolus) is used to increase patient surface dose. Unwanted air gaps between bolus and patient surface may occur for several reasons, e.g. due to lack of alignment of the fixation mask to the patient surface. In this study the dosimetric effect of air gaps between bolus and patient surface in VMAT treatments was investigated. The practical aim is to improve the assessment of surface dose when air gaps are observed in patient setup imaging during the course of treatment. **Materials and methods:** VMAT treatment plans were generated (Eclipse v.10.0, Varian Medical Systems, Inc.) with 6 MV photons based on a CT scan of the anthropomorphic Alderson ART-300A phantom: One full and one double half arc both with 3 and 5 mm bolus linked to the treatment field. Two PTV locations were investigated, one at the neck and one at the forehead. Air gaps of 5, 10 and 15 mm were moulded into fixation masks. The treatment plans were delivered by the Varian 2300 iX Clinac and measured using GafChromic EBT3 film (forehead) and the in-house developed ME40 dosimetry system (DTU Nutech) (forehead and neck) based on a fiber-coupled plastic scintillator. **Results:** Results show a decrease in surface dose with increasing air gap, irrespectively of PTV location, arc technique, and bolus thickness. The dose reduction at 5 mm air gab is about 10% and decreases to about 80% at 15 mm air gab, confirmed by both dosimetry systems. In addition, EBT3 film measurements revealed that only about 90% of the prescribed dose (2 Gy in mean dose to PTV) was delivered with no air gab and double half arc technique using 3 mm bolus (Fig. 1). **Conclusions:** This study indicates that there is a critical reduction in dose at air gaps of 5 mm and above. The dose coverage of the PTV may therefore easily be compromised. Our results may be used for estimation of dose deficiencies in the clinical setting when air gaps between bolus and patient surface are observed.

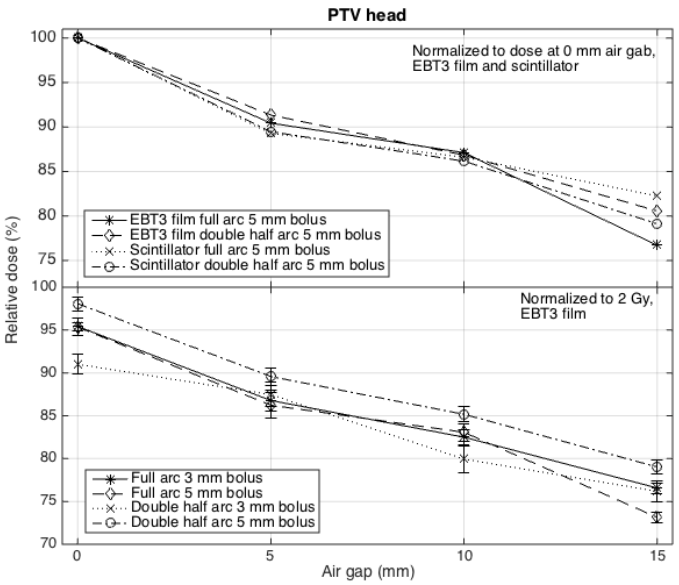

Fig. 1 – A selection of data for PTV head is shown. Top: 5 mm bolus measurements with scintillator and EBT3 film. Bottom: Film measurements with 3 and 5 mm bolus (error bars indicate ± 1 SD).

Poster #71

Steffen Nielsen, Aarhus, Denmark

Hypoxia-regulated Gene Expression as an Endogenous Marker in Prostate Adenocarcinoma

Nielsen S, Wittrup CF, Busk M, Horsmann MR, Overgaard J, Alsner J and Sørensen BS. Department of Experimental Clinical Oncology, Aarhus University Hospital, Aarhus, Denmark

INTRODUCTION: A 15-gene hypoxia classifier has previously shown prognostic and predictive value in head and neck cancer. Hypoxia in prostate adenocarcinoma is associated with an aggressive phenotype and early biochemical relapse after radiotherapy. It is desired to use the classifier to identify patients with prostate cancer that would benefit from intensified treatment. The aim of this initial study was to identify optimal reference genes for relative quantification of gene expression and to investigate, whether hypoxia treatment induce expression of the 15 classifier genes in prostate cancer cell lines. METHOD: Quantitative real-time PCR was used to quantify expression of the 15 classifier genes in prostate cancer cell lines DU145, LNCaP and PC-3 after exposure to either hypoxic (0% O2) or normoxic conditions for 24 hours. From a 22-gene panel, PSMC4, TBP and NDFIP1 were identified as optimal reference genes across cell lines by using the software application geNorm. The original reference genes used for gene expression analysis in head and neck biopsies were ACTR3, RPL37A and NDFIP1. RESULTS: Both the original and the newly selected set of reference genes were used as normalization factors to determine expression of the hypoxia induced genes. There was no significant difference in relative expression levels. 14 of the 15 classifier genes were induced by hypoxia treatment. The ALDOA gene was not significantly upregulated in DU145 and LNCaP. It may be necessary to eliminate or substitute the ALDOA gene to optimize the classifier for use in prostate adenocarcinomas. CONCLUSION: 14 of 15 genes were significantly upregulated by hypoxia treatment in vitro. In vivo experiments could provide more information on the hypoxia induced expression of the classifier genes. These initial findings indicate that the classifier has potential to be used for identification of patients with hypoxic prostate adenocarcinomas in a clinical setting.

Poster #72

Maria Sjölin, Herlev, Denmark

The effect of different dosimetric leaf gap on patient specific quality assurance

Sjölin M, Edmund JM. Radiotherapy Research Unit, Department of Onoclogy, Herlev Hospital, Herlev, Denmark

Introduction: Dose calculations of dynamic treatment plans use a dosimetric leaf separation (DLS) parameter. The purpose of this study was to quantify the dosimetric effect of varying the DLS parameter in treatment planning and investigate if the sensitivity of the patient specific QA system could detect this effect. Material and Methods: 17 clinical IMRT/VMAT treatment plans for the pelvis and head and neck (H&N) were optimized and calculated with two different settings of the DLS (2.10 and 1.02 mm). The DLS difference represents a MLC gap of about 0.6 mm. The plans were delivered on an accelerator corresponding to a DLS=1.02 and measured on the diode-based Delta4 phantom. Gamma evaluation (2%/2mm, 3%/2mm and 3%/3mm, global dose difference) were carried out for the composite plan and per beam with the two different DLS settings used in the dose calculation. The difference in Dmean was recorded for the PTV. Results: The range in DVH differences for the Dmean parameter was 0.5 to 4.0%. The largest deviations (3.3±0.7%) were observed for IMRT H&N, followed by the VMAT H&N plans (1.8±0.4%), and the pelvis VMAT plans (1.38±0.64%). The composite plan gamma passing rates for the correct and incorrect DLS setting showed a significant difference for both the H&N IMRT and VMAT plans ($p<0.05$). Non-significance was observed for the pelvic plans. A small difference was further observed for the per beam gamma evaluation. Conclusion: The investigated difference in DLS parameter can affect the dosimetric accuracy up to about 4%. This difference could only be detected in the composite H&N plans, and not the pelvic plans in the patient specific QA.

Poster #73

Oscar Casares-Magaz, Aarhus, Denmark

Towards spatial dose-response relationships for the rectum in prostate radiotherapy

O. Casares-Magaz1, L. P. Muren1, V. Moiseenko2, J. Deasy3, S. Petersen1, M. Høyer1 and M. Thor3. 1) Department of Oncology, Aarhus University Hospital, DK. 2) Department of Radiation Medicine and Applied Science, UCSD, USA. 3) Department of Medical Physics, MSKCC, NY, USA.

INTRODUCTION: Rectal morbidity is one of the most studied complications following prostate cancer RT. Since spatial dose information has typically been disregarded, the internal rectal dose-response remains ambiguous. The aim of this study was therefore to assess spatial metrics of the rectal surface and to demonstrate the use of these metrics in the setting of outcome modelling for rectal morbidity. MATERIAL AND METHOD: A total of 105 prostate patients treated to 78Gy@2Gy fractions where patient-reported rectal morbidity was assessed at a median of 3.6 years post-RT. The rectum was defined from the recto-sigmoidal junction to the anal canal. 2D dose maps were generated by unfolding the rectum at the most posterior location, and dose was sampled in 100 equally spaced points for each rectal slice. The dose maps were divided in three regions (lower, middle and upper), and dose threshold areas (Ax: % area receiving ≥x Gy) were computed for each region and correlated using univariate logistic regression with three defecation urgency, U1: 5-10min to defer defecation before toilet visit; U2: re-defecate<1h after last bowel movement; U3: immediate toilet visit due to urgency, with U2 and U3 experienced on a monthly basis. RESULTS: We found that the Ax values calculated for a region were significantly different from corresponding Ax values of the two other regions ($p<0.0001$ for all comparisons using a Student's t-test). Weak correlations were found between A30 and U2 at the lower portion of the rectum ($p=0.06$), and between A70 and U3 at the upper part of the rectum ($p<0.06$). Future work will explore measurements over the 3D rectum surface to improve accuracy of dose-endpoints correlations. CONCLUSIONS: We have presented a method to take into account spatial measures of dose distributions and demonstrated its applicability for predicting various rectal morbidity endpoints. Future work will involve 3D rectal surface metrics and development of dose surface/volume constrains.

Poster #74

Britta Weber, Aarhus, Denmark

VMAT makes it possible to treat more advanced stages of NSCLC compared to 3D-CRT

Weber B, Bergman A, Berthelet E, Carolan H, Fong M, Goddard K, Lai A, Liu M. Department of Oncology, Aarhus University Hospital, Aarhus, Denmark, Radiation Oncology, British Columbia Cancer Agency, Vancouver Centre, Canada, Cancer Surveillance & Outcomes, Population Oncology, BCCA, Vancouver, Canada

Background: To evaluate our first cohort of advanced non-small cell lung cancer (NSCLC) patients treated with definitive radiotherapy using volumetric modulated arc therapy (VMAT) at British Columbia Cancer Agency. Materials and Methods: We analysed 72 consecutive patients who received radical non-stereotactic radiotherapy with either VMAT (n=33) or 3D-CRT (n=39). Dosimetric comparison between the two groups was made. Radiation pneumonitis was graded according to the Common Terminology Criteria for Adverse Events (CTCAE) v. 4.0. The Chi-square test, Fishers exact test or Wilcoxon-Mann-Whitney test were used to compare the two groups. Results: A significantly higher proportion of VMAT treated patients had supraclavicular lymph node involvement (24% vs. 3%, p=0.009). The mean length of the PTV volume was significantly longer in the VMAT treated group (11.7 cm vs. 10.0 cm, p=0.018), but there was no difference in V20Gy (24.0 vs. 23.2%, p=0.586), V5Gy (56.4 vs. 52.5%, p=0.228), V5Gy to contralateral lung (49.8 vs. 46.8%, p=0.417) or mean lung dose (13.7 vs. 14.0 Gy, p=0.782). The risk of developing pneumonitis ≥ gr. 2 was 12% in the VMAT group vs. 18% in the 3D-CRT group (p=0.497). Conclusions: VMAT treatment of NSCLC enabled the inclusion of patients with more advanced stages compared to 3D-CRT without any significant increase in lung dose.

Poster #75

Nina Boje Kibsgaard Jensen, Aarhus, Denmark

Application of library plan selection and margin reduction in locally advanced cervical cancer.

Jensen NBK1, Nyvang L2, Assenholt MS2, Vestergaard A2, Ramlov A1, Lindegaard JC1, Fokdal L1, Tanderup K2. 1) Department of Oncology, Aarhus University Hospital, Aarhus, Denmark. 2) Department of Medical Physics, Aarhus University Hospital, Aarhus, Denmark

Introduction: Pelvic organ motion for cervical cancer patients can be considerable during external beam radiotherapy (EBRT). This study evaluates dosimetric consequences of interfractional motion, and investigates the potential of adaptive plan selection to decrease PTV margin while improving target coverage. Materials and methods: Nine patients treated with definitive chemoradiation and brachytherapy (BT) were analyzed. EBRT was delivered as 45-50Gy using a bladder filling protocol. Two planning CTs were carried out with full and empty bladder, respectively. A plan library was generated with 2-3 plans depending on uterus movement at treatment planning: Two plans with uterus-PTV margins of 15mm and 5mm on the full bladder scan and one plan with 5mm margin on the empty bladder scan. A 15mm GTV-PTV margin was used. Daily onboard CBCTs acquired for setup were used retrospectively for contouring the primary tumour related CTV (uterus/GTV/cervix /upper vagina) and bladder, and contours were projected to the planning CTs. The margin reduction strategy was evaluated on the full bladder scan by summation of D98 across all CTVs and the plan selection was evaluated. Results: In total 245 CBCTs were available, 20 (8%) were excluded due to poor quality for contouring. The median and range of summed D98 of the CTV was 97.0% [84.4%-97.4%] and 95.7% [75.3%-98.0%] for 15mm and 5mm plans (full bladder), respectively. In 4/9 patients D98 was less than 95% with 5mm plans. D98 was increased with plan selection to median and range of 96.1% [87.2%-96.8%]. Adding the BT dose contribution, D98 was >45Gy [45.5Gy-54.8Gy] for all patients with the plan selection strategy. Conclusions: Our results showed that with daily CBCT monitoring, a reduced margin could be applied in 5/9 patients. Additionally, plan selection would increase the uterus dose in all patients. The BT dose may to a large extend compensate for possible EBRT dose loss due to uterus movements when narrow margins are applied.

Poster #76

Ziad Saleh, West Harrison, USA

Multiple-image based approach to evaluate the performance of deformable image registration and identify scan outliers in a longitudinal data set

Saleh Z, Thor M, Apte A, Sharp G, Tang X, Volpe T, Margiasso R, Veeraraghavan H, Muren LP and Deasy JO. Department of Medical Physics, Memorial Sloan-Kettering Cancer Center, New York, NY, USA; Department of Radiation Oncology, Massachusetts General Hospital, Boston, MA, USA; Department of Medical Physics, Aarhus University/Aarhus University Hospital,

Purpose: Adaptive radiotherapy of tumor sites prone to motion relies on deformable image registration (DIR). However, there is a lack of robust quantitative methods to evaluate DIR-related uncertainties. The aim of this study was to evaluate intra-patient DIR of the pelvis using the quantitative distance discordance metric (DDM). Moreover, DDM was used to identify anatomical regions of poor registration and scan outliers when DIR was performed on a longitudinal imaging dataset. Materials and Methods: The investigated data consisted of repeated CT scans (six scans/patient) for 38 patients previously treated with radiotherapy for prostate cancer. The rectum and bladder were delineated on all CT scans. For each patient, DIR was performed using a B-Spline algorithm, and voxel-by-voxel uncertainties were evaluated using DDM. Furthermore, intra-patient DIR was preformed on a group of five CT scans using leave-one-out technique (LOO) to establish the range of variation and examine scan outliers. The DDM map was superimposed on the first acquired CT scan and DDM statistics were assessed. Results: The DDM varied across different structures and among patients with the highest values observed near the skin and lowest in the bones. The mean rectal and bladder DDM ranged from 1.1-11.1 mm and 1.5-12.7 mm, respectively. The mean DDM for set of registered images from the same patient ranged from 3.8-4.2 mm. Conclusion: The DDM distributions were similar when multiple “similar” images from the same patient were used for longitudinal DIR. The highest variations were observed inside the regions which suffer from organ motion (bladder filling or presence of air in the rectum). Meanwhile, regions of high contrast showed the lowest variations (bony anatomy). This suggests that DDM can be a useful metric to identify scan outliers and regions of large DIR uncertainties in a longitudinal data set.

Poster #77

Steffen Hokland, Aarhus, Denmark

Evaluation of external beam radiotherapy CT-based dose plans recalculated on MRI-generated density maps

Steffen Hokland (1), Max Köhler (2), Kari Tanderup (3). 1: Department of Medical Physics, Aarhus University Hospital, Aarhus, Denmark 2: Philips Healtcare, MR Therapy, Vantaa, Finland 3: Department of Experimental Clinical Oncology, Aarhus University Hopsital, Aarhus, Denmark

Introduction: MRI-generated density maps are needed if radiotherapy is to be based on MRI alone. Here we present CT based radiotherapy plans re-calculated on density maps generated using a proprietary algorithm - Magnetic Resonance for Calculating Attenuation (MRCAT). Methods: Nine prostate cancer patients referred for standard radiotherapy received an mDixon-scan (Ingenia 1.5T Philips Healthcare, 3D cartesian Fast Field Echo, FOV: 350mm×478mm×300mm, Voxel size: 1.7mm×1.7mm×.25mm, TR=5.7ms, TE1=1.6ms, TE2=3.9ms, Flip angle=10°) in addition to the normal scan protocol. Five-value stratified HU-maps were calculated off-line using the MRCAT algorithm assigning Hounsfield values as either water (42), fat (-106), compact (798) or cancellous bone (160) or finally extra corporeal air (-968). Treatment plans (prescribed dose: 78Gy in 39 fractions) were optimised on CT with the requirement that they fulfil local dose constraints. The plans were subsequently re-calculated on the simulated CT images. DVH-parameters, PTV_V95, PTV_D98, PTV_Dmean, 2cc_Dmax and Rectum_D2cc, were compared across the two scans using a pairwise Student's ttest. Results: For overall target coverage we found (values listed as 95% confidence interval and p-value) PTV_V95(CT)=94.5% [93.6:95.7]% , PTV_V95(MRCAT)=96.3% [95.2:97.4]% (p=0.048) and PTV_D98(CT)=72.3Gy [72.0:72.6]Gy, PTV_D98(MRCAT)=73.3Gy [72.9:73.7]Gy (p=0.003). For MRCAT PTV_Dmean we found 100.9% [100.7:101.1]% which was significantly greater than 100% for the original plan. Rectal dose was also overestimated with MRCAT: D2cc(CT)=73.0Gy [72.7:73.3]Gy and D2cc(MRCAT)=74.1Gy [73.3:74.9]Gy (p=0.008) as well as the global maximum dose to 2cc 80.4Gy [80.3:80.6]Gy (CT) and 81.1Gy [80.9:81:3]Gy (MRCAT). Discussion: Although significantly greater when compared to the generic plan CT, DVH-parameters calculated on the synthetic CT-scans were comparable with a mean dose overestmation of 0.9% for mean dose. Rectum D2cc was overestimated by 1.5%.

Poster #78

Aniek Even, Maastricht, The Netherlands

Dual-energy CT for the combined assessment of changes in lung perfusion and morphology after radiotherapy in non-small cell lung cancer patients

Even A.J.G., Das M.*, Lambin P., van Elmpt W. *Department of Radiology, Maastricht University Medical Centre, Maastricht, The Netherlands

Introduction: Radiation induced damage to healthy lung parenchyma is a major dose limiting factor in radiotherapy for the treatment of non-small cell lung cancer (NSCLC). Objective measures are desirable to quantify and predict lung toxicity. Hounsfield units (HU) can be used to quantify lung fibrosis; dual-energy CT (DECT) allows indirect quantification of lung perfusion. In this study we compared both measures to the delivered radiation dose. Materials and methods: Six NSCLC patients included in an on-going clinical trial (NCT01024829) underwent contrast-enhanced DECT (100 and 140kV) before and 3 months after radiotherapy. Lungs were segmented and iodine-related attenuation (IRA) as surrogate for perfusion was calculated by subtracting the 140kV CT from the 100kV CT. The 100kV scans were used to assess changes in CT density (HU). Differences in IRA and CT density were calculated between both DECT scans and correlated to the dose distribution of irradiated and non-irradiated lung. CT density dose-response relationship was fitted with a sigmoidal dose-response curve with a fixed slope ɣ of 1.3. Free parameters were maximum HU and D50. Results: The mean CT density difference between post- and pre-treatment CT was higher for the irradiated lung (54±85 HU) compared to the non-irradiated lung (20±54 HU) for 5 of the 6 patients. The dose-response curves for those 5 patients had a HUmax of 155±92 and D50 of 35±8 Gy. In 5 of the 6 patients an average increase of perfusion was observed, for both irradiated (increase IRA: 6.1±7.8 HU) and non-irradiated lung (IRA: 7.0±8.7 HU). No clear relationship between IRA and treatment dose was observed. Conclusion: Dual-energy CT allows a quick assessment of changes in both morphology and functional perfusion in NSCLC. Larger morphological changes after radiotherapy were observed for high dose regions, although highly variable between patients. Changes in lung perfusion seem to be independent of treatment dose and lung density differences.

Poster #79

Angela Botticella, Leuven, Belgium

Optimization of gross tumour volume definition in lung-sparing volumetric modulated arc therapy for pleural mesothelioma: Implications for radiotherapy planning

A. Botticella1*, G. Defraene1, K. Nackaerts2, C. Deroose3, J. Coolen4, P. Nafteux5, S. Peeters1,6, D. De Ruysscher1,6. 1KU Leuven - University of Leuven, Department of Oncology, Experimental Radiation Oncology, B-3000 Leuven, Belgium

Introduction: High dose lung-sparing pleural radiotherapy for malignant pleural mesothelioma (MPM) is difficult. Accurate target delineation is critical. The optimal imaging modality to define radiotherapy target volumes has not been studied in depth. This is the aim of the present study. Materials and methods: Twelve consecutive patients with a histopathological diagnosis of stage I-IV MPM (6 left-sided and 6 right-sided) were included. CT scans with IV contrast, 18F-FDG PET/CT scans and MRI scans (post-contrast T1-weighted, T2 and diffusion-weighted images [DWI]) were obtained and downloaded from the institutional database onto a standalone image fusion workstation (MIM Software Inc., Cleveland, OH, USA) for image registration and contouring. CT scans were rigidly co-registered with 18FDG-CT-PET, with MRI scans and with DWI scans. Four sets of pleural GTVs were defined: 1) a CT-based GTV (GTVCT); 2)a PET/CT-based GTV (GTVCT+PET/CT); 3) a T1/T2-weighted MRI-based GTV (GTVCT+MRI); 4) a DWI-based GTV (GTVCT+DWI). Only the pleural tumor was contoured; mediastinal nodes were excluded. “Quantitative” and “qualitative” (visual) evaluation of the volumes was performed. Results: Compared to CT-based GTV definition, PET/CT identified additional tumour sites in 12/16 patients. Compared to either CT or PET/CT, MRI and DWI identified additional tumour sites in 15/16 patients. Mean GTVCT, GTVCT+PET/CT, GTVCT+MRI and GTVCT+DWI (+ standard deviation [SD]) were respectively 630.1 mL (+302.81), 640.23 (+302.83), 660.8 (+290.8) and 655.2 mL(+290.7). Mean Jaccard index was lower in MRI-based contours versus all the others. Conclusions: To the best of our knowledge, this is the first study showing that the integration of MRI into the target volume definition in hemithoracic radiotherapy in MPM may allow to improve the accuracy of target delineation and reduce the likelihood of geographical misses.

Poster #80

Ester Thøgersen, Aarhus, Denmark

Quantification of interfractional movement of the oesophagus and the influence on the dose to the oesophagus.

Thøgersen E.H., Møller D.S, Hoffman L. Department of Medical Physics. Aarhus University Hospital. Denmark

Introduction: Dose escalation in lung cancer patients may increase the survival rate. This requires a high precision in the patient setup to avoid increased dose to organs at risk. The aim of this study was to identify how much the oesophagus moves during the RT course and the impact on the dose distribution. Material and methods: Twenty lung cancer patients treated with chemo-RT were included. All patients had a 4D planning-CT scan (p-CT) and two additional 4DCT control scans (c-CT). For each patient, an experienced radiographer contoured the oesophagus in two different structures: The full extent of the oesophagus (oes), and the extent of the tumour (oes-T). In the Eclipse registration module, a rigid 6D tumour match between the p-CT and each of the c-CT scans was performed and the shift of the oesophagus was obtained for the segments oes and oes-T. The treatment plan was copied to the c-CTs using the 4D registration and the dose was re-calculated by using fixed monitor units and the mean and the maximum dose to the oesophagus were read out. Results: The mean shift of the oesophagus was 7.5 mm ± 5.3 mm with a maximum shift of 23.3 mm. The mean shift in the region of the tumour was 3.8 mm ± 3.0 mm with a maximum shift of 13.5 mm. The mean dose to the oesophagus at the region of the tumour (eso-T) increased by 0.4% ± 4.4%. In three patients, an increase in mean dose above 5% was observed. These patients had anatomically changes such as pneumonia and atelectasis. The maximum dose increased by 1.3% ± 2.6%, with a maximum increase of 10% in one patient. In this patient only minor anatomical changes are observed. Conclusion: The oesophagus moves during the RT course. Patients with anatomical changes like disappearance of an atelectasis are more likely to receive an increased dose to the oesophagus during the RT course. In the case of dose escalation, these patients may benefit from an adaptive treatment plan during treatment to avoid severe oesophageal toxicity.

Poster #81

Bregtje Hermans, Maastricht, The Netherlands

Weekly cone beam computed tomography for detection of discrepancies between planned and delivered dose in head and neck cancer patients treated with radical (chemo)radiotherapy

Hermans B.C.M. (I), Persoon L.C.G.G. (I), Hoebers F.J.P. (I), Troost E.G.C. (I, II), Verhaegen F. (I). I) Department of Radiation Oncology (MAASTRO), Maastricht University Medical Centre, Maastricht, the Netherlands. II)Helmholtz Zentrum Dresden-Rossendorf, Department of Radiation Oncology, Universitätsklinik Carl Gustav Carus der TU Dresden, Germany

Introduction: Curative-intent treatment for patients with squamous cell carcinomas of the head and neck (HNSCC) consists of surgery and/or (chemo)radiotherapy. The use of volumetric modulated arc therapy (VMAT) may lead to under-/overdosage of gross target volume (GTV) and organs at risk (OAR) due to changes in patient anatomy. An increase of dose to parotid glands of 0-3Gy or 0-6% has been reported in small studies (N≤15). The next step to more effective radiation treatment combined with less toxicity is dose-guided radiotherapy (DGRT). The aim of this study was to evaluate discrepancies between planned and actually delivered radiation dose to GTV and OARs in HNSCC patients and to identify predictive factors. Methods: In this retrospective analysis of prospectively collected data, 20 patients with cT2-4N0-3M0 HNSCC (all subsites except for nasopharynx) treated with primary (chemo)radiotherapy and receiving weekly CBCT scans were included. Contours delineated on the planning CT were propagated to registered CBCTs and manually adapted. The dose was recalculated on CBCTs and quantified by D95% (GTV), Dmean (parotid and submandibular glands) and D2% (spinal cord). Predictive factors investigated were: gender, age, cT/N-stage, tumor grade, HPV-status, systemic therapy, BMI at start of treatment, weight loss and volume change. Results: A total of 139 CBCTs was evaluated. There was no significant difference between the planned and delivered dose for GTV and OARs of week 1 to subsequent weeks. However, 1 patient showed a relevant increase of cumulative dose to the left parotid gland (Dmean increase from 31,1 Gy to 33,5 Gy). No clinically relevant correlations between dose changes and predictive factors were found. Conclusion: None of the patients investigated had putative clinical benefit from replanning and thus weekly dose calculations may be unnecessary for the disease sites investigated. This analysis will be repeated for patients with nasopharyngeal carcinomas.

Poster #82

Jacob Rasmussen, Copenhagen, Danmark

Spatio-temporal stability of pre-treatment 18F-Fludeoxyglucose uptake in head and neck squamous cell carcinomas sufficient for dose painting

Rasmussen JH1, Vogelius IR1, Aznar MC1, Fischer BM2, Christensen CB2, Friborg J1, Loft A2, Kristensen CA1, Bentzen SM3, Specht L1.. 1) Department of Oncology, Section of Radiotherapy, Rigshospitalet, Denmark. 2) Department of Clinical Physiology, Nuclear Medicine and PET, Rigshospitalet, Denmark. 3) Division of Biostatistics and Bioinformatics, University of Maryland, Baltimore, USA

Introduction The pre-treatment 18F-Fludeoxyglucose (FDG) avid sub-volume of the tumor is hypothesized to be a relevant target for dose painting in patients with in head and neck squamous cell carcinomas (HNSCC). Studies for FDG based dose painting are recruiting patients, however the spatio-temporal stability of the FDG avid sub-volume is unknown. This study assess (1) the pre-treatment spatio-temporal variability of FDG PET/CT target volumes and (2) the impact of this variability on dose distribution in dose painting plans in patients with HNSCC. Materials and methods: Thirty patients were enrolled and scanned twice in treatment position prior to treatment with FDG PET/CT. Delineation of the FDG avid sub-volume of the tumor and lymph nodes was performed by a specialist in nuclear medicine yielding GTVPET1 and GTVPET2 and segmentation based on SUV iso-contours were constructed yielding two metabolic target volumes, MTV1 and MTV2. Planning target volumes were constructed by expanding the target volumes with an isotropic margin of 4 mm for all four target volumes yielding PTVPET1, PTVPET2, PTVMTV1 and PTVMTV2. Images were co-registered rigidly and dose painting plans with dose escalation up to 82 Gy (EQD2) to GTVPET1 were planned and GTVPET2 was copied from the co-registered images to the dose planning scan. Afterwards the same was done for MTV1 and MTV2. Mean dose and the percentage volume receiving 95% of prescribed dose were assessed. Results: Twenty-four patients were available for full analysis. The median mismatch between GTVPET1 and GTVPET2 was 14.2%(1.7 cc.) corresponding to a median DICE coefficient =0.74(range 0.42-0.91). The median difference in dose to the FDG planning target volume is 0.3 Gy (PTVPET) and 0.4 Gy (PTVMTV). Median difference in tumor control probability (TCP) was <0.2%. Conclusions: Day-to-day variability of pre-treatment FDGPET/CT target volumes has no relevant impact on dose distribution and expected tumor control in dose painting plans.

Poster #83

Jens Edmund, Herlev, Denmark

CBCT guided treatment delivery and planning verification for MRI-only radiotherapy of the brain

Edmund JM (1), Andreasen D (1,2), Mahmood F (1) and Van Leemput K (2,3). 1. Copenhagen University Hospital, Department of Oncology, Herlev, Denmark. 2. Technical University of Denmark, DTU Compute, Lyngby, Denmark. 3. Harvard Medical School, Department of Radiology, Boston, USA.

Introduction. Radiotherapy based on MRI as the sole modality, so-called MRI-only RT, shows a promising potential for treatment sites such as the brain. Most research, however, focus on creating a pseudo CT (pCT) from the MRI for treatment planning while little attention is paid to the treatment delivery. Here, we investigate if the CBCT can be used for MRI-only IGRT and for verification of the correctness of the corresponding pCT. Materials and methods. Six patients receiving palliative cranial RT were included. Each patient had a 3D T1W MRI (TE/TR = 6.9/25 ms, resolution = 0.85 x 0.85 x 1.2 mm and FOV = 16 x 16 x 18 cm), a CBCT and a CT for reference. A pCT was generated using a patch based approach. All scans were re-sliced and cropped to the MRI. The MRI, pCT and CT were put in the same frame of reference, matched to the CBCT and the differences in the transformation matrix noted. Paired pCT-CT and pCT-CBCT data were created in bins of 10 HU and the absolute difference calculated. The data were then transformed to relative electron densities (RED) using the default CT or a CBCT specific calibration curve. The latter was either based on a Cirs CBCT phantom (phan) or a paired CT-CBCT population (pop) of the 5 other patients. Results. Non-significant (NS) differences in the pooled CT-CBCT, MRI-CBCT and pCT-CBCT transformations of the patients were detected. The largest deviations from the CT-CBCT were < 1 mm and 1 degree. The median absolute error (MeAE) in HU was 203±49 and 299±49 on average for the pCT-CT and the pCT-CBCT, respectively, and was significantly different ($p<0.01$) in each patient. The average MeAE in RED was 0.108±0.025, 0.104±0.011 and 0.099±0.017 for the pCT-CT, pCT-CBCT phan ($p<0.01$ on 2 patiens) and pCT-CBCT pop (NS), respectively. Conclusions. The CBCT can be used for patient setup with either the MRI or the pCT. The correctness of the pCT can be verified from the CBCT using a population based calibration curve in the treatment geometry.

Poster #84

Grete May Engeseth, Bergen, Norway

Effect of range uncertainty and setup errors in cranio-spinal treatment plans

Grete May Engeseth 1, Camilla Hanquist Stokkevåg 1,2. 1. Department of Oncology and Medical Physics, Haukeland University Hospital, Bergen, Norway 2. Department of Physics and Technology, University of Bergen, Bergen, Norway

Introduction: Both CTV dose coverage as well as organs at risk (OAR) can be compromised due to inaccuracies between planned and delivered dose distributions. The aim of this study was to analyse the effect of range uncertainties and setup errors in cranio-spinal (CS) proton treatment plans. Material and methods: Intensity Modulated Proton Treatment plans (IMPT) were created for 6 pediatric patients. The CTV consisted of the whole brain and the spinal including the thecal sac. The PTV was defined by extending the CTV by 4 mm as well as including the vertebrae. The effects of range uncertainties were investigated by changing the Relative Stopping Power in the CT calibration curve by ±1-5 %, while setup errors were introduced by shifting the isocenter by ±1-5 mm. The treatment plans were recalculated with the initial spot distribution and the changes in V95% for the CTV and V5Gy(RBE) for the heart, thyroid and lungs were considered. Results: A reduction in the 95% dose coverage of the CTV was observed following increasing setup- and range errors. The largest impact on the CTV dose was caused by a 5 mm caudal setup error and a undershoot in (proton) dose range of 5 %, which resulted in a reduction of 2.3 % and 2.7 % to the V95 %, respectively. The heart dose was most sensitive to the range uncertainties, increasing the V5Gy(RBE) from 4.2% to 6,7 % with a 5 % overshoot. Range uncertainty also had the largest impact on the thyroid dose, increasing the V5Gy(RBE) from 50.9 % to 72.3 % following a 5% overshoot. Conclusion: For the IMPT plans in this study, range- and setup errors resulted in a loss in the CTV 95% dose coverage of less than 3%. The OARs appeared to be more sensitive to uncertainties, in particularly the thyroid, which suffered a significant dose increase. Considering the risk of radiation induced thyroid dysfunctions following peadiatic CS irradiaton, the use of robust planning– and optimization strategies should be applied during the planning process.

Poster #85

Maria Luisa Belli, Milano, Italy

PET positive lymph nodes variations during treatment as predictors of treatment outcome

Belli Maria Luisa1, Fiorino Claudio1, Zerbetto Flavia2, Raso Roberta1, Sara Broggi1, Anna Chiara2, Cattaneo Giovanni Mauro1, Di Muzio Nadia2, Dell'Oca Italo2, Calandrino Riccardo1. 1) Medical Physics, and 2) Radiotherapy, S.Raffaele Scientific Institute, Milano,Italy

Introduction.We investigated the possibility to early identify non responding patients(pts)based on in-room images evaluation of FDG-PETpositive lymph nodes(PNs). Materials and methods.27pts with≥1pre-treatment PNs were retrospectively analyzed; they received 54Gy,66Gy,69Gy in30fr on precautionary lymph nodal(N),primary(T) and PET positive(BTV) PTV volumes respectively (Tomotherapy SIB approach).PNs volume changes during treatment were assessed based on MVCTs used for image guidance(ratio between PNs volume at fr30/20/10 and at 1stfr).The correlation between PNs changes and T,N,M relapses,death,cancer specific death (rT,rN,rM,OD,CSD) was investigated. The difference of the volume changes between the groups was tested(patients with relapse/death vs without relapse/alive,Mann-Withney test).The impact of shrinkage on the corresponding survival curves (Cox proportional-hazard regression),dividing between no/moderate and large shrinkage based on the best cut off value(ROC curve),was also investigated. Results. Median follow-up was 27.4m(3.7-108.9).The number of rT,rN,rM,OD and CSD was 5,4,5,8,6 respectively. Differences in PNs shrinkage were found between pts with and without rT/rN at all considered timing(fr20, rT:0.56vs1.07(median),p=0.06; rN:0.57vs1.25,p=0.07). Differences were lower for rM and OD/CSD. Survival curves provide higher hazard-ratios(HR) between rT,rN,OD and PNs changes at fr20 and 10 (fr20, rT:best-cut-off=0.58,HR=5.1[95%CI=0.5–49.4],p=0.12; rN:best-cut-off=0.98,HR=14.9[1.6–142.9],p=0.01). No significant correlation was found between pre-RT BTV volumes and PNs changes. Conclusion. A limited shrinkage of PNs during treatment is associated with poorer outcome in terms of T/N relapses. The early variation of PNs observed on in-room images may provide useful information about the individual response with potential application in guiding an early adaptation of the treatment.

Poster #86

Roshan Karunamuni, La Jolla, California, United States of America

Adaptive replanning for brain IMRT treatment to achieve sparing of eloquent cortex in glioblastoma

Karunamuni R, Seibert T, Moore K, Li N, White N, Marshall D, Bartsch H, McDonald C, Farid N, Brewer J, Moiseenko V, Dale A, Hattangadi-Gluth J. Department of Radiation Medicine and Applied Sciences, University of California San Diego, La Jolla, California, USA

Introduction: Dose-dependent cortical thinning has been observed in glioblastoma patients, suggesting that limiting exposure of the cortex to high radiation doses can prevent severe cortical atrophy. High-resolution magnetic resonance imaging (MRI) has been used to reliably visualize and segment structures within the brain. We used MRI in conjunction with robust, auto-segmentation tools to delineate the cortex in treatment planning images and re-plan a glioblastoma patient with added cortical dose constraints. Materials and Methods: Cerebral cortex of a representative glioblastoma patient was parcellated on high-resolution T1-weighted pre-contrast MR images with well-validated segmentation software (Freesufer). MR images were co-registered to the treatment-planning CT images so as to project the cortical segmentation into CT space. For each CT slice, the binary segmentation image was converted into vertex locations describing multiple closed polygons. Vertices were saved in the existing radiation structure (RS) file as an additional contour. Updated RS and CT files were imported into an Eclipse workstation and used to re-plan the patient, both with- and without- cortical dose constraints. Constraints to the remaining structures mirrored those used clinically. Results: By penalizing against cortical voxels receiving dose greater than 30 Gy, the volume percentage of cortex receiving at least 20, 30, 40 and 50 Gy, decreased by 10, 7, 7 and 5%, respectively. Planning treatment volume (PTV) coverage was maintained, at the cost of an increase in the overall 3D maximum dose from 65.0 to 66.9 Gy. The point source for the hot spot was located within the gross tumor volume. Conclusion: We found that radiation dose to the cerebral cortex can be reduced while maintaining clinically practiced PTV coverage. Future studies will attempt to correlate radiation sparing of the cortex with improved neurocognitive outcome post-therapy.

Poster #87

David Hansen, Aarhus, Denmark

A Gadgetron based hyperpolarised 13C analysis module for multi-vendor clinical translation

Hansen DC, Schulte R, Sørensen TS, Ringgard S, Stødkilde-Jørgensen H, Laustsen C. Medical Physics, Aarhus University Hospital, Aarhus, GE Healthcare, Munich, Germany; Clinical Medicine, Aarhus University, Aarhus, Denmark; MR Rsearch Center, Aarhus University, Aarhus, Denmark

Introduction: Magnetic resonance spectroscopy (MRS) using hyperpolarised 13C is showing great promise for molecular imaging of cancer patients and was recently used in humans for prostate cancer. While 13C MRS has been done using many different MRI machines, there is currently no vendor providing reconstruction facilities and simple in-house software is typically used instead. Thus, clinical state-of-the-art techniques such as multi-channel parallel imaging and compressed sensing are not used and translation from small-animal MRI as well as multi-center trials are difficult. Here we introduce an easily extensible hyperpolarisation module for the open source reconstruction framework Gadgetron, allowing for state-of-the-art reconstruction from all major MRI vendors demonstrating its use for a multi-center trial with pancreatic cancer patients. Materials and Methods: A 30 kg pig was sedated and mechanically ventilated during the MRI session. [1-13C]pyruvic acid was polarised in a SpinLab (GE Healthcare) and the solution was injected via a femoral vein catheter. Metabolic images of the kidneys and pancreas were acquired using a specialized 13C RF coil with 16 receive channels and an IDEAL spiral CSI sequence. Image reconstruction was done in the Gadgetron framework. Noise adjustment and coil reduction was done, followed by a MATLAB module, which separated the metabolites into standard spiral datasets using IDEAL chemical shift modeling. This data was directly passed into the Gagetron reconstruction, which in this case was TV-SENSE with the coil sensitivity maps estimated from the pyruvate data. Results and conclusion: The Gadgetron framework provides fast and accurate reconstruction, which compared favorably with the simpler in-house method. The MATLAB IDEAL extension allowed for quick integration of the chemical shift modeling, without compromising image quality. Further, using multi vendor raw data format is crucial in upcoming multicentre trials.

Poster #88

Finn von Eyben, Odense, Denmark

Management of prostate cancer with dominant intraprostatic lesion: a systematic review and meta-analysis

Finn Edler von Eyben. Center of Tobacco Control Research

Background. Prostate cancer is usually multifocal but a dominant intraprostatic lesion (DIL) may control the clinical course. Up to a third of patients treated with radiotherapy recur, and DIL is often the site for a recurrence. Thus our meta-analysis aimed to assess i) the diagnostic accuracy of detecting DIL with imaging, and ii) the effects of an imaging-based radiation boost for DIL. Methods. We undertook searches for studies about DIL and a boost for DIL in Pubmed, Embrace, and ClinicalTrials, and undertook a manual search. One investigator extracted primary data. Results. We identified 64 studies with 5102 cases. DIL volume varied from median 0.7 to 4.4 cm3 in 14 studies with 694 patients. Often median DIL volume was less than a tenth of the median volume of the prostate. 19 studies evaluated 1256 patients with multiparametric MRI of 18262 prostate segments. We used histopathology after radical prostatectomy as reference test. 4115 (23%) prostate segments were true-positive. A boost for DIL with a planned target volume delineated with imaging was carried out for 977 patients in 12 studies. In seven studies, the boost for DIL was given with an EQD2 dose >90 Gy. 239 patients with low-, intermediate-, or high-risk in one of the studies had 94%, 79%, and 58% 10-years prostate specific antigen (PSA) recurrence-free survival. Conclusions. A radiotherapy boost for DIL was safe and effective. Current trials assess tumor control and toxicity of a DIL boost against conventional EBRT.

List of participants *(per May 26, 2015)*

Azadeh Abravan
PhD candidate
physics
University of Oslo
Oslo, Norway
azadeh.abravan@fys.uio.no

Ninna Aggerholm-Pedersen
PhD student
Experimental clinical Oncology
Aarhus University hospital
Aarhus, Danmark
aggerholm@oncology.dk

Ahmad Ali
Lecturer
Clinical Oncology
Cairo University
Cairo, Egypt
thedrahmadali@gmail.com

Jan Alsner
Professor
Experimental Clinical Oncology
Aarhus University Hospital
Aarhus C, Denmark
jan@oncology.au.dk

Andreas Gravgaard Andersen
Bachelor Student
Department of Medical Physics
Aarhus University Hospital/Aarhus University
Aarhus C, Denmark
andreasg@phys.au.dk

Margit Holst Andersen
RTT & Nurse
Department of Oncology, AUH
Radiotherapy (Stråleterapien)
Aarhus, Denmark
margande@rm.dk

Nicolaj Andreassen
MD
Dept. of Oncology
Aarhus University Hospital
Aarhus, Denmark
Nicolaj@oncology.au.dk

Lena Andreasson-Haddad
Acta Oncologica
Solna, Sweden
lena.andreasson-haddad@actaoncologica.se

Marius Arnesen
Medical Physicist/Phd-fellow
Department of Medical Physics
Oslo University Hospital
Oslo, Norway
marius.arnesen111@gmail.com

Sadia Asghar Butt
PhD
Clinical science
Philips Denmark a/s
Copenhagen SV, Denmark
Sadia.asghar.butt@philps.com

Marianne Sanggaard Assenholt
Medical Physicist
Department of Clinical Oncology
Aarhus university hospital
Aarhus N, Denmark
mariasse@rm.dk

Mariwan Baker
PhD candidate
Department of Oncology (R)
Division of Radiophysics
Herlev, Denmark
mariwan.baker@regionh.dk

Michael Baumann
Head of department
Dept. of Radiation Oncology
University Hospital Carl Gustav Carus Dresden
Dresden, Germany
michael.baumann@uniklinikum-dresden.de

Lise Bentzen
MD., Ph.D
Dept. of Oncology
Aarhus University Hospital
Aarhus, Denmark
lise@oncology.dk

Patrick Berkovic
Radiation Oncologist
Radiotherapy
CHU Liege
Liege, Belgium
p.berkovic@gmail.com

Jenny Bertholet
PhD student
department of Oncology
Aarhus University Hospital
Aarhus, Danemark
jennbe@rm.dk

Thomas Björk-Eriksson
Medical director
Skandion Clinic
Uppsala, Sweden
thomas.bjork-eriksson@vgregion.se

Josep M. Borras
Professor
Department of Clinical Sciences
University of Barcelona
Barcelona, Spain
jmborras@iconcologia.net

Line Brøndum
PhD-studerende
Experimental Clinical Oncology
Aarhus University Hospital
Aarhus, Danmark
line@oncology.au.dk

Kia Busch
Student
Dept. of Medical Physics
Aarhus University
Aarhus, Denmark
busch505@hotmail.com

Morten Busk
Ph.D
Experimental Clinical Oncology
Aarhus University Hospital
Aarhus, Denmark
morten@oncology.dk

Jan Bussink
MD PhD
Department of Radiation Oncology
Radboud University Medical Center
Nijmegen, The Netherlands
Jan.Bussink@radboudumc.nl

Annette Bøjen
Head of the Learning Centre, RTT
Department of Oncology
Aarhus University Hospital
Aarhus, Denmark
annette.boejen@aarhus.rm.dk

Sara Carvalho
PhD student
Dep of Radiation Oncology (MAASTRO)
GROW-School for Oncology and Developmental Biology, Maastricht University Medical Center (MUMC+)
Maastricht, The Netherlands
sara.carvalho@maastro.nl

Oscar CasaresMagaz
PhD Student
Oncology Department
Aarhus University Hospital
Aarhus, Denmark
oscar.casares@oncology.au.dk

Joachim Chan
Clinical Oncology Trainee
Clinical Oncology
Clatterbridge Cancer Centre NHS Foundation Trust
Bebington, Wirral, UK
joachim.chan@clatterbridgecc.nhs.uk

Haley Clark
Graduate Student
Physics and Astronomy
University of British Columbia
Vancouver, Canada
hdclark@phas.ubc.ca

Olav Dahl
Professor
Oncology Dept.
University of Bergen
Bergen, Norway
olav.dahl@helse-bergen.no

Einar Dale
Radiation oncologist
Avdeling for kreftbehandling
Oslo universitetssykehus
Oslo, Norway
einardale@yahoo.com

Sidsel Damkjær
Medical Physicist
Deptment of Radiation Oncology
Næstved Sygehus
Næstved, Denmark
sidd@regionsjaelland.dk

Joseph Deasy
Chair
Department of Medical Physics
Memorial Sloan Kettering Cancer Center
New York, United States
deasyj@mskcc.org

Timo Deist
PhD Student
Radiotheraphy
Maastro Clinic
Maastricht, The Netherlands
timo.deist@maastro.nl

Marciana-Nona Duma
Department of Radiation Oncology,
Technische Universität München,
Klinikum rechts der Isar, Münich
Germany
Marciana.Duma@mri.tum.de

Catarina Dinis Fernandes
PhD
Radiation Oncology
The Netherlands Cancer Institute
Amsterdam, The Netherlands
d.v.dinten@nki.nl

Sarah Edwards
BLM Market Access Manager
Business Line Development
Elekta
Crawley, UK
sarah.edwards@elekta.com

Pernille Byrialsen Elming
PhD-student
Department of Experimental Clinical Oncology
Aarhus University Hospital
Aarhus, Denmark
peljen@rm.dk

Ulrik Vindelev Elstrøm
Medical Physicist
Medical Physics
Aarhus University Hospital
Aarhus, Danmark
ulrielst@rm.dk

Kenni Engstrøm
MSc
Department of physics and astronomy
Science and technology
Aarhus, Denmark
Kenniengstroem@gmail.com

Katherina Farr
MD, PhD-student
Department of Oncology
Aarhus University Hospital
Aarhus, Denmark
katherina@oncology.au.dk

Emilie Finnerup
Student
Department of Oncology, Radiotherapy Research Unit
Herlev Hospital
Herlev, Denmark
emilie.finnerup@hotmail.com

Christina Fjeldbo
Post doc
Department of Radiation Biology
The Norwegian Radium Hospital
Oslo, Norway
Christina.Saten.Fjeldbo@rr-research.no

Cecilia Futsæther
Associate Professor
Dept. of Mathematical Sciences and Technology
Norwegian University of Life Sciences
Aas, Norway
cecilia.futsaether@nmbu.no

Ghazaleh Ghobadi
postdoc
Radiation Oncology
The Netherlands Cancer Institute
Amsterdam, The Netherlands
g.ghobadi@nki.nl

Cai Grau
professor
Department of Oncology
Aarhus University Hospital
Aarhus, Denmark
caigrau@dadlnet.dk

Caroline Grønborg
Medical physicist
Medical Physics
Aarhus University Hospital
Aarhus, Denmark
carolinegroenborg@gmail.com

Endre Grøvik
MRI Physicist
The Intervention Centre
Oslo University Hospital
Oslo, Norway
endre.grovik@mn.uio.no

David Hansen
Researcher
Department of Oncology
Aarhus University Hospital
Aarhus, Denmark
daviha@rm.dk

Rune Hansen
Medical Physicist
Department of Medical Physics
Aarhus University Hospital
Aarhus, Denmark
rune.hansen@aarhus.rm.dk

Anders Traberg Hansen
Medical Physicist
department of Medical Physics
Aarhus University Hospital
Aarhus, Denmark
andehans@rm.dk

Ate Haraldsen
MD
Nuklearmedicinsk Afdeling & PET Center
Aarhus Universitetshospital
Aarhus, Danmark
karhar@rm.dk

Karin Haustermanns
Professor
Department of Radiation Oncology
UZ-KULeuven
Leuven, Belgium
karin.haustermans@uzleuven.be

Taran Paulsen Hellebust
Medical Physicist
Dep. for Medical Physics
Oslo University Hospital
Oslo, Norway
TPH@ous-hf.no

Richard Hill
Senior scientist
Princess Margaret Cancer Centre
UHN Research
Toronto, Canada
Richard.Hill@uhnresearch.ca

Lone Hoffmann
Medical physicist
Medical Physics
Aarhun University Hospital
Aarhus, Denmark
Lone.Hoffmann@aarhus.rm.dk

Anne Holm
Medical Physicist
Medical Physics
Aarhus University Hospital
Aarhus, Denmark
annivaho@rm.dk

Tord Hompland
Post. Doc.
Radiation Biology
The Norwegian Radium Hospital
Oslo, Norway
tord.hompland@rr-research.no

Michael Horsman
Professor of Experimental Radiotherapy
Dept. Experimental Clinical Oncology
Aarhus University Hospital
Aarhus, Denmark
mike@oncology.au.dk

Peter Hoskin
Professor
Department of Oncology
Mount Vernon Cancer Centre
Northwood, UK
peterhoskin@nhs.net

Ellen Marie Høye
PhD
Department of Oncology
Aarhus University Hospital
Aarhus, Denmark
elhoey@rm.dk

Morten Høyer
Professor
Department of Oncology
Aarhus University Hospital
Aarhus, Denmark
hoyer@aarhus.rm.dk

Søren Haack
MR Physicist
Dept. of Clinical Engineering / Dept. of Oncology
Aarhus University Hospital
Aarhus, Denmark
soehaa@rm.dk

Ane Iversen
MD, PhD student
Dept of Experimental Clinical Oncology
Aarhus University Hospital
Aarhus, Denmark
ane.bundsbaek.iversen@oncology.au.dk

Kirsten Legård Jakobsen
Physicist
Oncological department, division of radiotherapy
Herlev University Hospital
Herlev, Denmark
Kirsten.Legaard.Jakobsen@RegionH.Dk

Maria Fuglsang Jensen
Post. doc.
Department of Oncology
Aarhus University Hospital
Aarhus, Denmark
marfugje@rm.dk

Ingelise Jensen
Hospitalsfysiker
Afd. for Medicinsk Fysik, Onkologisk Afdeling
Aalborg Universitetshospital
Aalborg, Danmark
inje@rn.dk

Nina Boje Kibsgaard Jensen
MD, Resident
Department of Oncology
Aarhus University Hospital
Aarhus, Denmark
nina.boje@rm.dk

Christoffer Johansen
Professor
Survivorship Unit
Danish Cancer Society Research Centre
Copenhagen, Denmark
christof@CANCER.DK

Jørgen Johansen
MD, PhD
Dept. of Oncology
Odense University Hospital
Odense, Denmark
j.johansen@dadlnet.dk

Maria Kandi
Med.Dr.
Oncology
Aarhus university Hospital
Aarhus, Denmark
marikand@rm.dk

Azza Khalil
Clinical Oncologist
Oncology
Aarhus University Hospital
Aarhus, Denmark
azzakhal@rm.dk

Marianne Knap
MD
Oncology
Aarhus University Hospital
Aarhus, Denmark
mariknap@rm.dk

Stine Korreman
Head of Department
Department of Science, Systems and Models
Roskilde University
Roskilde, Denmark
stine.korreman@gmail.com

Stine Kramer
MD
NUK-PET
Aarhus Universitetshospital
Aarhus C, Denmark
stinkram@rm.dk

Alexander Kristian
PhD Student
Department of Tumor Biology
Institute for Cancer Research, OUS
Oslo, Norway
alexandr.kristian@gmail.com

Svetlana Kunwald
overlæge
onkologisk
Aalborg Universitets hospitel
Aalborg, Danmark
svk@rn.dk

Christopher Kurz
PostDoc
Department of Radiation Oncology and Department of Medical Physics
Ludwig-Maximilians-University Munich
Garching, Germany
christopher.kurz@physik.uni-muenchen.de

Jan Lagendijk
Professor
Radiotherapy
University medical center Utrecht
Utrecht, Netherlands
J.J.W.Lagendijk@umcutrecht.nl

Ferenc Lakosi
radiation oncologist
radiotherapy
CHU de Liege
Liege, Belgium
lakosiferenc@yahoo.com

Philippe Lambin
Professor
Radiation Oncology
Maastro Clinic
Maastricht, The Netherlands
philippe.lambin@maastro.nl

Mette Lange
Medical secretary
Dept. of Oncology
Aarhus University Hospital
Aarhus, Denmark
metejens@rm.dk

Anne Larsen
Ph.d. studerende
Klinisk Biokemisk Afdeling
Aarhus University Hospital
Aarhus C., Denmark
anlarsen@rm.dk

Yasmin Lassen
Afdelingslæge
Department of Oncology
Aarhus University Hospital
Aarhus, Danmark
yasmlass@rm.dk

Louise Laursen
Postdoc/Administrator
Experimental Clinical Oncology
Aarhus University Hospital
Aarhus C, Denmark
louise@oncology.au.dk

Marta Lazzeroni
Post Doc
Medical Radiation Physics, Dept. Oncology-Pathology
Karolinska Institute
Solna (Stockholm), Sweden
marta.lazzeroni@ki.se

Ralph Leijenaar
PhD candidate
radiation oncology
MAASTRO clinic
Maastricht, Netherlands
ralph.leijenaar@maastro.nl

Anna Li
Medical Physicist
Department of Medical Physics
Oslo University Hospital
Oslo, Norway
lianna2@ous-hf.no

Yolande Lievens
Professor
Radiation Oncology
UZ Ghent
Ghent, Belgium
Yolande.Lievens@uzgent.be

Jacob Lilja-Fischer
PhD student
Experimental Clinical Oncology
Aarhus University Hospital
Aarhus, Denmark
jacob@oncology.au.dk

Emely Lindblom
PhD student
Medical Radiation Physics, Department of Physics
Stockholm University
Stockholm, Sweden
emely.lindblom@gmail.com

Jacob Christian Lindegaard
Consultant
Department of Oncology
Aarhus University Hospital
Aarhus, Denmark
jacolind@rm.dk

Lotte Lutkenhaus
PhD-student
Radation Oncology
Academic Medical Center
Amsterdam, The Netherlands
l.j.lutkenhaus@amc.uva.nl

Christina Maria Lutz
PhD Student
Department of Oncology
Aarhus University Hospital
Aarhus C, Denmark
chrilutz@rm.dk

Armin Lühr
Postdoc
OncoRay / German Cancer Consortium (DKTK)
TU Dresden
Dresden, Germany
armin.luehr@oncoray.de

Heidi Lyng
Scientist
Department of Radiation Biology
Oslo University Hospital
Oslo, Norway
heidi.lyng@rr-research.no

Christina Daugaard Lyngholm
PhD student, MD
Dep of Experimental Clinical Oncology
Aarhus University Hospital
Aarhus, Denmark
Christina@oncology.dk

Faisal Mahmood
Physicist, PhD
Oncology
Herlev Hospital
Herlev, Denmark
fama@regionh.dk

Philippe Maingon
Radiation Oncologist
Radiotherapy
Centre Georges-Francois LECLERC
DIJON CEDEX, FRANCE
pmaingon@cgfl.fr

Eirik Malinen
Professor
Department of Physics
University of Oslo
Oslo, Norway
eirik.malinen@fys.uio.no

Anfinn Mehus
Chief physicist
Department of oncology and medical physics
Haukeland University hospital
Bergen, Norway
anfinn.mehus@helse-bergen.no

Anni Morsing
Chief Physician
Nuclear Medicine & PET Centre
Aarhus University Hospital
Aarhus, Denmark
anni.morsing@aarhus.rm.dk

Ludvig Muren
Professor
Dept of Medical Physics
Aarhus University Hospital
Aarhus, Denmark
ludvmure@rm.dk

Ida Mølholm
Student
Department of Oncology, Radiotherapy Research Unit
Herlev Hospital
Herlev, Denmark
ida_moelholm@yahoo.dk

Søren Møller
Senior resident
Dept. of Oncology
Rigshospitalet, University of Copenhagen
Copenhagen, Denmark
dr.smoller@gmail.com

Ditte Sloth Møller
Medical Physicist
Department of Medical Physics
Aarhus University Hospital
Aarhus C, Denmark
dittmoel@rm.dk

Maria Najim
Radiation Oncologist
Radiation Oncology
Crown Princess Mary Cancer Centre, Westmead
Sydney, australia
maria.najim@health.nsw.gov.au

Steffen Nielsen
Research Assistant
Experimental Clinical Oncology
Aarhus University Hospital
Aarhus, Denmark
steffen.nielsen89@gmail.com

Thomas Nielsen
Postdoc.
Center of Functionally Integrative Neuroscience
Aarhus University Hospital
Aarhus, Denmark
thomas@cfin.au.dk

Marie E K Nielsen
Medical Physicist
Deptment of Radiation Oncology
Næstved Sygehus
Næstved, Denmark
maeln@regionsjaelland.dk

Martin Nielsen
Medical Physicist
Department of Medical Physics
Aalborg University Hospital
Aalborg, Denmark
martin.skovmos.nielsen@rn.dk

Marianne Nordsmark
Associate professor
Dept Oncology
Aarhus University Hospital
Aarhus, Denmark
marnor@rm.dk

Tine Bisballe Nyeng
Medical Physicist
Medical Physics
Aarhus University Hospital
Aarhus, Denmark
tinenyen@rm.dk

Ole Nørrevang
Chief Physicist
Department of Medical Physics
Aarhus University Hospital
Aarhus, Denmark
olenoerr@rm.dk

Giske Opheim
Scientific research assistent
Dept. of Oncology, Radiation Therapy unit
Herlev Hospital, University of Copenhagen
Herlev, Denmark
giske.fiskarbekk.opheim@regionh.dk

Wiviann Ottosson
Medical Physicist
Department of Oncology
Radiotherapy Research Unit
Herlev, Denmark
wivott01@heh.regionh.dk

Jens Overgaard
Professor
Department of Experimental Clinical Oncology
Aarhus University Hospital
Aarhus, Denmark
jens@oncology.au.dk

Leen Paelinck
Physicist
Radiotherapy
UZ Ghent
Ghent, Belgium
Leen.Paelinck@uzgent.be

Parag Parikh
MD
Department of Radiation Oncology
Washington University School of Medicine
St Louis, MO, USA
pparikh@radonc.wustl.edu

Jesper Pedersen
Master Student
Dept. of Medical Physics
Aarhus University Hospital
Aarhus, Denmark
yllemanden@hotmail.com

Marta Peroni
Imaging Physicist
Paul Scherrer Institut
Villigen, Schweiz
marta.peroni@psi.ch

Lucas Persoon
PhD student
medical physics
MAASTRO clinic
MAASTRICHT, The Netherlands
lucas.persoon@maastro.nl

Gitte Persson
Afdelingslæge
Onkologisk Klinik
Rigshospitalet
Copenhagen, Denmark
gitte.persson@regionh.dk

Marie Tvilum Petersen
Research Year Student
Department of Oncology
Aarhus University Hospital
Aarhus, Denmark
maiepter@rm.dk

Stine Elleberg Petersen
MD, PhD
Department of Oncology
Aarhus University Hospital
Aarhus, Denmark
stinpete@rm.dk

Jørgen Petersen
Medical Physicist
Dept. of Medical Physics
Aarhus University Hospital
Aarhus, Denmark
joerpete@rm.dk

Marielle Philippens
Medical physicist
Radiotherapy
University medical center Utrecht
Utrecht, Netherlands
m.philippens@umcutrecht.nl

Jean-Philippe Pignol
Professor
Department of Radiation Oncology
Erasmus MC
Rotterdam, The Netherlands
j.p.pignol@erasmusmc.nl

Kathinka Elinor Pitman
PhD student
Physics
UIO
Oslo, Norway
kathinka.pitman@fys.uio.no

Per Poulsen
Associate Professor
Department of Oncology
Aarhus University Hospital
Aarhus, Denmark
per.poulsen@rm.dk

Toke Printz Ringbæk
PhD student
Instituts für Medizinische Physik und Strahlen-schutz (IMPS)
Technische Hochschule Mittelhessen (THM)
Marburg, Germany
printzri@med.uni-marburg.de

Lars Hjorth Præstegaard
Medical Physicist
Medical Physics
Aarhus University Hospital/Aarhus University
Aarhus, Denmark
larsprae@rm.dk

Tanuj Puri
Postdoctoral PET Physicist
Oncology
University of Oxford
Oxford, England
tanuj.puri@oncology.ox.ac.uk

Richard Pötter
Head of Radiotherapy department
Radiotherapy
Medical University Vienna
Vienna, Austria
richard.poetter@akhwien.at

Shirin Rahmanian
PhD student
Medical Physics in Radiation Oncology
German Cancer Center (DKFZ)
Heidelberg, Germany
s.rahmanian@dkfz.de

Anne Ramlov
Ph.d. student
Department of Oncology
Aarhus University Hospital
Aarhus C, Denmark
anraml@rm.dk

Gregers B. D. Rasmussen
Ph.D. student
Dept. of Oncology, Section of Radiotherapy
Rigshospitalet
Copenhagen, Denmark
gras0038@regionh.dk

Laura Rechner
Hospital Physicist
Department of Oncology
Rigshospitalet
Copenhagen, DK
laura.ann.rechner@regionh.dk

Kathrine Rø Redalen
Postdoc
Department of Oncology
Akershus University Hospital
Lørenskog, Norway
kathrine.roe@medisin.uio.no

Bernt Louni Rekstad
Physicist
Department of Medical Physics
Oslo University Hospital
Oslo, Norway
bernt.louni.rekstad@ous-hf.no

Espen Rusten
PhD
Department of Physics
University of Oslo
Oslo, Norge
espen.rusten@gmail.com

Susanne Rylander
Medical physicist
Department of Clinical Medicine
Aarhus University Hospital
Aarhus, Denmark
susaryla@gmail.com

Jan Rødal
Head of department
Department of medical physics
Oslo University Hospital
Oslo, Norway
jan.rodal@ous-hf.no

Cornelis Raaijmakers
Medical Physicist
Radiotherapy
University Medical Centre Utrecht
Utrecht, The Netherlands
c.p.j.raaijmakers@umcutrecht.nl

Hella Sand
Physicist
Medical physics, Oncology
Aalborg University Hospital
Aalborg, Denmark
hmbs@rn.dk

Alina Santiago
Research Associate
Radiotherapy Department
University of Marburg
Marburg, Germany
santiago@staff.uni-marburg.de

Line M H Schack
MD, PhD student
Dep. of Experimental Clinical Oncology
Aarhus University Hospital
Aarhus, DK
schack@oncology.au.dk

Mai Schmidt
PhD-student
Department of Oncology
Aarhus University Hospital
Aarhus, Denmark
maiscmid@rm.dk

Annette Schouboe
RTT
Department of oncology
Aarhus University Hospital
Aarhus, Denmark
annescho@rm.dk

Joao Seco
Assistant Professor
Department of Radiation Oncology
Francis H Burr Proton Therapy Center
Boston MA, USA
JSECO@mgh.harvard.edu

Patrik Sibolt
Ph.D. Student
Nutech Radiation Physics
Technical University of Denmark, Risø¸ Campus
Roskilde, Denmark
pasi@dtu.dk

Maria Sjölin
Medical Physicist
Department of Oncology
Radiotherapy Research Unit
Herlev, Denmark
maria.sjoelin@regionh.dk

David Sjøstrøm
Deputy Chief Physicist
Departement of Oncology
Herlev Hospital
Herlev, Danmark
David.sjostrom@regionh.dk

Camilla Skinnerup Byskov
Postdoc
Medical Physics
Aarhus University Hospital
Aarhus, Denmark
c.skinnerup@gmail.com

Jan-Jakob Sonke
Physicist
Radiation Oncology
The Netherlands Cancer Institute
Amsterdam, The Netherlands
j.sonke@nki.nl

Camilla Stokkevåg
PHD student
Dep. of oncology and medical physics
Haukeland University Hospital
Bergen, Norway
camilla.stokkevag@ift.uib.no

Jonathan Sykes
Head of Physics
Blacktown Cancer Care Centre
Western Sydney Local Health District
Sydney, Australia
jonathan.sykes@health.nsw.gov.au

Brita Singers Sørensen
Associated Professor
Dep Experimental Clinical Oncology
Aarhus University Hospital
Aarhus, Danmark
bsin@oncology.dk

Kari Tanderup
Professor
Department of Oncology
Aarhus University Hospital
Aarhus, Denmark
karitand@rm.dk

Sara Thörnqvist
Postdoc
Department of oncology and medical physics
Haukeland university hospital
Bergen, Norway
sarathoe@rm.dk

Beate Timmermann
Professor
WPE
University Clinic Essen
Essen, Germany
Beate.Timmermann@uk-essen.de

Jakob Toftegaard
PhD student
Department of Oncology
Aarhus Univerty Hospital
Aarhus, Denmark
jaktofte@rm.dk

Turid Torheim
PhD student
Dept. of Mathematical Sciences and Technology, Norwegian University of Life Sciences
Ås, Norway
turid_torheim@hotmail.com

Klaus R. Trott
Professor
Department of Radiation Oncology,
Technische Universität München,
Klinikum rechts der Isar, Münich
Germany
klaustrott@yahoo.it

Laura Tuomikoski
Clinical Physicist
Department of Oncology
Helsinki University Central Hospital
Helsinki, Finland
laura.tuomikoski@hus.fi

Vicki Taasti
PhD student
Oncology
Aarhus University Hospital
Aarhus, Danmark
v.taasti@gmail.com

Niels Ulsø
Physicist
Medical Physics
Aarhus University Hospital
Aarhus, Denmark
niels.ulsq@gmail.com

Vincenzo Valentini
Professor
Radiation Oncology Department
Gemelli-ART
Rome, Italy
vvalentini.it@gmail.com

Uulke van der Heide
PhD
Medical physics
The Netherlands Cancer Institute
Amsterdam, The Netherlands
u.vd.heide@nki.nl

Mikkel Holm Vendelbo
MD, PhD
Department of Nuclear Medicine and PET-centre
Aarhus University Hospital
Aarhus, Denmark
mhve@clin.au.dk

Anne Vestergaard
Medical Physicist
Department of Medical Physics
Aarhus University Hospital
Aarhus, Denmark
annveste@rm.dk

Ivan Richter Vogelius
Medical physicist
Department of Oncology
Rigshospitalet
Copenhagen, Denmark
ivan.richter.vogelius@regionh.dk

Finn von Eyben
leder
Hovedkontor
Center of Tobacco Control Research
Odense, Denmark
finn113edler@mail.tele.dk

Linda Wack
PhD student
Section for Biomedical Physics
University Hospital Tübingen
Tübingen, Germany
linda-jacqueline.wack@med.uni-tuebingen.de

Hanlin Wan
PhD Student
Department of Radiation Oncology
Washington University School of Medicine
St Louis, MO, USA
hwan@radonc.wustl.edu

Daniel Warren
Postdoctoral physicist
Department of Oncology
University of Oxford
Oxford, United Kingdom
daniel.warren@oncology.ox.ac.uk

Britta Weber
MD, PhD
Department of Oncology
Aarhus University Hospital
Aarhus, Denmark
britwebe@rm.dk

Dan Welsh
Pre-Registration Clinical Student
Oncology Physics
NHS Lothian
Edinburgh, UK
dan.welsh@nhs.net

Mette Winther
PhD student
Dept. of Experimental Clinical Oncology
Aarhus University Hospital
Aarhus, Denmark
mette@oncology.dk

Thomas Wittenborn
Postdoc
Dept. Experimental Clinical Oncology
Aarhus University Hospital
Aarhus, Denmark
Wittenborn@oncology.au.dk

Esben Worm
Medical Physicist
Medical Physics
Aarhus University Hospital
Aarhus N, Denmark
esbeworm@rm.dk

Karen Zegers
Phd-student
Radiation Oncology
Maastro-Clinic Maastricht
Maastricht, Netherlands
karen.zegers@maastro.nl

Daniel Zips
Professor
Radiation Oncology
University Hospital Tübingen
Tübingen, Germany
Daniel.Zips@med.uni-tuebingen.de

Ruta Zukauskaite
MD/ph.d stud
Oncology
Odense University Hospital
Odense, Danmark
ruta.zukauskaite@rsyd.dk